U.S. DEPARTMENT OF COMMERCE
National Technical Information Service

AD/A-055 824

DEMONSTRATION OF THE MICROWAVE ICE PROTECTIO CONCEPT

BERTRAM MAGENHEIM

MECHANICS RESEARCH, INCORPORATED
MCLEAN, VIRGINIA

MAY 1978

AD-A058824

USAAMRDL-TR-77-34

DEMONSTRATION OF THE MICROWAVE ICE PROTECTION CONCEPT

Bertram Magenheim
Mechanics Research, Inc.
7929 Westpark Drive
McLean, Va. 22101

DDC FILE COPY

May 1978

Final Report for Period June 1976 - June 1977

Approved for public release;
distribution unlimited.

Prepared for

APPLIED TECHNOLOGY LABORATORY
U. S. ARMY RESEARCH AND TECHNOLOGY LABORATORIES (AVRADCOM)
Fort Eustis, Va. 23604

APPLIED TECHNOLOGY LABORATORY POSITION STATEMENT

The primary purpose of this R&D effort was to verify the applicability of microwave surface guide theory as a method of helicopter rotor blade ice protection, and to estimate the performance characteristics and penalties imposed by the system to provide a sound basis for further development or abandonment of the concept. Primary conceptual concerns were: accuracy of analytical prediction techniques for surface wave guide performance, system complexity and weight, and detectability of the microwave energy during use of the ice protection system. Also of significance in determining feasibility for further development are features such as system cost, reliability, maintainability, electrical power requirements, and aircraft performance penalties. This effort has confirmed the applicability of surface wave guide theory and has produced estimates of microwave rotor blade ice protection features.

This Directorate concurs in the findings presented in this report and recommends use of the information contained herein for further R&D planning purposes. The information contained herein should not be used for production design purposes since complete test verification has not been accomplished and absolute confidence of estimated characteristics does not exist. Continued investigations are needed to gain further knowledge regarding methodology of concept implementation for use as an ice protection device for helicopter rotor blades, to demonstrate full-scale system function, and to refine the estimated design features.

The Project Engineer for this effort was Mr. Richard I. Adams of the Systems Support Division.

Unclassified
SECURITY CLASSIFICATION OF THIS PAGE (When Data Entered)

REPORT DOCUMENTATION PAGE

READ INSTRUCTIONS BEFORE COMPLETING FORM

1. REPORT NUMBER: USAAMRDL TR-77-34 (18) (19)	2. GOVT ACCESSION NO.
3. RECIPIENT'S CATALOG NUMBER	
4. TITLE (and Subtitle): DEMONSTRATION OF THE MICROWAVE ICE PROTECTION CONCEPT (6)	5. TYPE OF REPORT & PERIOD COVERED: Final Report, June 1976 – June 1977 (9)
	6. PERFORMING ORG. REPORT NUMBER
7. AUTHOR(s): Bertram Magenheim (10)	8. CONTRACT OR GRANT NUMBER(s): DAAJ02-76-C-0052 (15)
9. PERFORMING ORGANIZATION NAME AND ADDRESS: Mechanics Research, Inc. 7929 Westpark Drive McLean, Virginia 22101	10. PROGRAM ELEMENT, PROJECT, TASK AREA & WORK UNIT NUMBERS: 62209A 1L262209AH76 00 172 EK
11. CONTROLLING OFFICE NAME AND ADDRESS: Applied Technology Laboratory, U. S. Army Research and Technology Laboratories (AVRADCOM) Fort Eustis, Virginia 23604	12. REPORT DATE: May 1978 (11) (17) 00
	13. NUMBER OF PAGES: 133 (12) 134p.
14. MONITORING AGENCY NAME & ADDRESS (if different from Controlling Office)	15. SECURITY CLASS. (of this report): Unclassified
	15a. DECLASSIFICATION/DOWNGRADING SCHEDULE

16. DISTRIBUTION STATEMENT (of this Report)

Approved for public release; distribution unlimited.

17. DISTRIBUTION STATEMENT (of the abstract entered in Block 20, if different from Report)

18. SUPPLEMENTARY NOTES

19. KEY WORDS (Continue on reverse side if necessary and identify by block number)

Feasibility	Ice	Dissipation
Helicopters	Adhesion	Cost
Rotors	Surface Waveguides	Weight
Blades	Dielectrics	Power
Microwaves	Heat	Experimental Verification

20. ABSTRACT (Continue on reverse side if necessary and identify by block number)

An experimental demonstration of the microwave ice protection concept for helicopter rotor blades is presented. By shedding ice samples from experimental ice protection devices, microwave ice protection theory was verified. Increased power density in the ice layer is achieved by operating at higher microwave frequencies, resulting in significantly shorter shed times for the same microwave power. The microwave concept offers the possibility of constructing ice protection systems totally out of nonmetallic materials that will not deteriorate the radar cross section of composite blades. Incremental weight, cost and power estimates for equipping

DD FORM 1473, 1 JAN 73 EDITION OF 1 NOV 65 IS OBSOLETE

Unclassified
SECURITY CLASSIFICATION OF THIS PAGE (When Data Entered)

392 011 78 06 29 011

Unclassified

SECURITY CLASSIFICATION OF THIS PAGE(When Data Entered)

Block 20. Abstract - continued.

various helicopters are presented. An evolving microwave tube technology promises significant improvements in cost, efficiency, weight, and power drain while providing higher microwave powers and consequently shorter shed times.

It is demonstrated that a combination erosion shield/surface waveguide constructed from ultrahigh molecular weight polyethylene (UHMWPE) fortified with a layer of polyurethane near the tip did not deteriorate the mean time between unscheduled maintenance (MTBUM) of the blade below that of the polyurethane erosion shield by itself. When the erosion shield/surface waveguide reaches the MTBUM it can be replaced without discarding the blade.

Unclassified

SECURITY CLASSIFICATION OF THIS PAGE(When Data Entered)

PREFACE

This report presents the findings of an investigation of the microwave ice protection concept for helicopter rotor blades performed by Mechanics Research, Inc., Electronic Systems Division, under Contract No. DAAJ02-76-C-0052 for the Eustis Directorate, U.S. Army Air Mobility Research and Development Laboratory (USAAMRDL),* Fort Eustis, Viriginia. The technical monitor of the project for USAAMRDL was Mr. R. I. Adams. The Mechanics Research, Inc. program was under the direction of Mr. B. Magenheim, Project Manager. Personnel contributing to the program included Mr. K. Atkins.

*On 1 September 1977, the Eustis Directorate, U.S. Army Air Mobility Research and Development Laboratory was redesignated Applied Technology Laboratory, U.S. Army Research and Technology Laboratories (AVRADCOM).

SUMMARY

The purpose of this program was to demonstrate the microwave ice protection concept for helicopter rotor blades and to estimate the characteristics and penalties of the concept. The work performed was based on the Feasibility Analysis (Reference 1) performed previously for the Eustis Directorate.

Ice Shed Tests

Scale model microwave deicers successfully shed ice samples at blade surface temperature of -20°C.

Scale model tests run at 2.45 GHz and scaled to 22 GHz indicate a significant improvement in performance at 22 GHz for the same amount of power used at 2.45 GHz, due primarily to the higher power concentration that can be achieved in the ice layer at the higher frequency.

Verification of Analytical Techniques

Analytical techniques for predicting surface waveguide deicer performance have been verified experimentally and can be reliably used to predict surface waveguide performance at any frequency.

Launch Efficiency

Launch efficiencies between 50% and 70% were obtained. The goal of this program was to achieve a sufficient launch efficiency to demonstrate deicer performance, not to optimize launchers. Data indicates that launch efficiencies in excess of 90% are achievable.

[1] Magenheim, Bertram and Hains, Frank, Feasibility Analysis for a Microwave Deicer for Helicopter Rotor Blades, Mechanics Research Inc., USAAMRDL-TR-76-18, Eustis Directorate, U.S. Army Air Mobility Research and Development Laboratory, Fort Eustis, Virginia, May 1977.

Dielectric Properties of Rotor Ice

A technique for measuring the dielectric loss properties of rotor ice was established and used to measure the loss tangents of the various ice samples used in the ice shed tests.

Cost, Weight and Power

Preliminary cost, weight and power estimated for UH-1, AH-1, CH-47, OH-58, UTTAS, AAH and ASH helicopters were made and are presented in Section 8. Costs range from approximately $9.3K for the UH-1 to $26K for the CH-47.

Reliability and Maintainability

The mean time between unscheduled maintainance (MTBUM) for a microwave deicer boot composed of ultrahigh molecular weight polyethelene (UHMWPE) out to 70% span and UHMWPE covered with a 25-mil polyurethane erosion coat for the remainder of the span was shown not to deteriorate the MTBUM obtainable with a polyurethane erosion shield over the full span of the blade.

Passive Countermeasures

It is shown in section 6 that the vulnerability of Army helicopters due to the possible detection of microwave deicer leakage radiation is negligable.

Ice Detection

Techniques have been identified that can be used to detect the presence of ice and measure its thickness and accretion rate. One technique is inherent in the deicer and consists of monitoring signals returning from the deicer boot. Other techniques would utilize separate and independent devices that are nonmechanical having no moving parts and conform to the contour of the surface being monitored. The readout is essentially instantaneous, giving ice presence, ice thickness and ice accretion rate as a function of time. The devices are small, lightweight and rugged so that they can be placed almost anywhere on the skin of the aircraft, including the rotor blade and in the engine inlet ducts.

TABLE OF CONTENTS

	Page
PREFACE	3
SUMMARY	4
LIST OF ILLUSTRATIONS	9
LIST OF TABLES	12
SECTION 1 - STATIC ICE SHED TESTS	13
Physical Removal of Ice by Microwave Deicers	13
Discussion of Ice Shed Data	15
Multilayer Model Surface Waveguide	23
Comparative Shedding Effectiveness of the TE_1 and TM_0 Modes	27
Shedding Time as a Function of Temperature	29
Experimental Procedures	29
SECTION 2 - VERIFICATION OF SURFACE WAVEGUIDE THEORY	34
Experimental Procedures	43
SECTION 3 - WAVE LAUNCHERS	54
Measurement of Coupling Efficiency of the TE_1 Mode	58
SECTION 4 - LOSS TANGENT OF ROTOR ICE	62
Loss Tangent Measurements	63
SECTION 5 - ICE DETECTORS	66
SECTION 6 - PASSIVE COUNTERMEASURES AND IMPACT ON COMPOSITE BLADES	69
Radar Reflectivity	70
Detectability	72
SECTION 7 - RELIABILITY AND MAINTAINABILITY STUDIES	78
SECTION 8 - POWER, WEIGHT, COST	82
System Power	82
System Weight	85
Weight of Tube and Power Supply	85
System Cost	87

TABLE OF CONTENTS

Page

SECTION 9 - CONCLUSIONS. 88

SECTION 10 - RECOMMENDATIONS. 89

LIST OF SYMBOLS. 90

LIST OF REFERENCES 92

APPENDIXES A - SUMMARY OF STATIC ICE SHED, TESTS 94

B - DERIVATIONS OF LOSS TANGENT EQUATIONS 118

C - RECOMMENDED WHIRLING ARM TESTS - UH-1 TAIL ROTOR EQUIPPED WITH MICROWAVE ICE PROTECTION IN SIMULATED ICING ENVIRONMENT. 122

Simulated Icing Environment. 122

D - RECOMMENDED DEVELOPMENT MICROWAVE ICE DETECTORS. 128

Microwave Ice Detectors. 128

Basic Concepts. 129

E - POWER DRAIN OF A MICROWAVE DEICER AT 33.7 GHz USING AN EXPERIMENTAL GYROTORN 131

LIST OF ILLUSTRATIONS

Figure		Page
1	Shed Time Versus Power In Surface Wave, $-17^{o}C < T_{\infty} < -20^{o}C$ 2.45 GHz.	14
2	Attenuation Constant Versus Ice Thickness For TE_1 mode, 2.45 GHz, $\varepsilon_1 = 2.1$.	19
3	Attenuation Constant Versus Ice Thickness for TE_1 mode, 22 GHz, $\varepsilon_1 = 2.2$.	20
4	Shed Time Versus Power In Surface Wave, $T_{\infty} = -20^{o}C$, 22 GHz.	22
5	TE_1 Mode Power Density Versus Distance From Surface, 2.45 GHz and 22 GHz.	24
6	Two and Three Layer Models	25
7	Attenuation Constant Versus Ice Thickness at 2.45 GHz.	28
8	Effect of Blade Temperature on Shed Time	30
9	Test Equipment for Performing Static Ice Shed Tests.	31
10	Comparison of Computed With Measured Guide Wavelength for TE_1 Mode.	35
11	Comparison of Computed and Measured Guide Wavelength TM_C Mode.	36
12	Comparison of Theoretical With Measured External Eigenvalue, TM_0 Mode.	37
13	Comparison of Theoretical With Measured Internal Eigenvalue, TM_0 Mode.	38
14	Comparison of Theoretical With Measured External Eigenvalue, TE_1 Mode.	39
15	Comparison of Theoretical With Measured Internal Eigenvalue, TE_1 Mode.	40
16	Attenuation as a Function of Distance Above Surface.	41

LIST OF ILLUSTRATIONS

Figure		Page
17	Attenuation as a Function of Distance Above Surface	42
18	TE_1 Mode Test Model No. 1	44
19	TM_0 Mode Test Model No. 1	45
20	Test Equipment for Measuring Surface Waveguide Performance - Low Power Configuration for Bench or Cold Chamber	50
21	Experimental Set-Up for Measuring Surface Waveguide Performance	51
22	Experimental Set-Up for Measuring Surface Waveguide Performance	52
23	Coupling Performance	
	(a) Measured Coupling Efficiency Versus Frequency	55
	(b) Voltage Standing Wave Ratio Versus Frequency for TE_1 Mode, Test Model No. 1, $d_1 = 1.6"$, $\epsilon_1 = 2.2$	55
24	Coupling Efficiency Versus Frequency, TM_0 Mode	56
25	Comparison of Theoretical Values of Coupling Efficiency With Measured Values	57
26	Measured Tuning Characteristics of Resonant TM_0 Mode Waveguide as a Function of Ice Thickness	67
27	Measured Tuning Characteristics of Resonant TE_1 Mode Surface Waveguide as a Function of Ice Thickness	68
28	Power Density at 22 GHz for the TE_1 Mode for Dielectric Slabs and Image Lines	71
29	Power Denisty at 22 GHz for the TM_0 Modes for Dielectric Slabs and Image Lines	73
30	Mean Time Between Unscheduled Maintenance (MTBUM) Versus Percent Exposure to Sand and Rain Erosion	81

LIST OF ILLUSTRATIONS

Figure		Page
C-1	Artists Conception of Whirling Arm Test Stand.	123
C-2	Schematic Diagram Whirling Arm Test Stand.	124
C-3	Perspective View UH-1 Tail Rotor Equipped With Microwave Deicer Boot and Wave Launcher.	125
C-4	Crossection - Deicer Boot and Wave Launcher.	126
E-1	The Dependence of the Efficiency (η), Cavity Losses (P_c) and Gryotron Output Power P on the Beam Current I in Continuous Mode of Operation: U_c = 19 kV	132
E-2	Outline Drawing of Soviet Gyrotron Prototype.	132

LIST OF TABLES

Table		Page
1	Measured and Scaled Shed Performance Data.	18
2	Measured Loss Tangents of Various Samples of Ice (Model 1 TE_1 Mode)	64
3	Helicopter Power Drain 400 Watts Per Blade	83
4	Time to Shed Ice Layer (Measured at Midspan Stagnation Point) Teflon Model, Ice Density = 0.9, Computed From eq B - 14 and 17 Reference 1 (lower ice density will result in shorter shed time).	84
5	System Incremental Weight and Cost.	86

SECTION 1
STATIC ICE SHED TESTS

PHYSICAL REMOVAL OF ICE BY MICROWAVE DEICERS

The physical removal of laboratory-grown ice from test articles equipped with experimental microwave ice protection devices was performed under various ambient temperatures and with various ice densities and compositions.

Test data are summarized in Figure 1, representing data from 70 tests at an ambient temperature of -20 degrees centigrade. Complete test data are given in Appendix A. Experiments were performed on scale model surface waveguides propagating the Transverse Electric (TE) and Transverse Magnetic (TM) modes,*designed for operation at a frequency of 2.45 GHz. These models represent scaled up versions of models for operation at 5.85 and 22 GHz.

Ice samples were approximately 3 inches in length and had a weight coupled mechanically to simulate the centrigugal force encountered by a 3-inch element of ice at approximately 100 inches from the rotor hub as shown in Figure 9. The wave launched into the surface waveguide first passed through the ice sample, which extracted a small fraction of the energy from the passing wave, sufficient to cause it to shed. Then, the energy remaining in the wave continued down the surface waveguide to be dissipated in the electrical load terminating it and simulating the remaining ice on the rotor blade. The amount of power extracted by the ice sample is dependent upon lossiness or the median loss tangent of the ice (tan δ).

---

*Modes are defined in Appendix A Reference 1

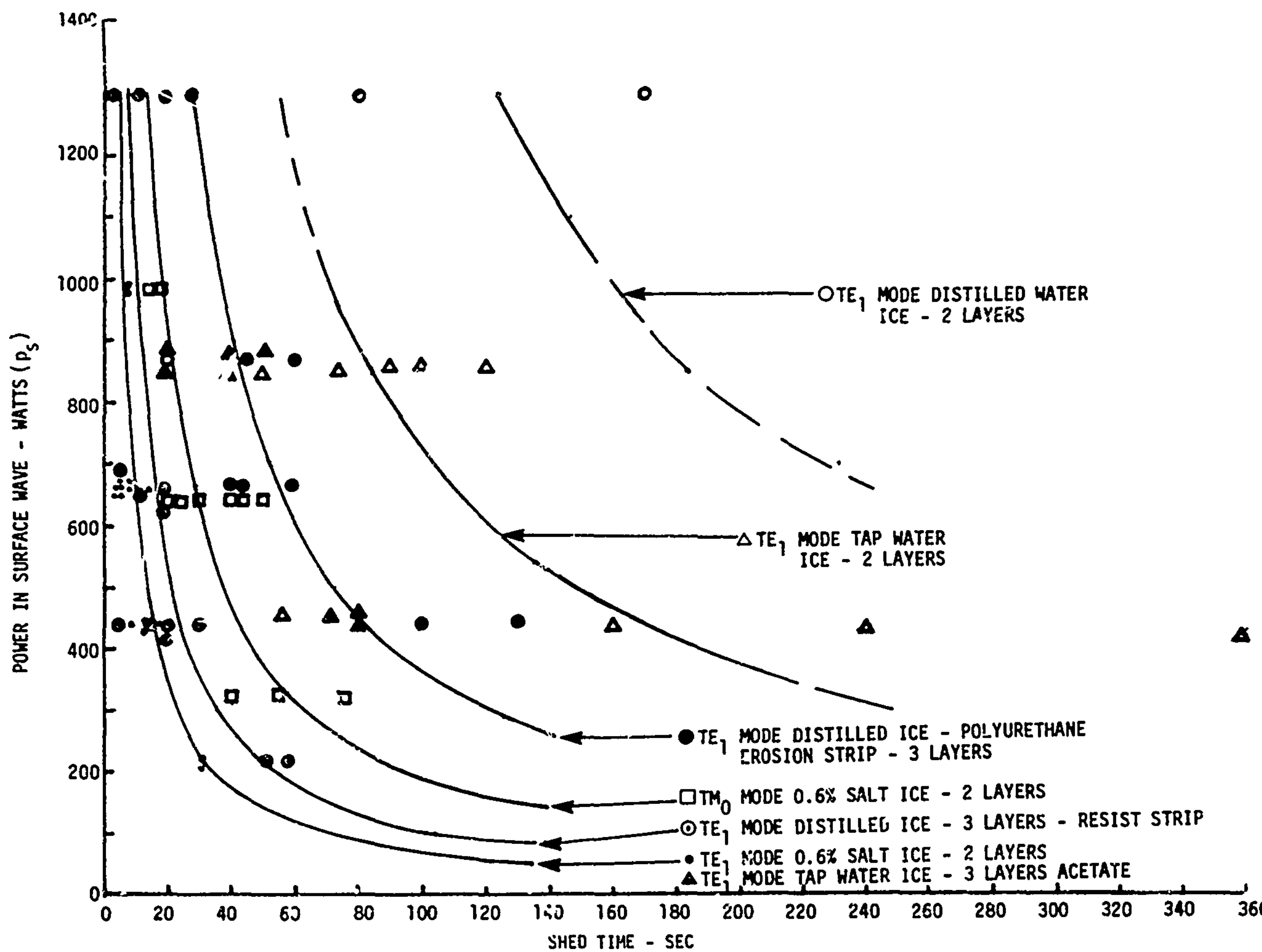

Figure 1. Shed Time Versus Power In Surface Wave, $-17^{\circ}C < T_{\infty} < -20^{\circ}C$, 2.45 GHz

Tests were performed on ice of the following compositions which may be considered to encompass the full range of tan δ to be expected in natural icing.

1. Salt water ice, 0.6% concentration, density 0.9 gm/cm^3
2. Salt water ice, 0.3% concentration, density 0.9 gm/cm^3
3. Salt water ice, 0.15% concentration, density 0.9 $gm/cm/^3$
4. Tap water ice, density 0.9 gm/cm^3
5. Tap water ice, density 0.75 gm/cm^3
6. Distilled water ice, density 0.9 gm/cm^3
7. Distilled water ice, density 0.75 gm/cm^3
8. CRREL* snow, density 0.35 gm/cm^3
9. CRREL* snow, density 0.25 gm/cm^3

DISCUSSION OF ICE SHED DATA

The data of Figure 1 demonstrate the shedding of ice elements from 2.45 GHz scale model surface waveguide deicers. The first and most obvious trend noted is the hyperbolic shape of the shed-time curves, that were fit to the data, of the form:

$$p_s t_s = k_\varepsilon \qquad (1)$$

where: t_s = Shed time (sec)

p_s = Power in the surface wave, (watts)

k_ε = Energy, (watt-sec)

*Cold Regions Research and Engineering Laboratory (CRREL)

High-loss ice samples, such as that with 0.6% salt, shed rapidly; whereas low-loss samples, such as distilled water ice, took longer and required more power to shed. The shed time of the low-loss ice was reduced considerably by the use of a lossier third layer (Figure 6): such as a polyurethane erosion strip. Values of k_ε for different ice samples are presented in Table 1.

The power in the surface wave, p_s, is much larger than the power dissipated in the ice sample; most of the energy in the wave passes through the ice and is dissipated in the load terminating the guide (as evidenced by the sharp rise in temperature of the termination). The energy that must be dissipated in the ice sample to cause it to shed is determined from:

$$p_d t_s = \frac{mc\Delta T}{0.2389} = k_s \qquad (2)$$

where: p_d = Power dissipated in the ice sample (watts)

t_s = Shed time (sec)

m = Mass of ice sample (gms)

c = Specific heat of ice

ΔT = Temperature rise required to shed ($^\circ$C)

k_s = Energy required to shed (watt-sec)

The ratio of Equation 1 to Equation 2 establishes the ratio of the power in the surface wave, p_s, to the power dissipated in the ice sample, p_d, since the shed times cancel.

$$\frac{p_d t_s}{p_s t_s} = \frac{mc\Delta T}{k_\varepsilon \quad (0.2389)}$$

or

$$\frac{p_d}{p_s} = \frac{mc\Delta T}{k_\varepsilon(0.2389)} \qquad (3)$$

where: 0.2389 is the factor required to convert $mc\Delta T$ in calories to watt-sec. Values of p_d/p_s computed from Equation 3 are presented in Table 1.

Knowing the power lost in the ice sample and the power input, the attenuation constant, α, in db/in can be computed and is presented in Table 1 for each of the ice sample types used in the test.

Extension of Shed Data to 22 GHz

Figures 2 and 3 show curves of the theoretically computed attenuation constant for the TE_1 mode as a function of ice thickness for operating frequencies of 2.45 and 22 GHz respectively. Computations are based upon techniques presented in Appendix A of Reference 1 which are well recognized techniques for computation of the attenuation constant of waveguides as substantiated by the experimental work of Cohn, Reference 2 and 3, King and Schlesinger Reference 4 and 5 and the standard textbooks - Ramo and

---

2 M. Cohn, "Propagation in Dielectric-Loaded Parallel Plane Waveguide," IRE Transactions on Microwave Theory and Techniques, pp. 202-208, April 1959.

3 M. Cohn, "TE Modes of Dielectric Loaded Trough Line," IRE Transactions on Microwave Theory and Techniques, pp. 449-454, July 1960

4 D.D. King and S.P. Schlesinger, "Losses in Dielectric Image Lines," IRE Transactions on Microwave Theory and Techniques, January 1957.

TABLE 1. MEASURED AND SCALED SHED PERFORMANCE DATA

SYMBOL	DESCRIPTION	2.45 GHz MEASURED DATA			FROM FIGURE 2	FROM TABLE 2	22 GHz SCALED DATA		
		k_ϵ	P_d/P_s	α	$\tan\delta$	$\tan\delta$	k'_ϵ	P'_d/P'_s	α'
		watt-sec $\times10^3$	-	db/in	-	-	watt-sec $\times10^3$	-	db/in
•	TE_1 MODE 0.6% SALT ICE 2 LAYER MODEL	7	.094	.143	.15	.095	0.663	.995	7.8
□	TM_0 MODE 0.6% SALT ICE 2 LAYER MODEL	18.9	.035	.051	NA	NA	NA	NA	NA
○	TE_1 MODE DISTILLED ICE 2 LAYER MODEL	162.5	.0041	.0059	.004	.007	3.25	.203	.32
△	TE_1 MODE TAP ICE 2 LAYER MODEL	74.3	.009	.0129	.013	.015	1.625	.406	.75
●	TE_1 MODE DISTILLED ICE - 3 LAYERS POLYURETHANE EROSION STRIP	36	.018	.0267	.015	NA	.325	.799	2.3
⊙	TE_1 MODE TAP ICE - 3 LAYERS MYLAR RESISTIVE STRIP	10	.066	.0988	.10	NA	.575	.977	5.4

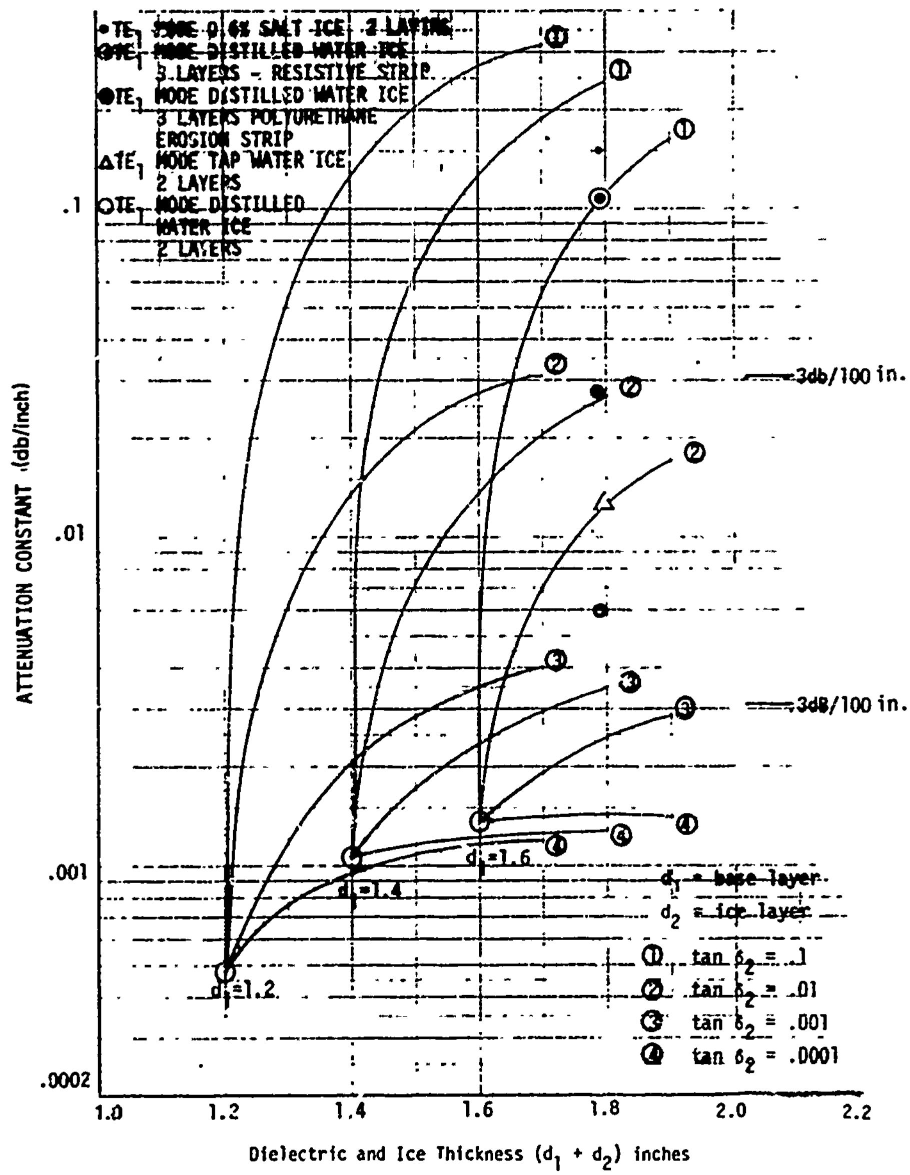

Figure 2. Attenuation Constant Versus Ice Thickness
TE_1 Mode, 2.45 GHz, ε_1 = 2.1

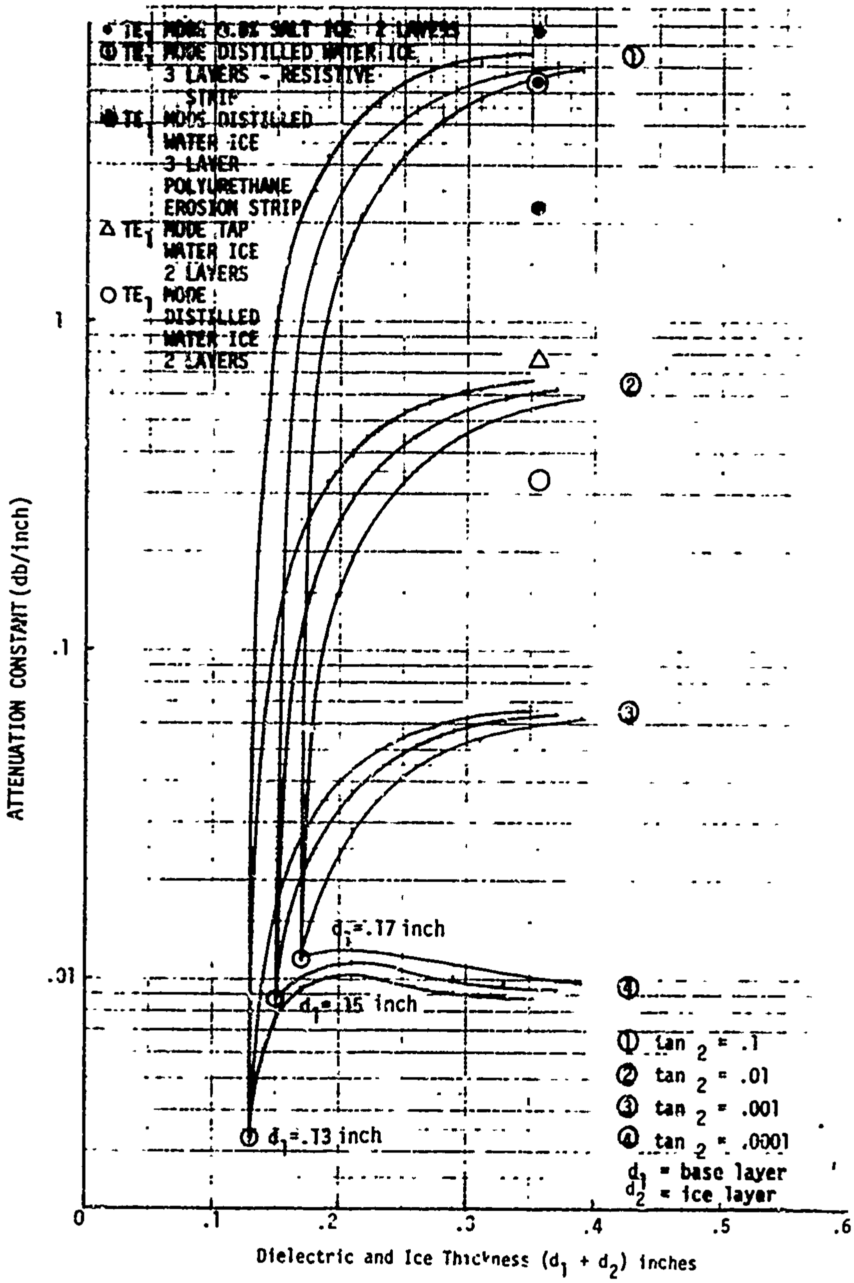

Figure 3. Attenuation Constant Versus Ice Thickness for TE_1 Mode, 22 GHz, $\varepsilon_1 = 2.2$

Whinnery Reference 7 and R. Collin Reference 6. The attenuation constants that were measured at a frequency of 2.45 GHz for the various ice samples are plotted on Figure 2. The loss tangents for each ice sample can be read off of Figure 2 and are presented in Table 1. (This method of establishing tan δ yields measurements that agree with measurements made separately in Section 4, which are also presented in Table 1). Using these values of tan δ and ice samples of the same thicknesses as those used in the 2.45 GHz tests, points on Figure 3 for 22 GHz can be plotted which correspond to the points plotted in Figure 2 for 2.45 GHz, permitting the attenuation constant α, p_d/p_s and k_ε to be determined at 22 GHz (these are denoted by α', p_d'/p_x' and k_ε'). Having determined k_ε' the curves of shed time versus surface wave power, p_s' t_s' can be established for 22 GHz and are plotted in Figure 4. Figure 4 snows a significant reduction in shed time at 22 GHz for the same surface wave power and ice samples. This reduction in shed time obviates the need for three layer models to enhance lossiness. Three-layer models may still be required, however, to improve sand and rain erosion.

---

5 S.P. Schlesinger and D.D. King, "Dielectric Image Lines," IRE Transactions on Microwave Theory and Techniques, July 1958.

6 R. Collin, Field Theory of Guided Waves, New York: McGraw-Hill, 1960.

7 Ramo, Whinnery and Van Duzer, Fields and Waves in Communications Electronics, New York: John Wiley & Sons, 1965.

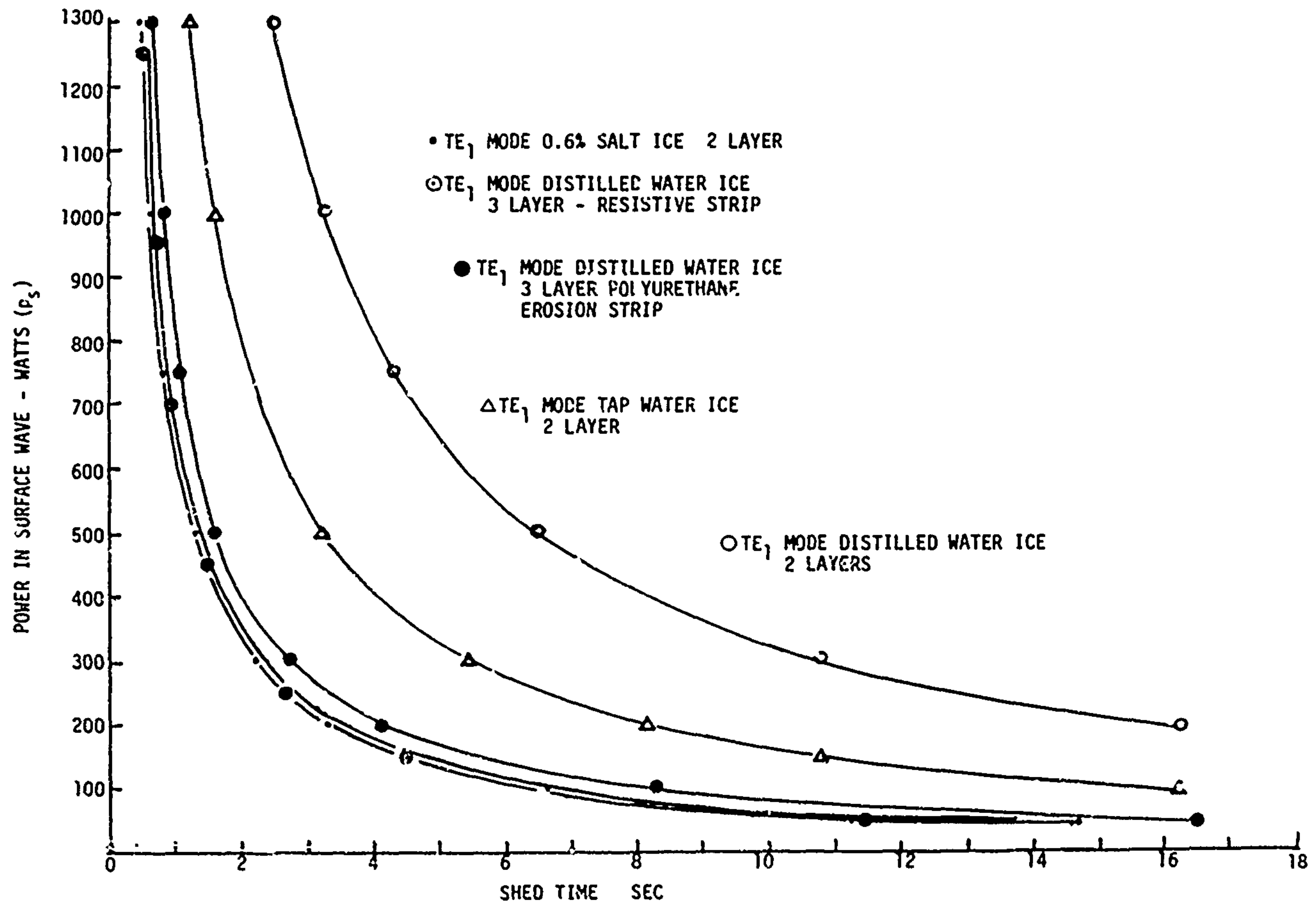

Figure 4. Shed Time Versus Power In Surface Wave, T_∞ = -20°C, 22 GHz

At 22 GHz, improved performance is obtained primarily by the higher concentration of energy that can be achieved in the ice layer and the consequently higher attenuation constant. A comparison of TE_1 mode power density at 2.45 GHz (where all data was taken) with that at 22 GHz is presented in Figure 5 for the same incident power and the same ice layer. The area under each curve represents the incident power (power launched into wave guide) and is the same for all curves. Figure 5 illustrates that the power density $:_i$ in the ice layer at 22 GHz is approximately nine times that achieved at 2.45 GHz. This is the reason for the order of magnitude increase in the attenuation constants illustrated by Figures 2 and 3. Figure 5 also illustrates the rapid increase in power density as a function of ice thickness and the migration of the peak power density into the ice layer. This shows up as a rapid increase of the attenuation constant as a function of ice thickness illustrated in Figure 3.

MULTILAYER MODEL SURFACE WAVEGUIDE

Static ice shed tests were run on a variety of two-layer and three-layer surface waveguide models These model types are shown in Figure 6. (Tests 50 to 59, 78 to 112 and 127 to 149 are three-layer tests, remaining tests were all two-layer.) The third layer was introduced to provide enhanced sand and rain erosion resistance and increased lossiness to speed up the shedding of low-loss ice. It is visualized that surface waveguide deicers or anti-icers may be constructed from two or three layers or combinations thereof.

Tests were performed on two types of lossy third layers:

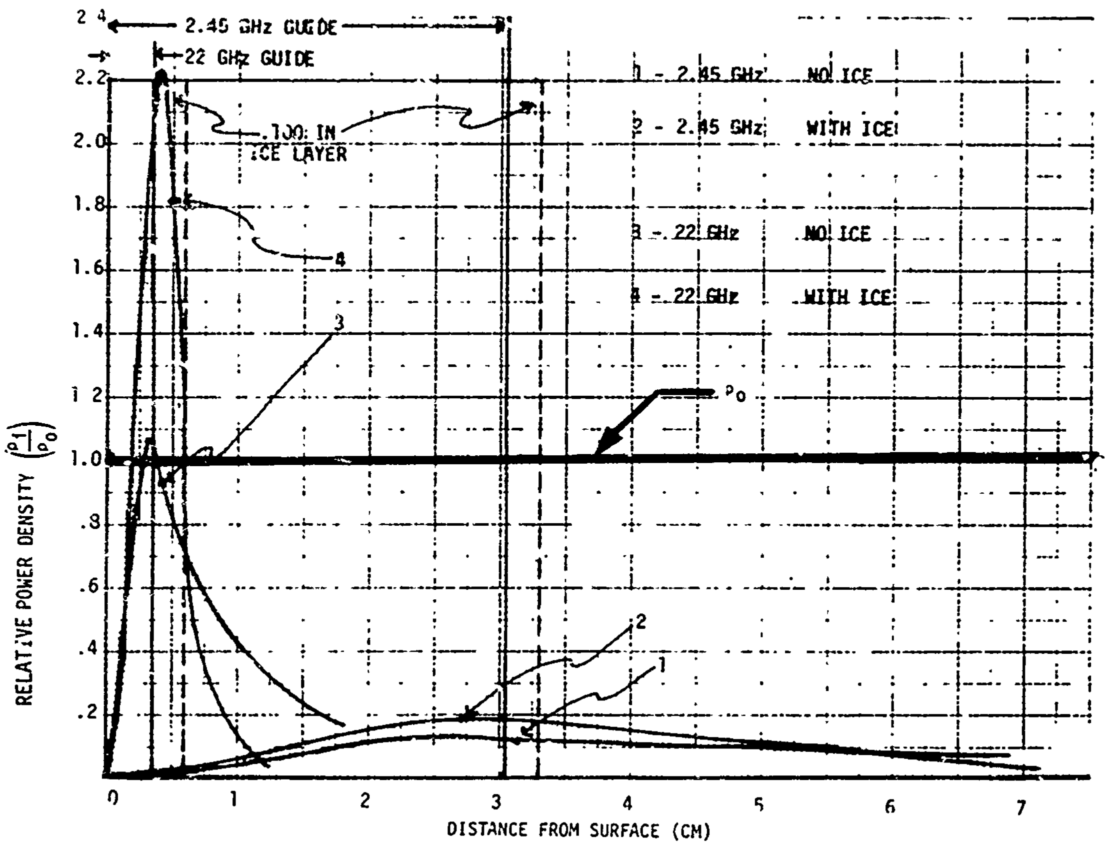

Figure 5. TE_1 mode Power Density Versus Distance From Surface, 2.45 GHz and 22 GHz

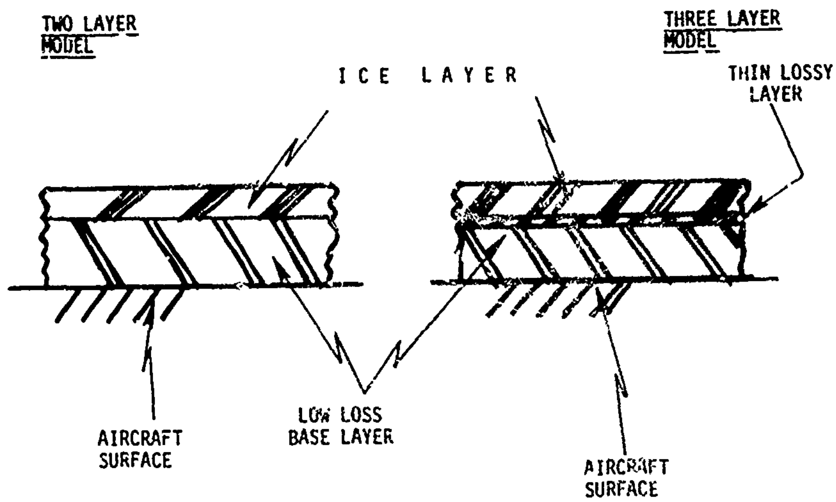

Figure 6. Two- and Three-Layer Models

1) Polyurethane erosion strips, 0.025-in. thick, which also show promise of high sand and rain erosion resistance.

2) Resistive-strip loss layers whose loss characteristics could be readily adjusted for experimental purposes to establish the effects of the variable loss on ice shed characteristics, these strips would be embedded below dielectric erosion strips for protection from sand and rain erosion.

Polyurethane Third Layers Tests

Test on three-layer surface waveguide models using 0.025-in. polyurethane erosion strips were conducted, (tests 140 to 149, Appendix A), the results of these tests are summarized in Figure 1 at -2[illegible]°C, illustrating shed time as a function of surface wave power for distilled water ice. The polyurethane erosion strips came with their own adhesive. However, the adhesive proved to be far more lossy at 2.45 GHz than the polyurethane itself and began to melt during the initial tests (tests 140 to 143, Appendix A). The data of Figure 1 for polyurethane erosion strips were obtained with the adhesive removed and the polyurethane taped in place (tests 144 and 149). Thus for microwave deicer service, a low-loss adhesive must be used or the polyurethane erosion coat must be applied as a liquid or a paint.

Variable-Resistivity Third Layer Tests

Third layer tests were run utilizing strips of variable resistivity. Variable resistivity strips, when used under a thin, low-loss erosion strip, can be used to control the surface guide's attenuation constant, offering the possibility of tailoring the attenuation constant to any desirable value. These strips are available commercially in a wide variety of standard resistivities, ranging from 25 ohms per square to 1000 ohms per square. Each consists of a vapor-deposited, molecular-thin pure-metal film on a 5-mil MYLAR (Polyethylene) or Kapton substrate. The metal film can be deposited directly underneath a polyethylene or polyurythane erosion strip to control the attenuation constant of the deicer as a function of blade radius.

Tests 127 to 139 were performed utilizing 300-ohm-per-square mylar strips in which attenuation constants 0.08 to 0.07 db/inch were obtained. These tapes were held in place by ten-mil low-loss tape and the ice samples on top. Exceptionally clean and rapid ice shedding (tests 127 to 139, Appendix A) were obtained and results were summarized in Figure 1, where they are compared to the polyurythane shedding tests.

COMPARISON OF THE SHEDDING EFFECTIVENESS OF THE TE_1 AND THE TM_0 MODES

Figure 1 shows shed time data for the TE_1 and the TM_0 modes (for identical 0.6% salt samples) that shows that the TE_1 mode is more effective since it takes less time to shed for the same incident power. These data further support theoretical predictions of shedding effectiveness based upon the calculated values of the attenuation constants for the TE_1 and the TM_0 modes. The TE_1 mode attenuation is always larger than the TM_0 mode, as illustrated in Figure 7.

The TM_0 mode is of practical interest, however, since it allows use of thinner surface waveguides than will the TE_1 mode at the same operating frequencies. Even though

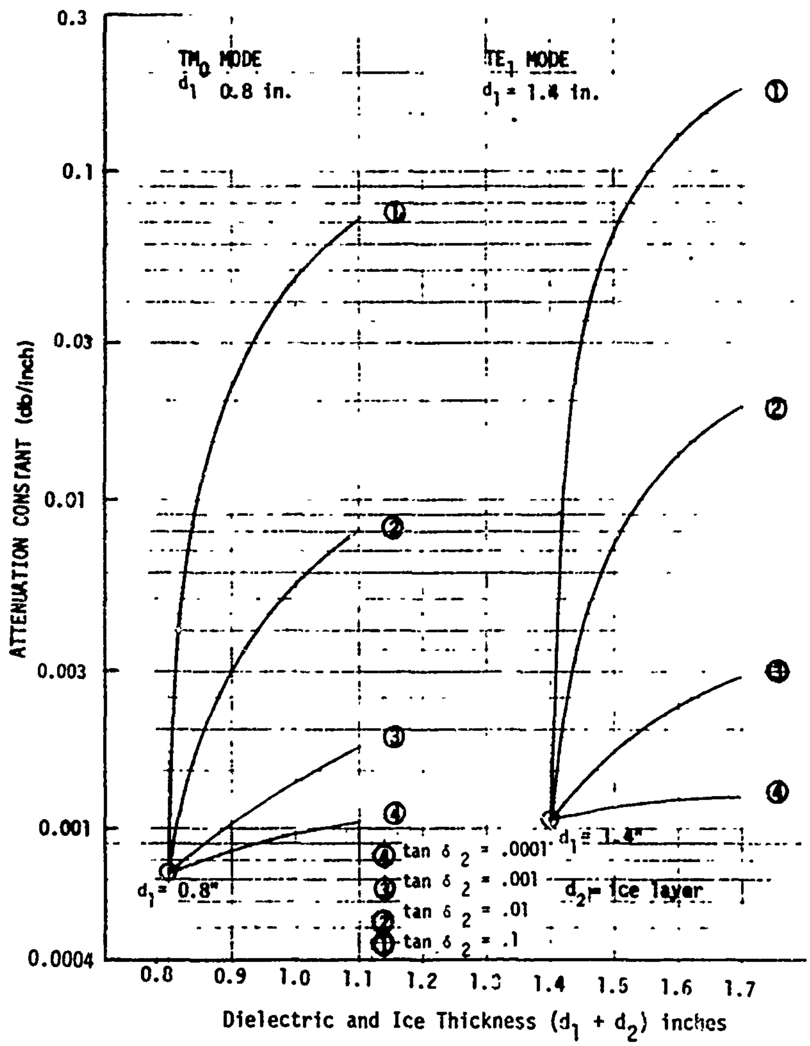

Figure 7. Attenuation Constant Versus Ice Thickness at 2.45 GHz

the TE_1 mode is more effective, the TM_0 mode still produces clean shedding, and in situations where waveguide thickness becomes the limiting consideration, the TM_0 mode might be considered for deicing purposes.

SHEDDING TIME AS A FUNCTION OF TEMPERATURE

While helicopter specifications require deicer performance down to an ambient temperature of -20°C the aerodyanmic heating of the blade will cause its temperature to be higher.

Shed data illustrated in Figure 1 was taken at blade temperatures between -17°C and -20°C. The effects of increased blade temperature due to aerodynamic heating or any other reason are illustrated in Figure 8, which was plotted from data obtained in tests 78 to 112, Appendix A. As shown, shed time is drastically reduced for the same incident power as the ambient temperature is increased, or alternately, the power required is reduced for the same shed time.

EXPERIMENTAL PROCEDURES

Figure 9 is a schematic of the setup for performing the ice shed tests. Figure 9 also shows the ice loading to simulate various centrifugal force fields. It became clear early in the tests that this method of simulating the centrifugal force field was only satisfactory for small ice elements, not exceeding about 3 inches in length and 2 inches in width. This limited most of the tests to samples not exceeding 3 inches.

When longer samples were used, those portions of the ice closest to the wave launcher (which are the first

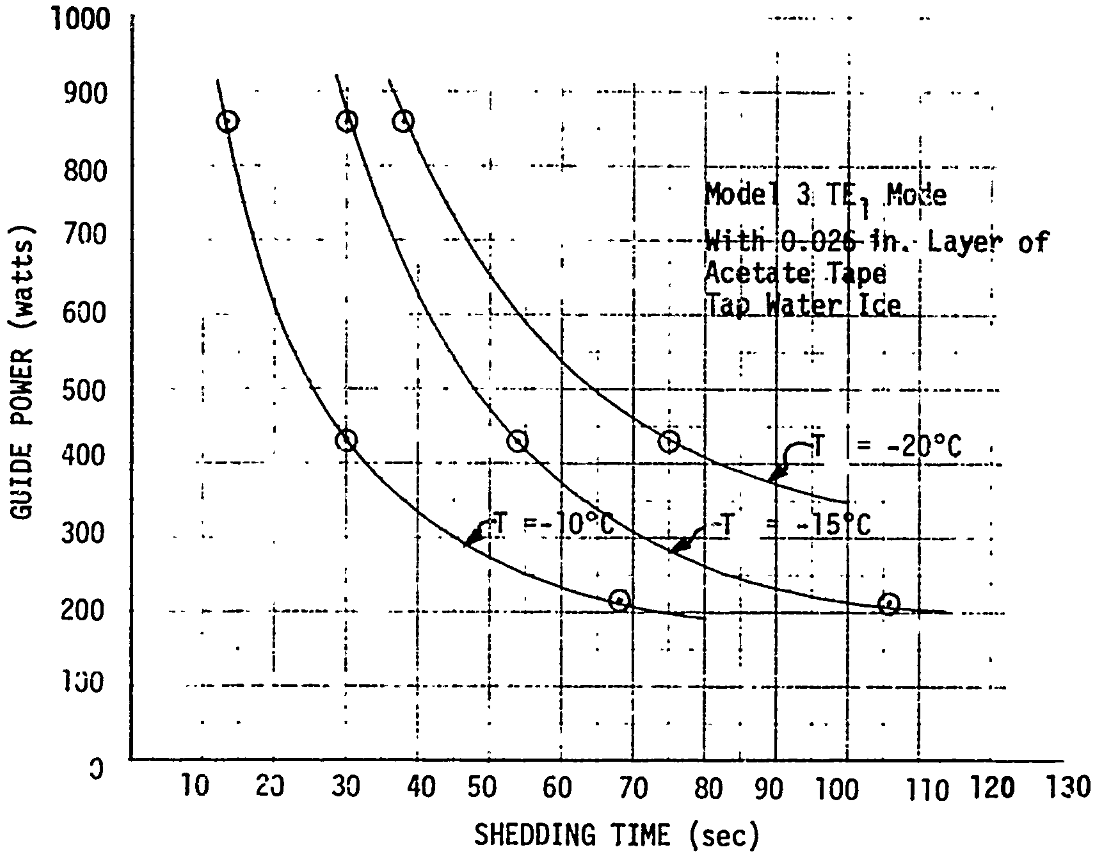

Figure 8. Effect of Blade Temperature on Shed Time

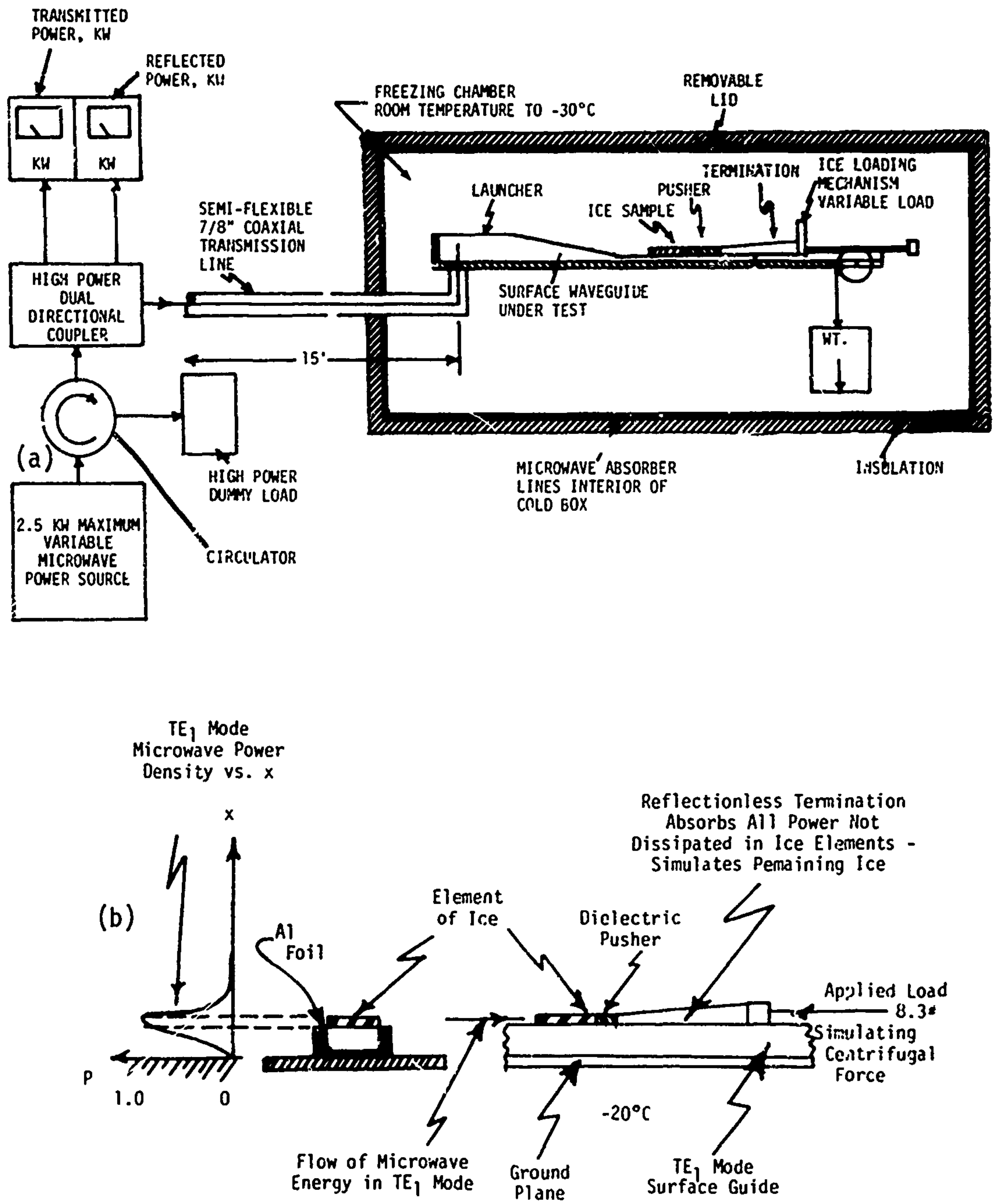

Figure 9. Test Equipment for Performing Static Ice Shed Tests

to be subjected to microwave heating and the first to be elevated to the shed temperature) were not removed from the surface waveguide by the simulated centrifugal load because this load was held in place by ice elements further down the waveguide that had not yet reached their shed temperature, thus preventing the shed force from traveling to the early elements of ice. This obviously is a poor simulation of conditions on a real rotor blade where all elements of the ice are simultaneously subjected to the centrifugal shear force.

Two types of microwave loads were used to terminate the surface waveguide: a totally reflecting plate and a reflectionless load. The force from the ice loading mechanism was transferred to the ice sample through the microwave termination (which was free to slide) and a dielectric pusher placed between the termination and the ice sample, as shown in Figure 9. The dielectric pusher, having approximately the same thickness and dielectric properties as the ice sample, is also a simulation of an additional length of the ice. The reflectionless load was replaced in some tests by the totally reflecting plate, which reflects essentially all energy, giving the wave an opportunity to make two passes through the ice sample. Under these conditions, the only thing supporting the weight of the loading mechanism was the adhesion strength of the bond between the ice and the surface waveguide. When this bond is broken by microwave energy the weight is free to fall, indicating that the ice has shed. The shed time was then measured as the time between the application of microwave energy and the instant that the weight fell.

The weight simulating the centrifugal force field was adjusted to be equivalent to that encountered by a similar ice sample at approximately 100 inches from the rotor hub. The simulated centrifugal forces used are tabulated in Appendix A.

The low power reflectionless load used for all low power tests consisted of a long taper (10-inches) of very lossy dielectric material which was placed on top of the surface waveguide and absorbed all incident microwave power in the surface wave, converting it to heat. For high power shed tests a water load was constructed which consisted of a long (10-inch) tapered block of low-loss polyethelene into which was drilled two intersecting round channels forming a long V, with the point of the V facing in the direction of the incident surface wave. Tap water was allowed to flow continuously through the V shaped channel absorbing most of the microwave energy in the surface wave, converting it to heat which was then carried off by the water flow.

SECTION 2
VERIFICATION OF SURFACE WAVEGUIDE THEORY

The theory of surface waveguides for use in microwave ice protection and significant parameters describing their performance were presented in the feasibility analysis, Reference 1. The performance parameters are listed below:

1. Guide Wavelength λ_g
2. Phase Constant β
3. Attenuation Constant α
4. External Eigenvalue K_x
5. Internal Eigenvalue k_x

Techniques for their prediction and measurement, given the surface waveguide dimensions and the operating frequency, were established in the feasibility analysis, Reference 1, Appendix A. In the present program, these parameters were measured and compared to theoretical values, for the purpose of verifying the theory. A summary of all measured and theoretical values of the parameters listed above appear in Figures 10 through 17. These data clearly verify theoretical values.

The significance of these comparisons is that surface waves, propagating in either the TE_1 o the TM_0 mode, behave essentially in the manner predicted in the feasibility analysis and that surface waves can be guided by dielectric materials such as ultra high molecular weight polyethelene (UHMWPE), that have been demonstrated to also

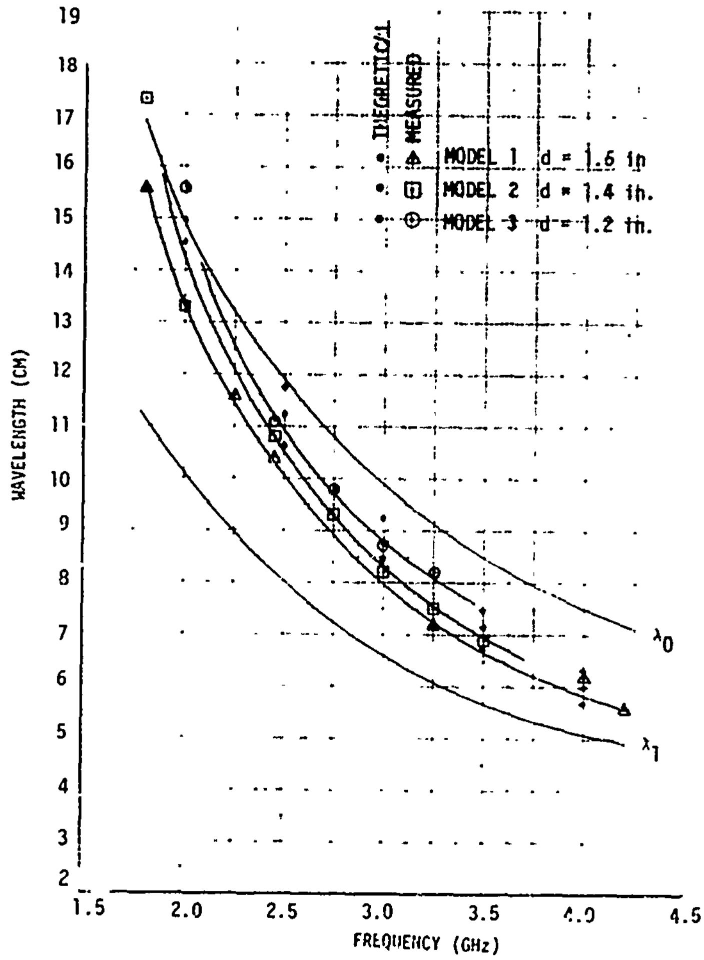

Figure 10. Comparison of Computed With Measured Guide Wavelength for TE_1 Mode

THIS PAGE IS BEST QUALITY PRACTICABLE
FROM COPY FURNISHED TO DDC

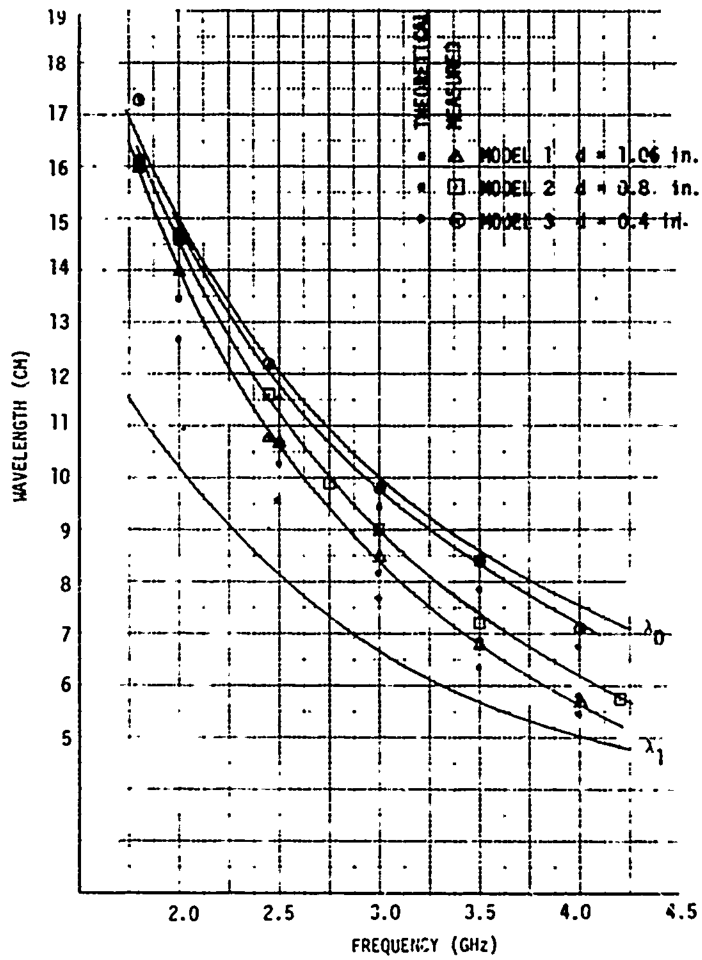

Figure 11. Comparison of Computed and Measured Guide Wavelength, TM_0 Mode

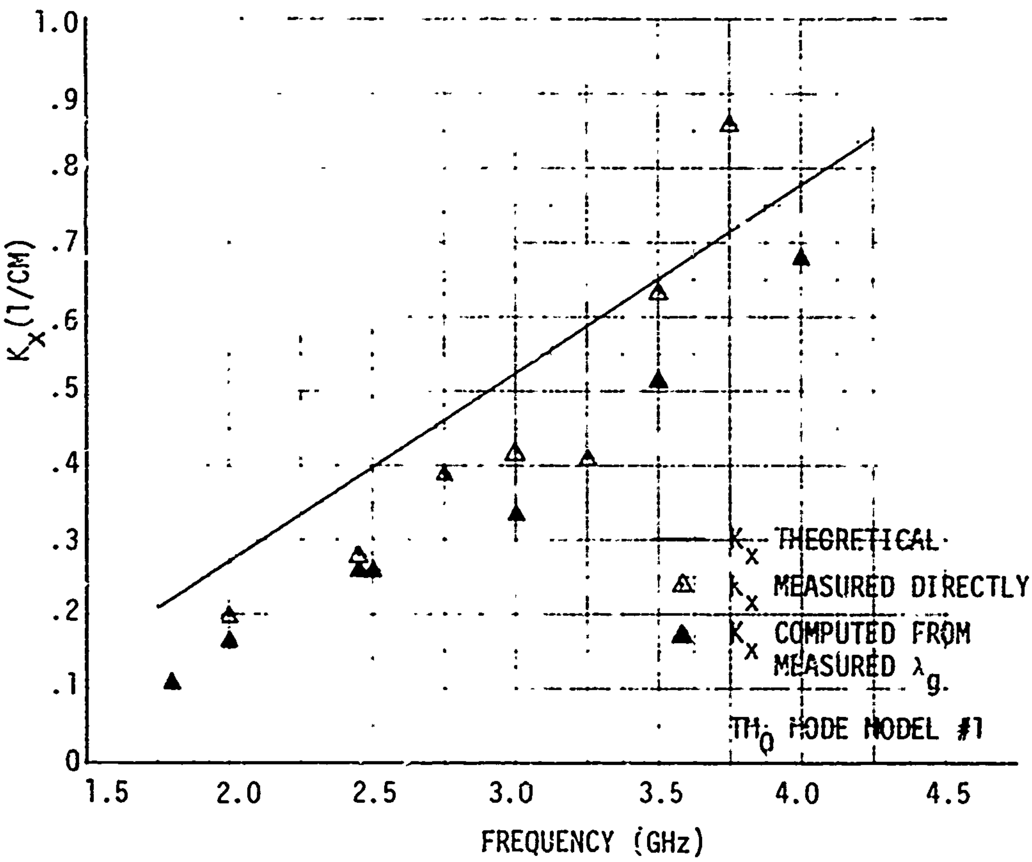

Figure 12. Comparison of Theoretical With Measured External Eigenvalue, TM_0 Mode

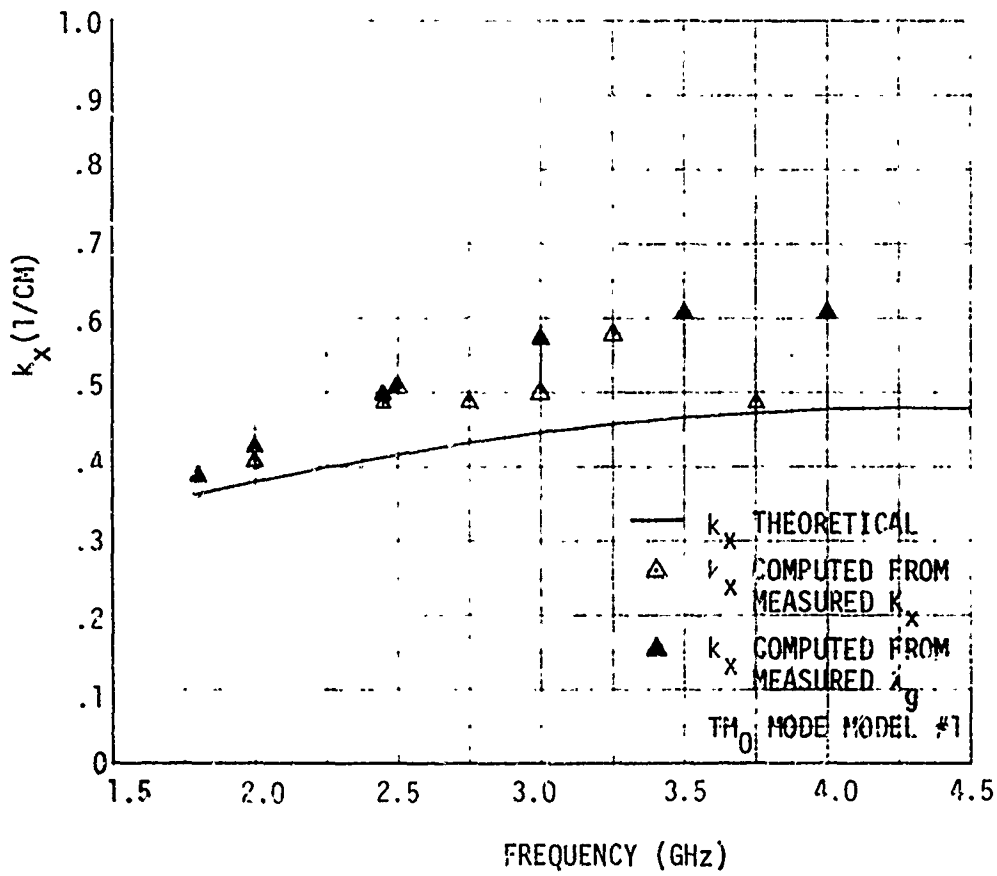

Figure 13. Comparison of Theoretical With Measured Internal Eigenvalue, TM_0 Mode

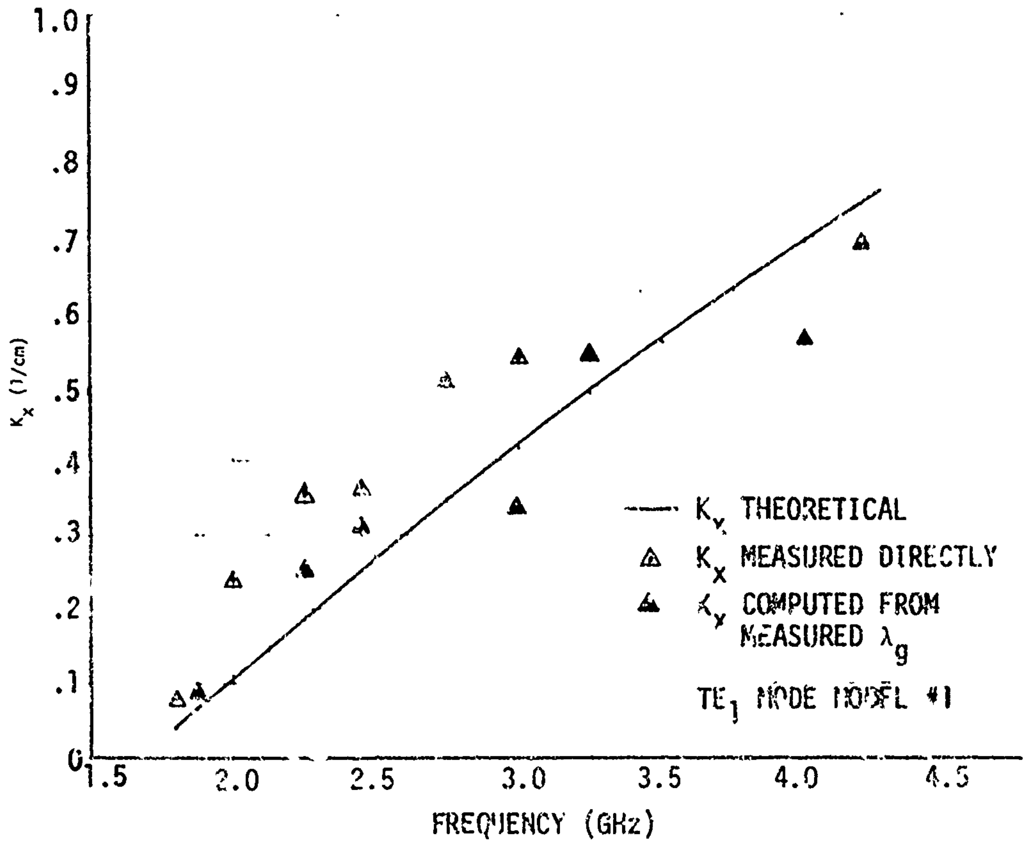

Figure 14. Comparison of Theoretical With Measured External Eigenvalue, TE_1 Mode

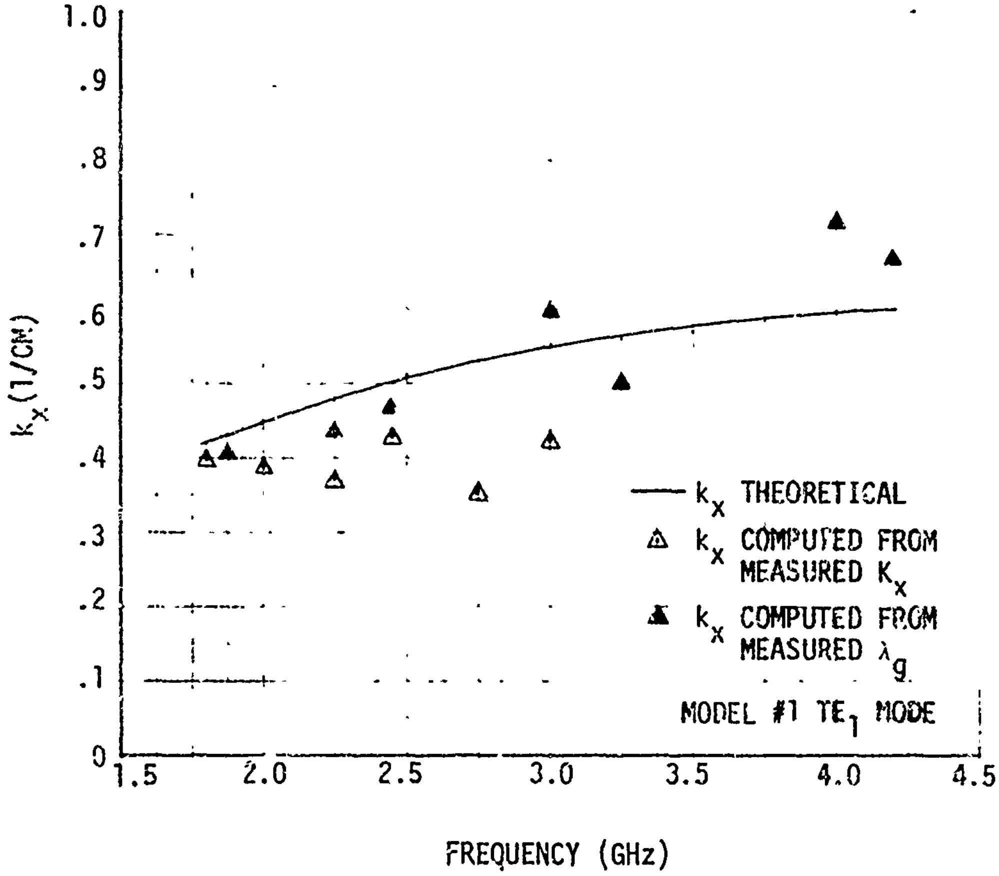

Figure 15. Comparison of Theoretical With Measured Internal Eigenvalue, TE_1 Mode

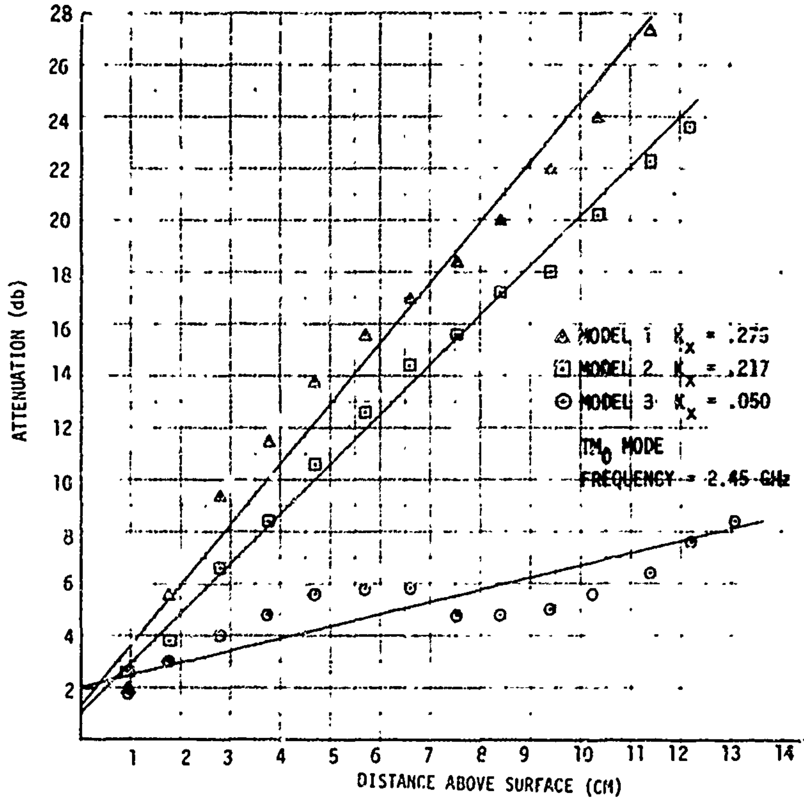

Figure 16. Attenuation as a Function of Distance Above Surface

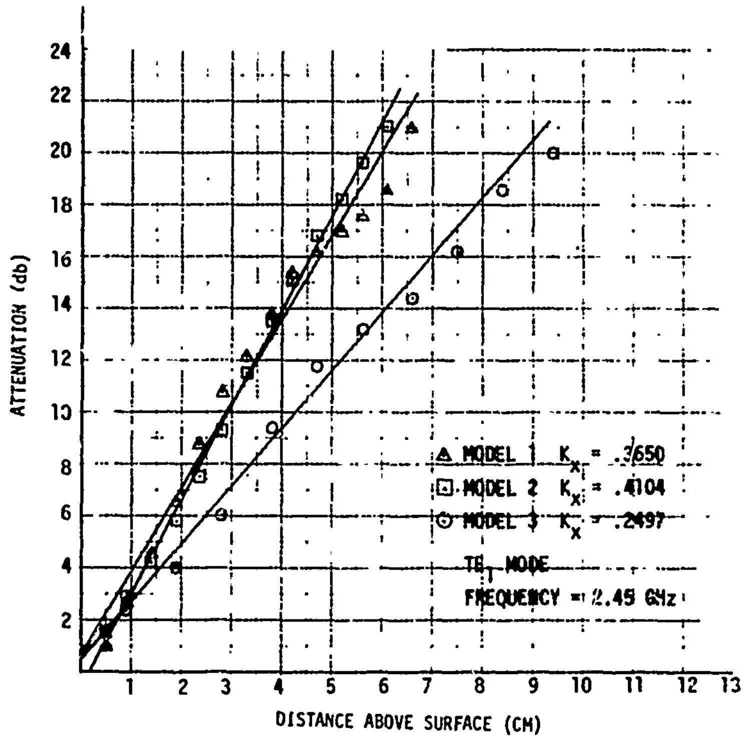

Figure 17. Attenuation as a Function of Distance Above Surface

offer high resistances to sand and rain erosion (Reference 8). It has been demonstrated that microwave energy exists in the air region immediately adjacent to the rotor blade and in the dielectric coating (surface waveguide) lining the blade, in a wave that propagates along the length of the blade. The power density being carried by the wave, as a function of distance above the blade, is numerically established by substituting the internal and external eignvalues, k_x and K_x (Figures 12 to 15), into equations A-72,74-88 and 90 of Reference 1. From this it can be seen that power density in the air region decays exponentially with distance from the surface.

EXPERIMENTAL PROCEDURES

Experiments were carried out on six scale-model surface waveguides in the 2- to 4-GHz band. Three of the models of varying thicknesses were used to verify the performance of the TE_1 mode (Figure 18), while the remaining three were used to verify performance of the TM_0 mode (Figure 19). After verification of the theory, these same models were used in the static ice shed tests discussed in Section 1. The theory presented in Reference 1, can be used to predict surface waveguide performance at any frequency; however, three frequencies were identified in Reference 1 for use in microwave ice protection. These are 2.45 GHz, 5.85 GHz, and 22.125 GHz. Measurements in this program were carried out in the 2 to 4 GHz bands. While

---

[8] Head, Robert E., Erosion Protection for the AH-1G Low Radar Cross-Section Main Rotor Blade, Volume I - Sand Rain Erosion Evaluation, Hughes Helicopters, USAAMRDL-TR-76-40A, Eustis Directorate, U.S. Army Air Mobility Research and Development Laboratory, Fort Eustis, Virginia, January 1977, AD A035961.

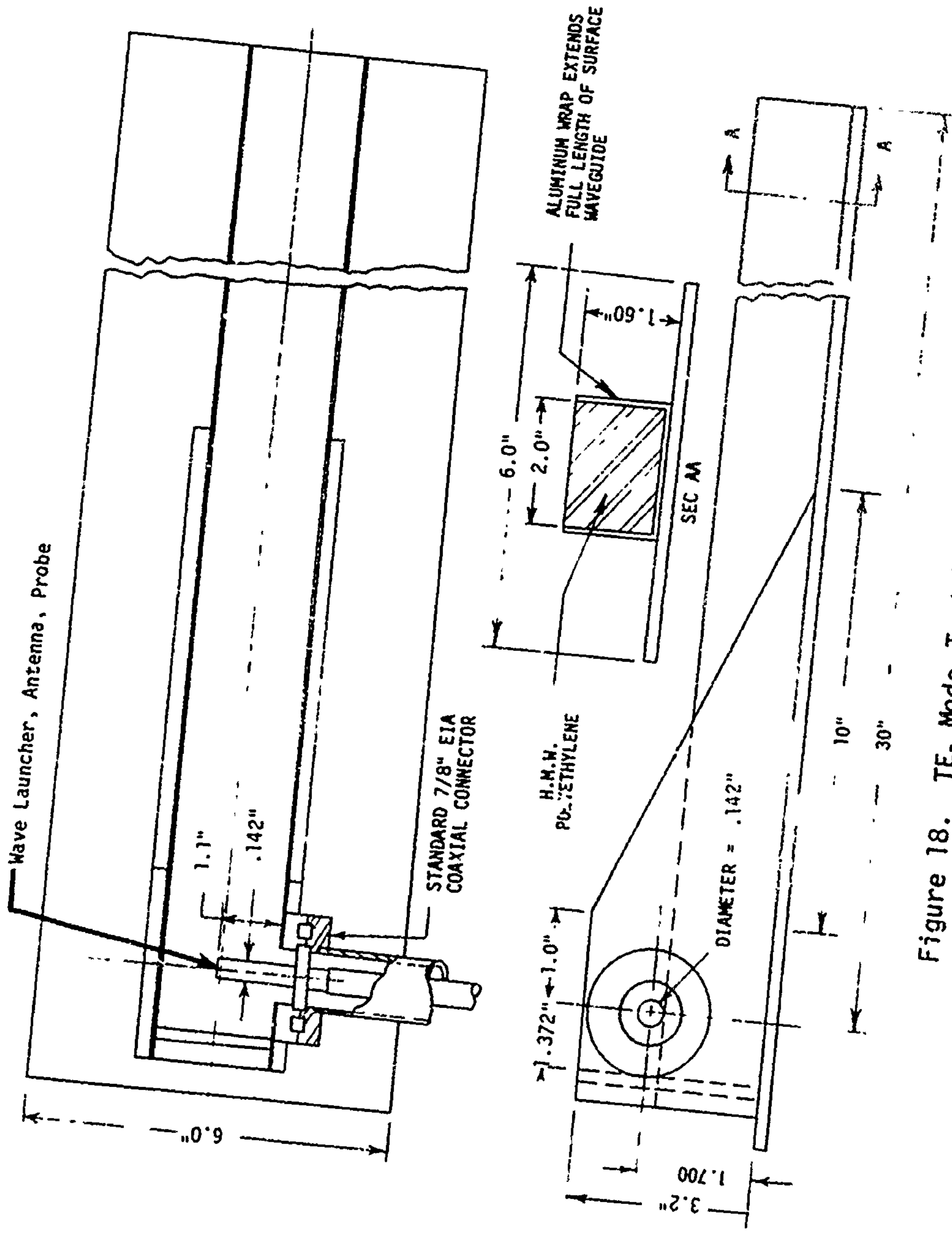

Figure 18. TE_1 Mode Test Model No. 1

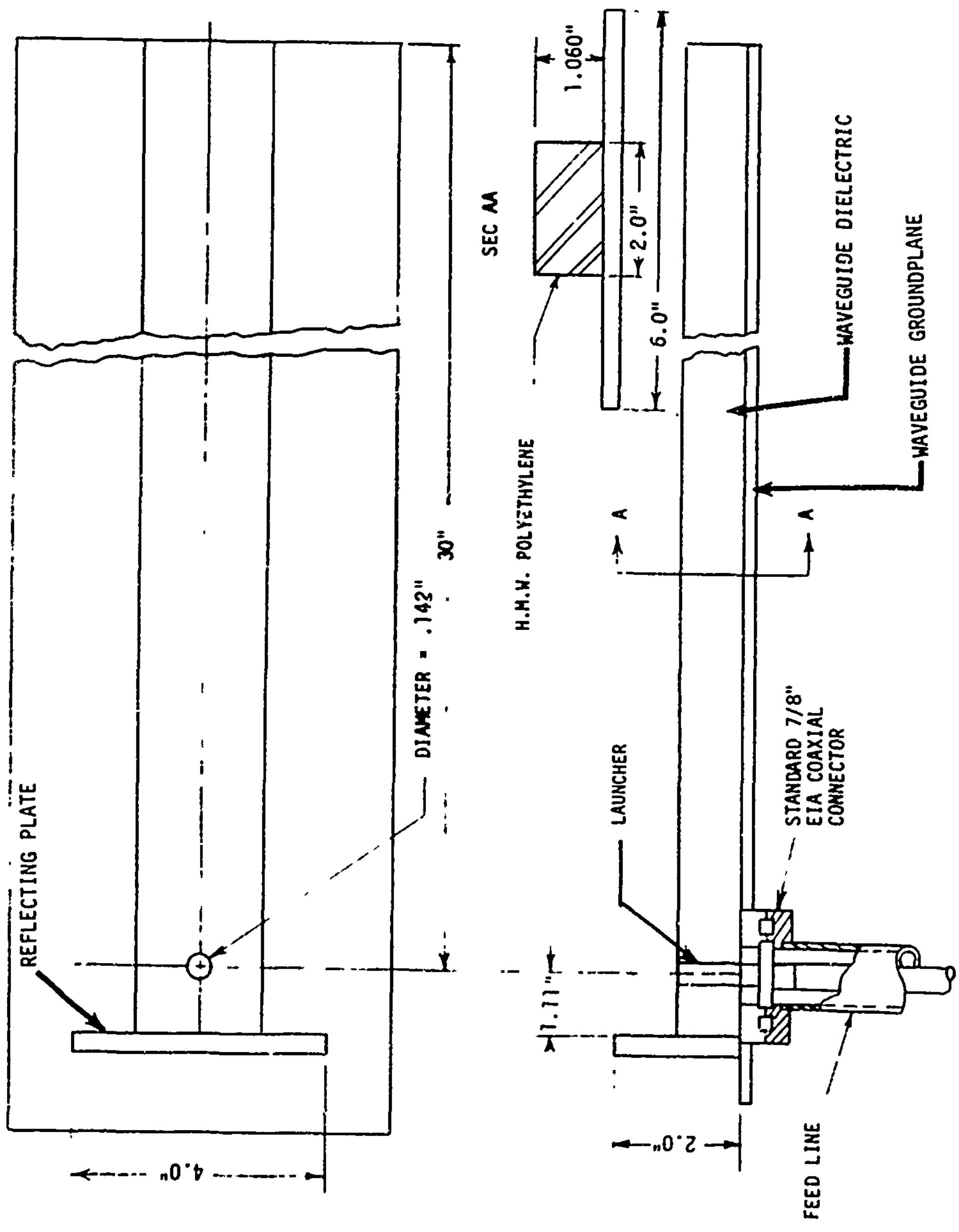

Figure 19. TM_0 Mode Test Model No. 1

the experimental surface waveguides are dimensioned for operation and measurement in the 2 to 4 GHz band, they also represent scale models for the same devices at 5.85 and 22.125 GHz, scaled in proportion to wavelength using the following scaling equations:

$$\frac{d}{\lambda} = \frac{d'}{\lambda'} \tag{4}$$

where: d = Physical dimension of test article on which measurements are performed

λ = Measurement wavelength

d' = Design dimension

λ' = Design wavelength

Equation 4 may be written for convenience as

$$\frac{d}{d'} = \frac{\lambda}{\lambda'} = \frac{f'}{f} \tag{5}$$

where: f = Measurement frequency

f' = Design frequency

Using these equations the following dimensional ratios were established:

Measurement Frequency MHz	2450	2450	2450
Design Frequency MHz	2450	5850	22,125
Scaling Ratio $\frac{d}{d'}$ =	1.00	2.388	9.031

This means that a 1-inch dimension at 2.45 GHz is equivalent to a (0.418) -inch dimension at 5.85 GHz and (0.111 -inch dimension at 22.125 GHz, (in any direction).

Thus, the actual test articles, operated at 2.45 GHz, appear much thicker than their true size at the design frequency.

Equivalent thicknesses at the scaled frequencies are given below:

EQUIVALENT SURFACE WAVEGUIDE THICKNESSES FOR THE TM_0 MODE WITH MEASUREMENTS PERFORMED AT 2.45 GHz

THICKNESS AT MEASUREMENT FREQUENCY 2.45 GHz (in.)	EQUIVALENT THICKNESS AT DESIGN FREQUENCY 5.85 GHz (in.)	EQUIVALENT THICKNESS AT DESIGN FREQUENCY 22.125 GHz (in.)
0.1	0.041	0.0111
0.2	0.0837	0.0221
0.4	0.1670	0.0442
0.8	0.335	0.0886
1.0	0.418	0.1110

The TE_1 mode must have a minimum thickness surface guide to permit propagation. This cutoff thickness is established from Equation 6 and is further explained in Appendix A, Reference 1.

$$f_c = \frac{Nc}{2(2d)\sqrt{\varepsilon_1 - \varepsilon}} \qquad (6)$$

f_c = cutoff frequency

where: N = 0,2,4,6,... for even modes

N = 1,3,5,7,... for odd modes

ε_1 = Relative dielectric constant of surface guide - 2.2 for UHMWPE

ε_2 = 1 = Relative dielectric constant of air

d = Thickness of surface guide

c = Speed of light = 2.9979×10^{10} $\frac{cm}{sec}$

Surface guides of various thicknesses were fabricated for the TE_1 mode. Equivalent thicknesses at the scaled frequencies are given below.

EQUIVALENT SURFACE WAVEGUIDE
THICKNESSES FOR THE TE_1 MODE WITH

MEASUREMENTS PERFORMED AT 2.45 GHz ε_1 = 2 2 (UHMWPE)

THICKNESS AT MEASUREMENT FREQUENCY 2.45 GHz inches	EQUIVALENT THICKNESS AT DESIGN FREQUENCY 5.85 GHz inches	EQUIVALENT THICKNESS AT DESIGN FREQUENCY 22.125 GHz inches
1.099*	.4605*	.1217*
1.100	.4606	.122
1.200	.503	.133
1.400	.586	.155
1.600	.670	.177
2.000	.8375	.2214

*cutoff thickness

A schematic of the experimental setup used for measuring surface waveguide performance is shown in Figure 20. Photographs of the test set up are presented in Figures 21 and 22.

The x-z positioning mechanism (Figure 20) was specially designed and fabricated for this program. It permitted probing the electric field intensity in the air region immediately adjacent to the surface waveguide. It is used to measure all significant performance parameters required.

The test equipment was all commercially available equipment capable of operating in the 2-to 4-GHz band.

Measurement of External Eigenvalue, K_x

Eigenvalues were measured by the technique outlined in Reference 1, Appendix D, Figure D-2. The electric field intensity was measured as a function of distance x above the surface waveguide with the x-z positioning mechanism and probe. Graphs of these measurements in decibels relative to the intensity value near the surface are shown in Figures 16 and 17 for the TE_1 and the TM_0 modes respectively. These graphs should be straight lines (indicating exponential decay), the slopes of which are the desired eigenvalues.

For the TE_1 mode attenuation is linear with only a minor periodic error as shown in Figure 17. The TM_0 mode produces a much larger periodic error from a straight line, but nevertheless, the linear trend is evident as shown in Figure 16. The periodic errors are due to interference patterns created between the desired mode and the undesired radiation component of the wave launcher. The external fields of the TM_0 mode are weaker than the corresponding fields for the TE_1 mode so that the unwanted interferring field has a relatively larger effect. Models used in the measurements were only 30 inches long. Consequently, measurement could only be made in the vicinity of the launcher. The interferring effects of the radiated components will

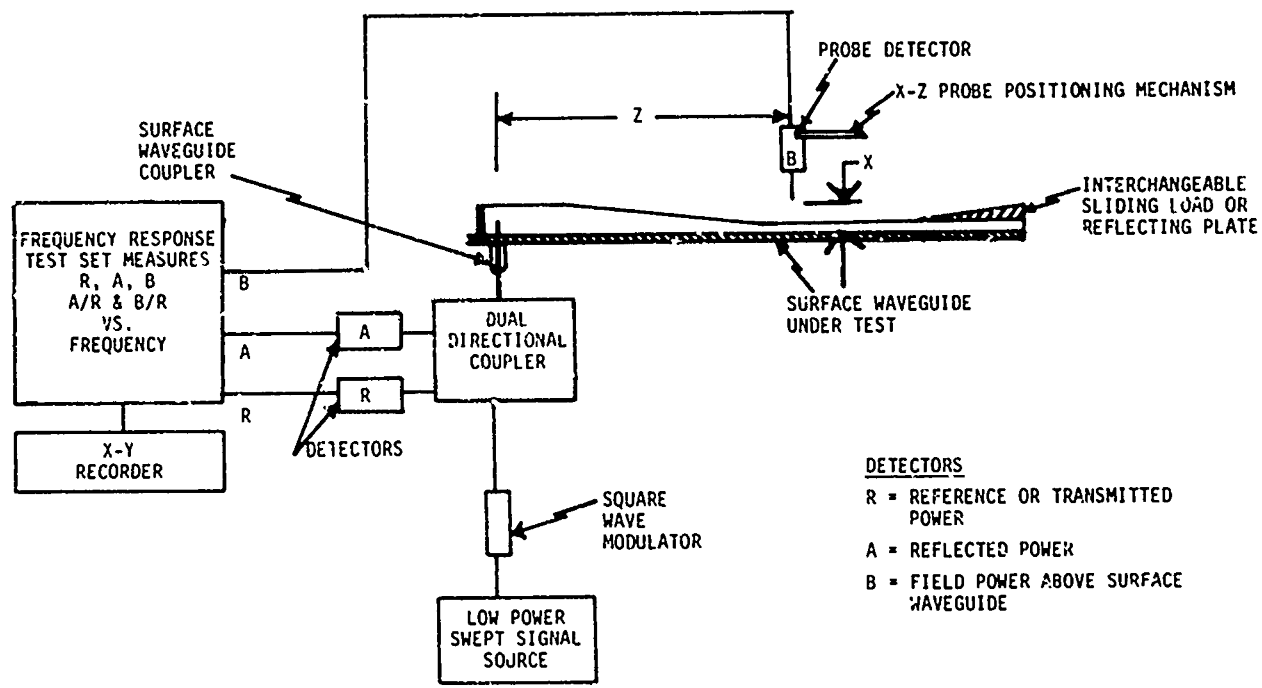

Figure 20. Test Equipment for Measuring Surface Waveguide Performance - Low-Power Configuration for Bench or Cold Chamber

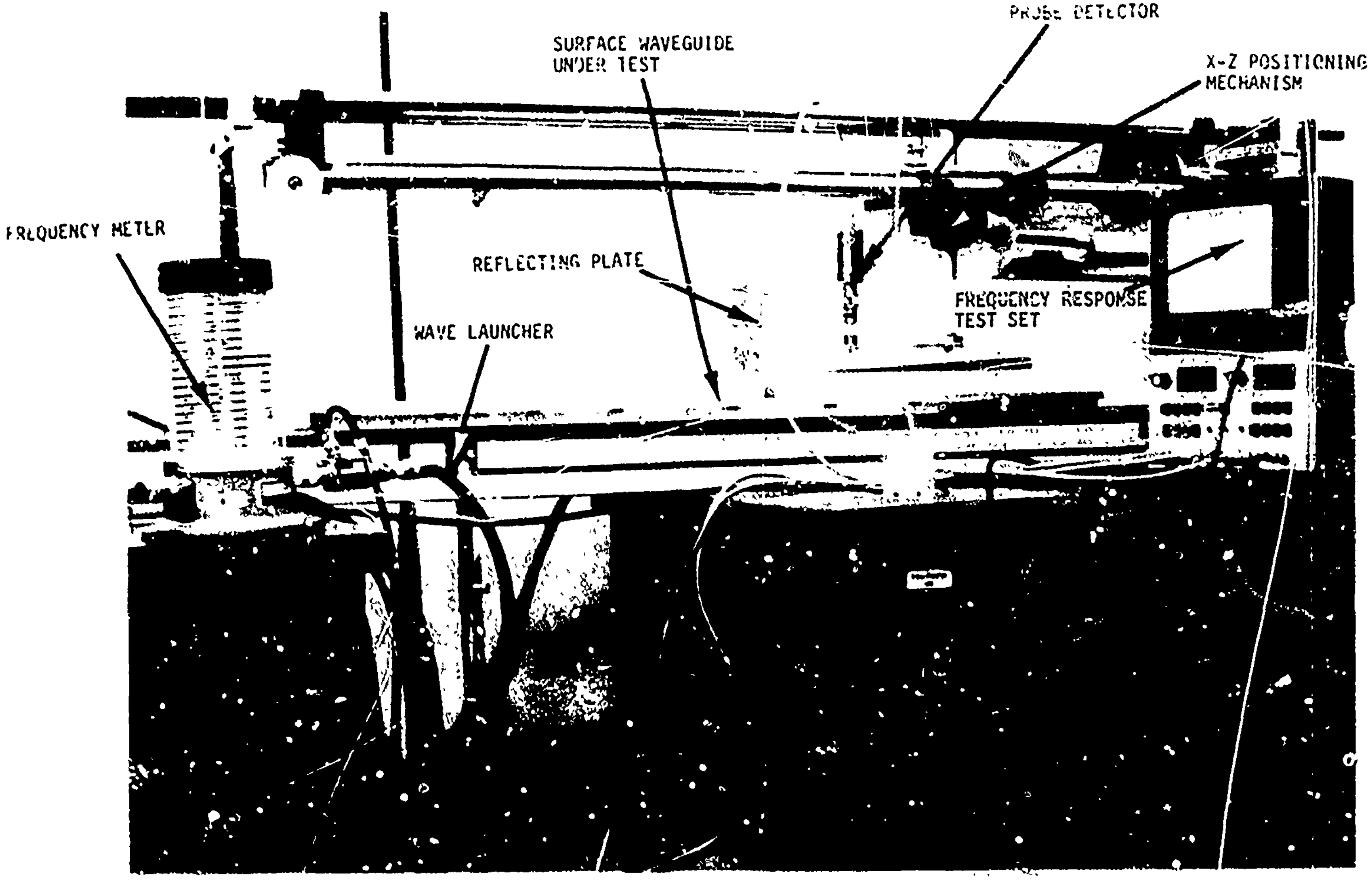

Figure 21. Experimental Set-Up for Measuring Surface Waveguide Performance

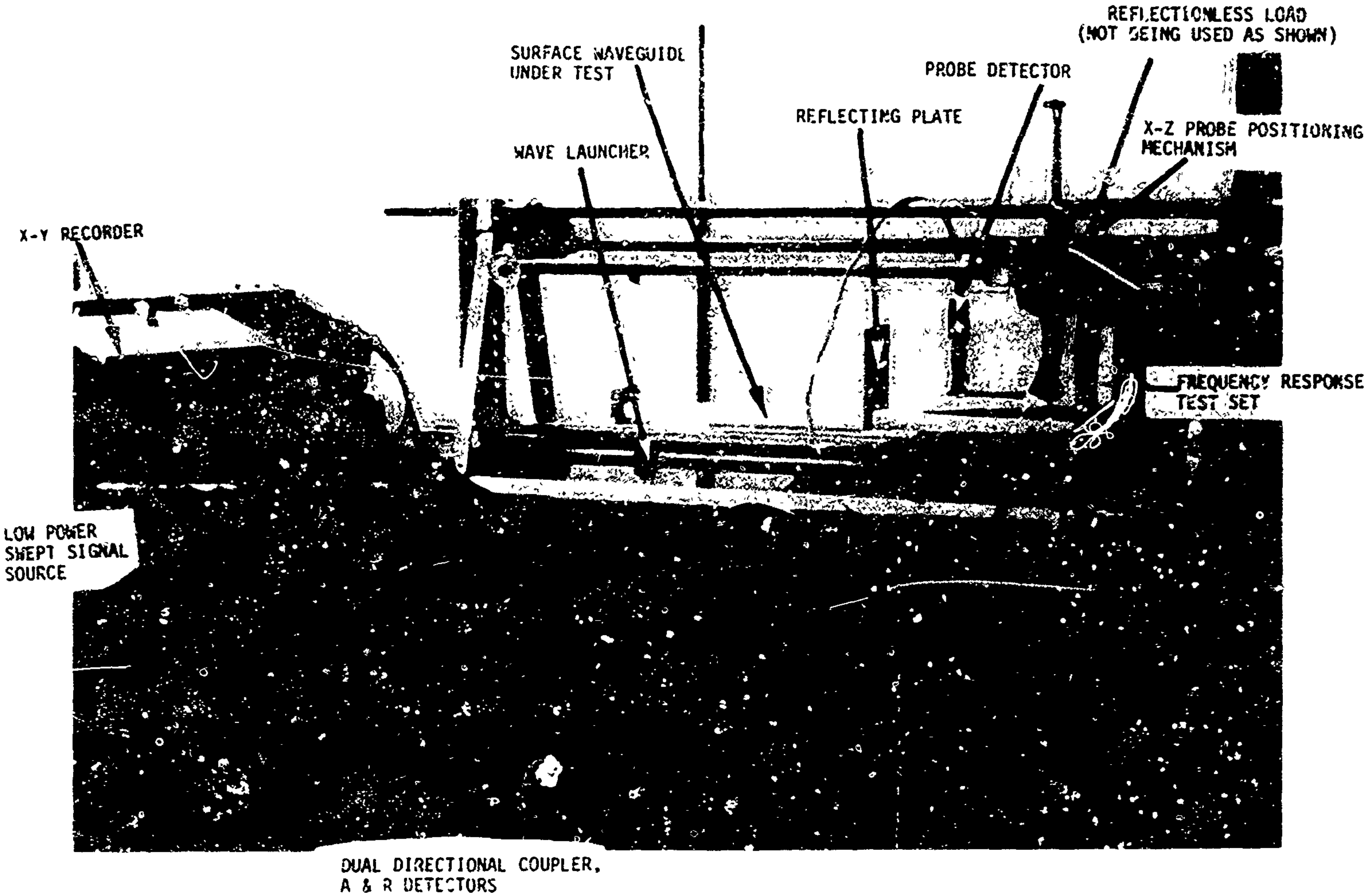

Figure 22. Experimental Set-Up for Measuring Surface Waveguide Performance

decrease if longer models are used.

The straight lines of Figures 16 and 17 were established using the linear least-square method of approximation and were used to determine the external eigenvalues (K_x).

The external eigenvalues were also determined indirectly by computing them from measured values of guide wavelength (λ_g).

SECTION 3
WAVE LAUNCHERS

The goal of this effort was to achieve wave launcher (coupling) efficiency necessary to demonstrate the microwave ice-protection concept. Coupling efficiencies as low as 25% would have been sufficient for this purpose. During this effort peak coupling efficiency was measured to be 68%, as illustrated in Figures 23 and 24.

Coupling techniques were studied in detail during the feasibility analysis. Two techniques emerged which appeared particularly attractive because of their simplicity and high coupling efficiency. These are the methods of Cohn, Reference 9, for the TE_1 mode and DuHamel and Duncan, Reference 10, for the TM_0 mode.

The design of the breadboard model TE_1 mode coupler is based upon experiments performed by Cohn, Reference 9, and is illustrated in Figure 18. The breadboard TM_0 mode launcher is based upon experiments performed by DuHamel and Duncan, Reference 10, and is illustrated in Figure 19. No attempt was made to optimize the coupling efficiency in this program; however, the relative ease in obtaining high coupling efficiency without a major effort lends confidence to the ability to design couplers with efficiencies in excess of 90%, as claimed by Cohn for the TE_1 mode.

If the measured data is plotted on Cohns theoretical coupling curves, Figure 25, it can be seen that while the shape of the curve is roughly in agreement with theory the magnitude of peak coupling falls short of maximum coupling.

[9] Cohn, Cassedy and Kott, "TE Mode Excitation on Dielectric Loaded Parallel Plane and Trough Waveguides," IRE Transactions on Microwave Theory and Techniques, pp. 545-552, September 1960.

[10] DuHamel, R.H. and Duncan, J.W., "Launching Efficiency of Wires and Slots for a Dielectric Rod Waveguide," IRE Transactions of Microwave Theory and Techniques, July 1958.

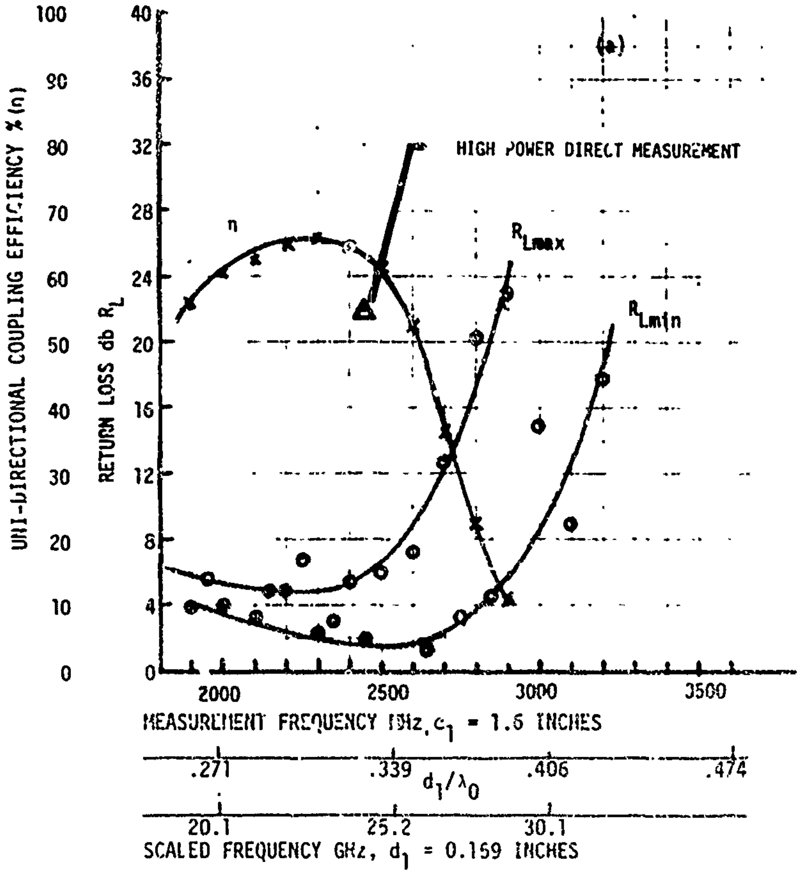

(a) Measured Coupling Efficiency Versus Frequency

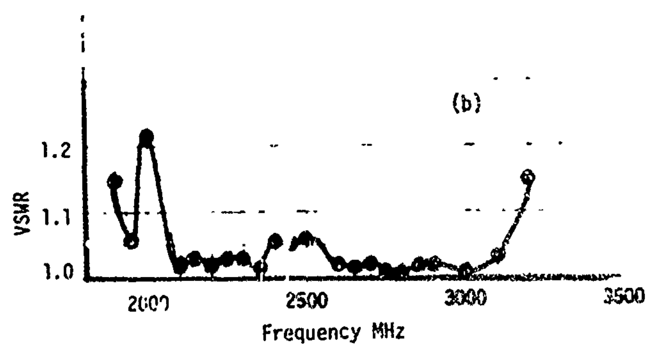

(b) Voltage Standing Wave Ratio Versus Frequency for TE_1 Mode, Test Model No. 1, d_1 = 1.6", ϵ_1 = 2.2

Figure 23. Coupling Performance

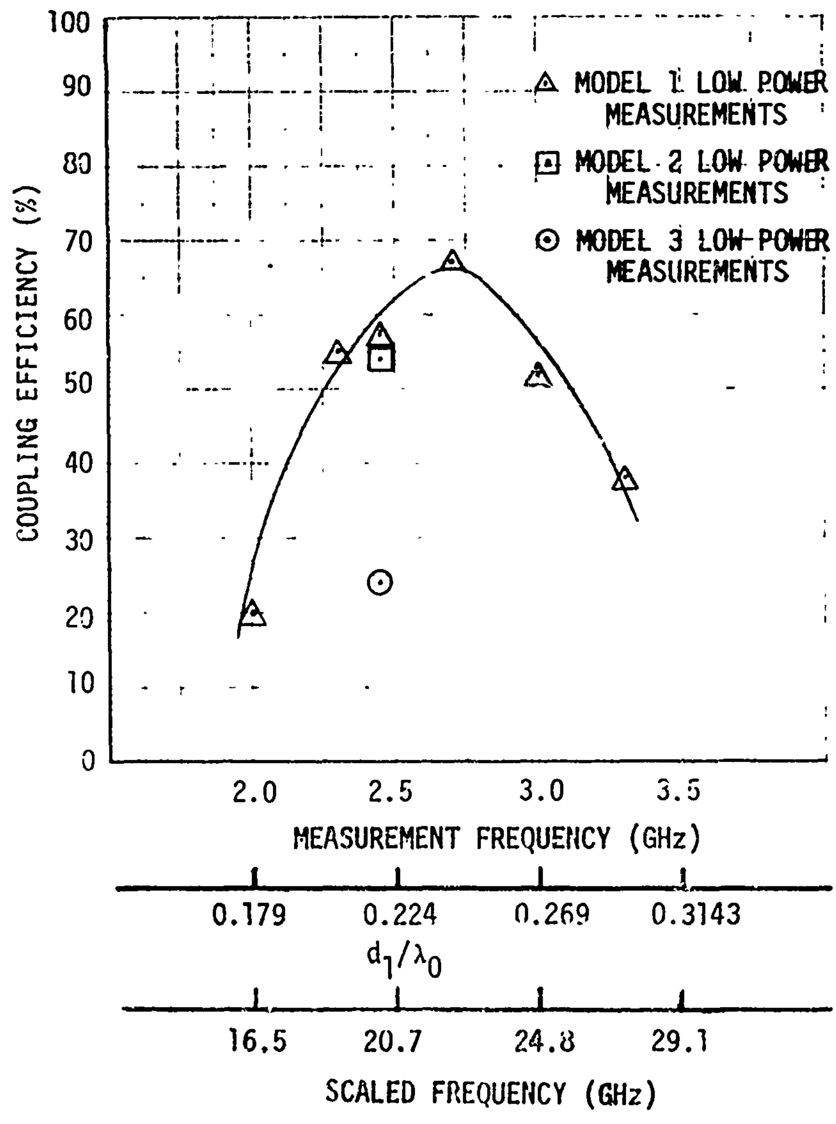

Figure 24. Coupling Efficiency Versus Frequency, TM_0 Mode

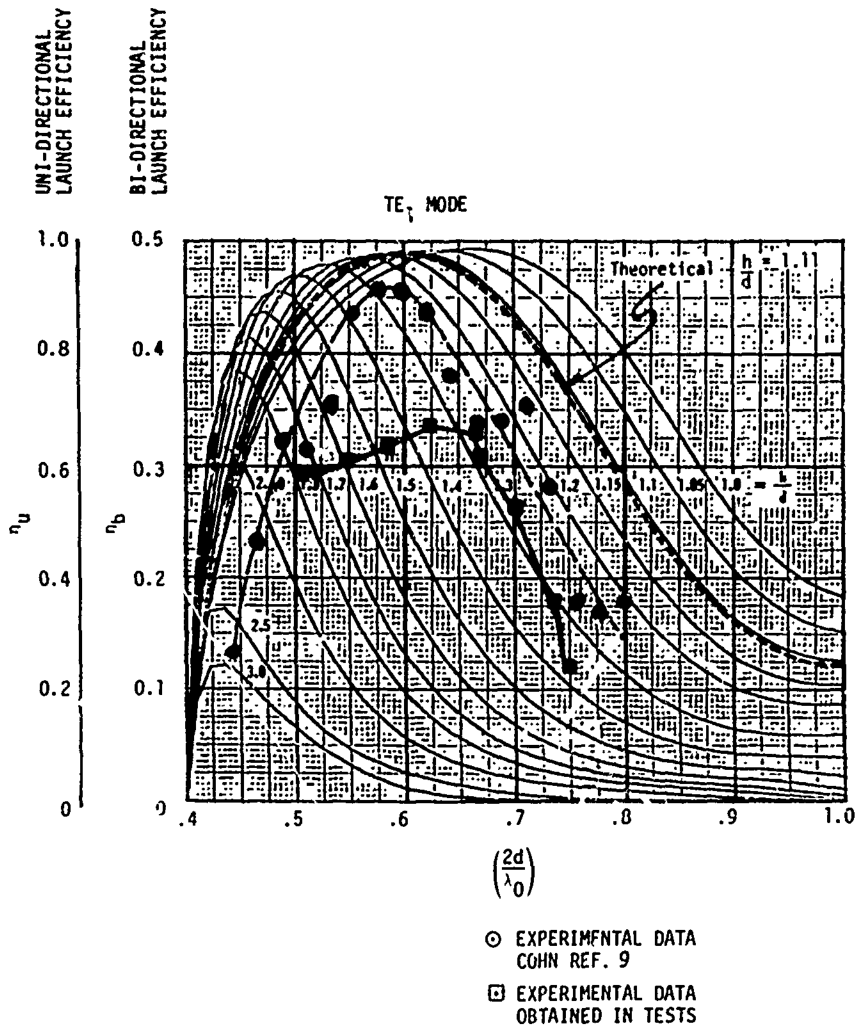

Figure 25. Comparison of Theoretical Values of Coupling Efficiency With Measured Values

Five coupling techniques were identified in Reference 1, from which only the two described here were tried in this program. Other promising techniques, such as that of Reference 11, can be used to couple to the surface waveguide from underneath the dielectric without disturbing the critical surfaces of the rotor. The technique of Reference 11 could be used to launch the surface wave from the tip or any intermediate point along the blade and could simplify the possibility of zoning the rotor blade in a manner similar to conventional electro-thermal devices, should this prove necessary.

MEASUREMENT OF THE COUPLING EFFICIENCY OF THE TE_1 MODE

The coupling efficiency of this mode was measured with two techniques: direct measurement with high power and indirectly with the techniques of Cohn, Reference 9, at low power. Both measurements are included in Figure 23a.

In Cohn's measurement, the following equations were used with a reflecting plate terminating the surface waveguide:

$$\eta = \frac{(r_{max} - 1)(r_{min} - 1)}{(r_{max} r_{min} - 1)} \tag{7}$$

where = r_{max} = Maximum voltage standing wave ratio
r_{min} = Minimum voltage standing wave ratio
η = Coupling efficiency

The frequency of operation was varied as a means of changing the electrical length of the surface guide so that the voltage standing wave ratio (vswr) would cycle through its maximum and minimum values. This was

[11] Frost, A.D., McGeoch, C.R., and Mingins, C.R., "The Excitation of Surface Waveguides and Radiating Slots by Strip-Circuit Transmission Lines," IRE Transactions on Microwave Theory and Techniques, October 1956.

done in lieu of varying the physical length of the line at a single frequency, which is impractical with dielectric lines, requiring that the dielectric be successively, physically cut.

The vswr (r_{max} and r_{min}) was actually determined by measuring minimum and maximum return losses and plotting these versus frequency, as illustrated in Figure 23a. The maximum and minimum return losses are then converted to maximum and minimum vswr with the following equation:

$$r = \frac{1 + [\Gamma]}{1 - [\Gamma]} = \frac{1 + [\log^{-1} \frac{R_L}{10}]^{1/2}}{1 - [\log^{-1} \frac{R_L}{10}]^{1/2}} \qquad (8)$$

where: r = vswr

Γ = Reflection coefficient

R_L = Return loss

The above procedure is valid provided that, when the surface guide is terminated in a reflectionless load, there is no mismatch at the input to the wave launcher. To insure this condition, the input vswr to the launcher was measured as a function of frequency, with the line terminated, and the data is plotted in Figure 23b, where it can be seen that the mismatch is less than 1.05 over most of the frequency band and no greater than 1.2. Actually, Equation 7 will give conservative estimates of launching efficiency. The true coupling efficiency is higher than given by Equation 7 and is given by Equation 9:

$$\eta_{true} = \frac{\eta_{measured}}{\Gamma_s} \qquad (9)$$

where Γ_s = reflection coefficient of the reflecting plate.

If the reflecting plate is totally reflecting, $\Gamma_s = 1$ $\eta_{true} = \eta_{measured}$. If the reflecting plate is less than totally reflecting, which is very likely in this case, $\Gamma_s < 1$ and $\eta_{true} > \eta_{measured}$.

Γ_s cannot be readily measured practically so that $\eta_{measured}$ must be considered only a lower bound, the true coupling efficiency being somewhat higher.

Although outside the scope of this program a direct measurement of the coupling efficiency was attempted to establish a rough order of magnitude correlation of coupling efficiency. This measurement was made possible by the availability of the high-power source at 2.45 GHz and a water load consisting of 3 rectangular polyethylene tubs placed end to end and terminating the waveguide, each containing 50 gms of water. The temperature rise of the water in each tub due to the absorbtion of energy in the surface wave, which was applied for 15 seconds, was measured. Data for an incident wave of 600 and 1200 watts is recorded below.

Tub	Water Mass gms	P_{in} = 600 watts			P_{in} = 1200 watts		
		ΔT °C	Power Absorbed Watts	Pr = Power Reflected Watts	ΔT °C	Power Absorbed Watts	Pr = Power Reflected Watts
1	50	17.5	244.17		36.1	503.69	
2	50	2.8	39.06	20	4.2	58.60	40
3	50	1.3	18.13		3.5	48.83	
Total Power P_a =			301.3			611.12	
Efficiency $= \frac{P_a}{P_{in} - P_r}$ =			51.9%			52.6%	

This measurement is also considered conservative. Coupling efficiency would be greater than measured because many sources of power loss exist with this method.

MEASUREMENT OF THE COUPLING EFFICIENCY OF THE TM_0 MODE

The measured coupling efficiency for the TM_0 mode is presented in Figure 24 as a function of frequency. Peak coupling efficiency, achieved at 2.7 GHz, is about 66%. Measurements were made by measuring the return loss, R_L, first with a termination on the surface guide and then with a short circuit. The launcher used was a lossy, four-terminal network with a one-way loss equal to one-half the measured return loss when the surface guide is terminated in a short circuit. The coupling efficiency in decibels is given by:

$$\eta = \frac{1}{2} R_L \tag{11}$$

In order to achieve the measured coupling efficiency, launcher reflections were reduced by using a coaxial double-slug tuner while the surface guide was terminated with a reflectionless tapered termination.

SECTION 4
LOSS TANGENT OF ROTOR ICE

The loss properties of rotor ice (glaze, rime, and any other form) are characterized electrically by their "loss tangent" (tan δ), for the purposes of establishing the effectiveness of the microwave ice protection concept.* A knowledge of the loss tangent permits the prediction of the performances of surface waveguide deicers in terms of attenuation constant (power dissipation per unit length of rotor blade), total power requirements and time to shed through the use of analytical techniques established in Reference 1.

As pointed out in Reference 1, the greatest unknown at the present time is loss tangent of ice that would form on rotor blades. Although the effects of various factors are not known, loss tangent may vary over a wide range depending upon:

1) Environment
   (a) Sea (salt content)
   (b) Land
   (c) Altitude
2) Unfrozen or free water content
3) Microwave frequency
4) Liquid water content of the icing cloud
5) Droplet diameter
6) Ambient temperature
7) Rate of freezing
8) Ice crystal structure
9) Surface Cleanliness
10) Hydrocarbon content (engine exhaust)
11) Air Content of ice
12) Other impurities

---

* A definition of the loss tangent was presented in the feasibility analysis, Reference 1, as being the ratio of the real to the imaginary part of the complex dielectric constant of the ice.

There is a sufficient number of variables that the loss tangent of rotor ice should be treated as a statistical variable and be expressed by its median value; (median tan δ). For this reason, a wide enough range of ice composition was chosen for testing here and in the static ice shed tests, Section 1, to fully encompass the range of loss tangents to be encountered in natural icing. The extreme values of salt water ice and distilled water ice are assumed to be the worst conditions, and the rationale for their choices was that if these samples could be shed in the laboratory, then median values could be shed in a natural icing environment.

It is expected that the most significant variable of those listed above is the "free water content of the ice", because the ice of interest to helicopter deicing is in the growth stage and there must exist an ice-water interface during ice growth. (Reference 12)

The second most significant variable is expected to be salt (NaCl) content. Salt water ice exhibits a cellular structure consisting of evenly spaced ice cells, the salt being present in liquid inclusions trapped between the cells (Reference 12).

It is generally accepted also that the loss tangent of pure ice increases with frequency in the microwave band, and therefore, an increase in median tan δ of rotor ice is expected in going to higher operating frequencies. This trend is evident in Figure 22 of Reference 1.

LOSS TANGENT MEASUREMENTS

Using techniques described below, the values of loss tangent for various samples of ice were measured and are presented in Table 2.

[12] Lofgren, Gary and Weeks, W.F., "Effect of Growth Parameters on Substructure Spacing in NaCl Ice Crystals", Journal of Glaciology, Vol. 8 No. 52, 1969.

Table 2. MEASURED LOSS TANGENTS OF VARIOUS SAMPLES OF ICE (MODEL 1 TE_1 MODE)

ICE TYPE	DATE	THICKNESS in	THICKNESS cm	TRANSMITTER POWER (WATTS)	T (°C)	ICE DEMINSIONS (cm)	MELTING TIME (sec)	T (dB/in)	TAN δ	TAN δ AV
DIS	2/4/77	9/32	.714	2000	- 7.3	.714 x 4.45 x 7.6	40	.0145	.0091	
DIS	2/7/77	3/16	476	2000	-11.0	.476 x 4.45 x 7.6	130	.0055	.0059	.0077
DIS	[illegible]7/77	3/32	.238	2000	-10.6	.238 x 4.45 x 7.6	80	.0046	.0062	
TAP	2/7/77	9/32	.714	2000	4.2	.714 x 4.45 x 7.6	30	.0238	.0152	
TAP	2/7/77	3/16	.476	2000	10.8	.48 x 4.5 x 7.6	35	.0164	.0145	.0150
TAP	2/8/77	3/32	.238	2000	[illegible]	.24 x 4.5 x 7.6	35	.0095	.0154	
6 g SALT/LITER	2/8/77	9/32	.714	400	- 9.6	.71 x 4.5 x 7.6	20	.1875	.1258	
"	2/8/77	3/16	.476	400	- 8.4	.48 x 4.5 x 7.6	30	.0709	.0667	.0953
"	2/8/77	3/32	.238	400	-10.0	.24 x 4.5 x 7.6	25	.0597	.0934	
3 g SALT/LITER	2/8/77	9/32	.714	400	- 9.9	.71 x 4.5 x 7.6	50	.0753	.0500	
"	2/8/77	3/16	.476	400	- 9.4	.48 x 4.5 x 7.6	50	.0477	.0448	.0515
"	2/8/77	3/32	.283	400	- 9.0	.24 x 4.5 x 7.6	35	.0329	.0597	
CRREL SNOW SAMPLE 9	2/9/77		.90	2000	-10.0	.9 x 3.4 x 17	160	.0028	.0019	.0014
"	2/10/77		.90	2000	-10.9	.9 x 3.4 x 17	390	.0020	.0009	
SPRAY ICE DIS	2/10/77		.23	2000	- 9.0	.23 x 4.45 x 7.6	40	.0053	.0077	
"	2/10/77		.14	2000	- 7.5	.14 x 4.45 x 7.6	30	.0040	.0083	.009
"	2/10/77		.31	2000	- 9.7	.31 x 4.45 x 7.6	30	.0091	.0115	

Surface Guide Parameter for Various Thickness of Ice

ICE THICKNESS			k_x	K_x	k_1	k_o	d	
(in)	(cm)	(cm^{-1})	(cm^{-1})	(cm^{-1})	(cm^{-1})	(cm^{-1})	(in)	(cm)
3/32	.238	.5856	.4855	.2815	.7616	.5135	1.6	4.064
3/16	.476	.5974	.4724	3053	.7616	.5135	1.6	4.064
9/32	.714	.6048	.4581	.3263	.7616	.5135	1.6	4.064

Because of the nature of rotor ice and variations in composition with time and temperature, it would be difficult, if not impossible, to simulate it in microwave test fixtures commonly used in the microwave industry for the measurement of the loss tangent of materials. A more meaningful approach would be to assess the effects of simulated rotor ice on actual test surface waveguides under a variety of icing environments.

This latter approach was taken in this effort and two different measurement techniques were attempted. The first method, based upon Reference 13, did not prove successful and was abandoned. This method relied on the perturbation of the resonant frequency of a resonant surface waveguide by the introduction of the ice sample on top of it. Attempts to perform this experiment indicate that the introduction of the ice sample into the resonant surface waveguide coupled small amounts of energy to the surrounding environment as well as dissipating energy in the sample. Since energy was lost in the surrounding environment as well as in the ice, computations of tan δ of the ice based on losses yielded unreasonably high values and this technique was abandoned as unreliable. The second method described below proved more successful and yielded reasonable values of tan δ which are listed in Table 2.

Basically the measurement concept is simple. In the feasibility analysis, Reference 1, analytical techniques had been established that could predict the time required to raise the temperature of a given ice sample from ambient to 0°C, the loss tangent could be computed by solving the equations for loss tangent in terms of time needed to raise the temperature to 0°C. Mathematical details are presented in Appendix B.

---

[13] Rueggebert, Werner, "Determination of Complex Permittivity of Arbitrarily Dimensioned Dielectric Modules at Microwave Frequencies", IEEE Transactions on Microwave Theory & Techniques, Vol. MTT-19, No. 6, pp. 517-521, June 1971.

SECTION 5
ICE DETECTORS

The detection of the presence of ice on a surface waveguide is possible because of the change in the reflection coefficient (or return loss) of the short-circuited surface waveguide. Utilizing the TM_0 mode at 2.45 GHz at low power (surface waveguide length = 30 inches), the following data was recorded:

Ice Thickness (in)	Return Loss db	Γ
0	-4.5	0.596
1/8	-6.0	0.501
1/4	-8.0	0.398

Observation of the reflected power during the high-power shed tests indicated that reflected power would cycle drastically between minimum and maximum values just prior to shedding. This was used throughout the shed tests as an indication of imminent ice shedding.

It was also observed that when the surface waveguide was made resonant, by intentionally mismatching the input wave launcher, the presence of small quantities of ice would make significant changes in the resonant frequency of the surface waveguide as illustrated in measurements taken on the TM_0 and TE_1 mode surface waveguide, Figures 26 and 27.

These measurements can be formalized into microwave ice detectors capable of measuring:

- Ice Presence
- Ice Thickness
- Ice Accretion Rate

These detectors would be nonmechanical, have no moving parts, and conform to the contour of the surface being monitored. Readouts would be essentially instantaneous. A more detailed description of the technology of these detectors is presented in Appendix D.

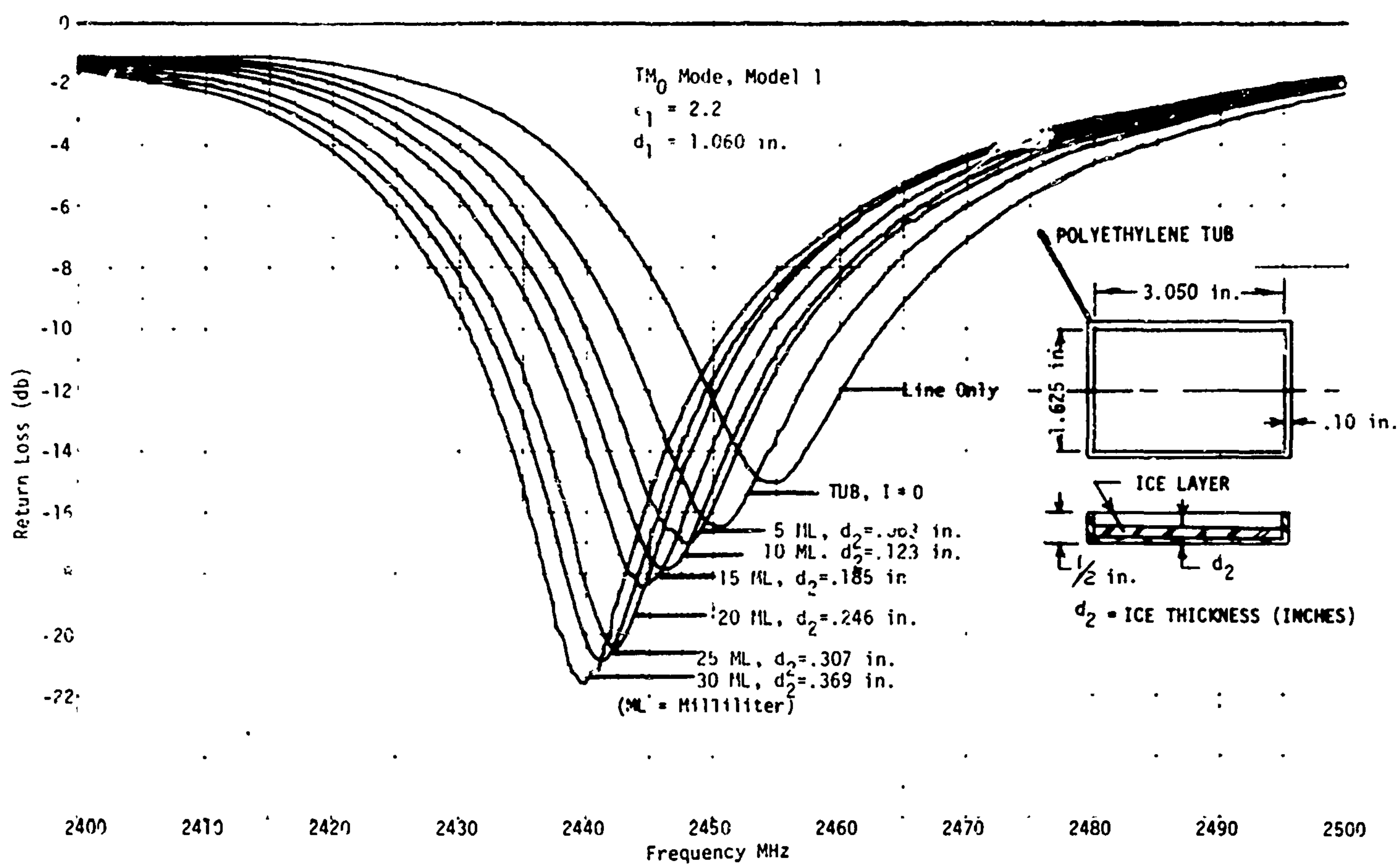

Figure 26. Measured Tuning Characteristics of Resonant TM_0 Mode Surface Waveguide as a Function of Ice Thickness

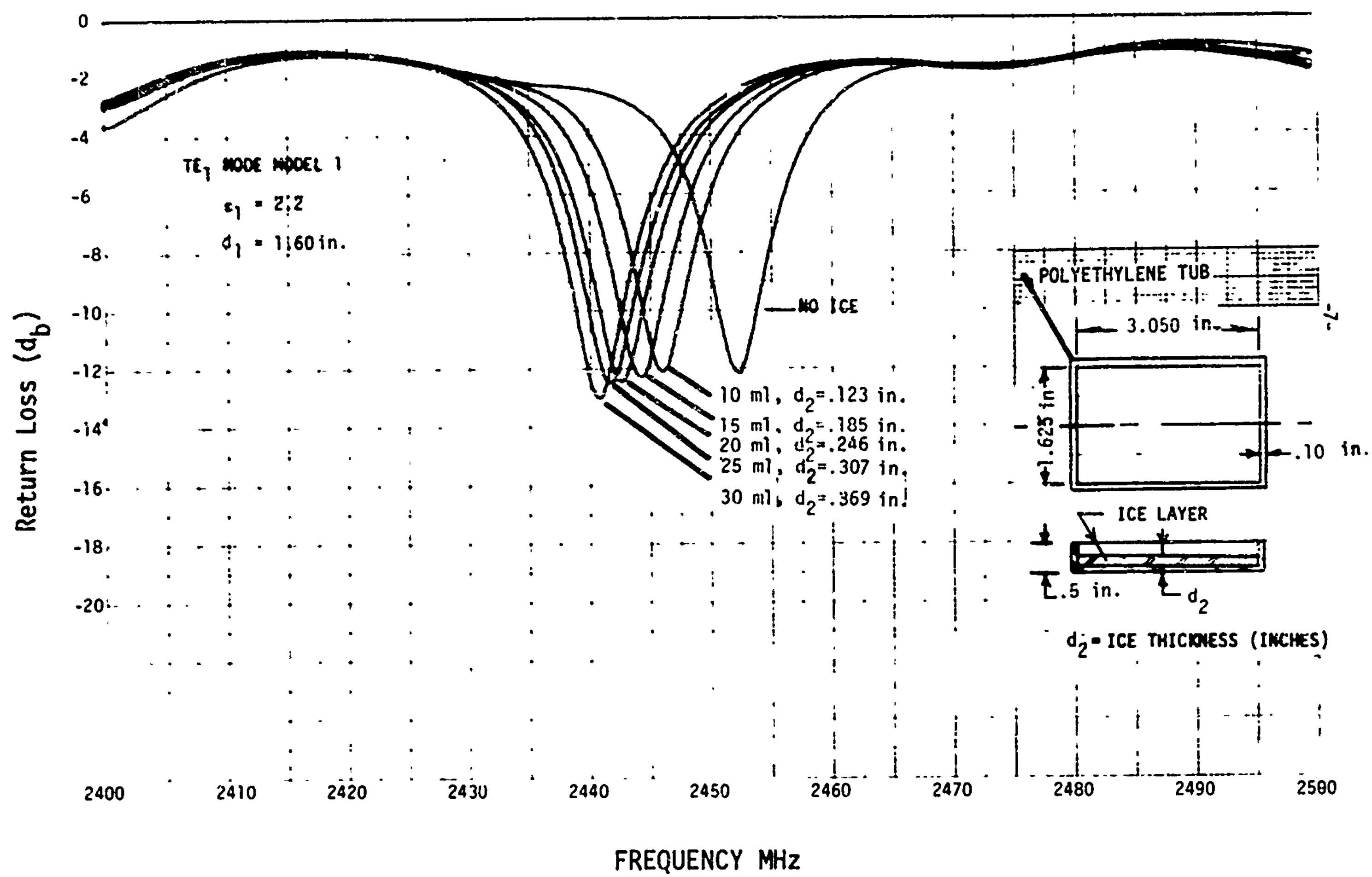

Figure 27. Measured Tuning Characteristics of Resonant TE_1 Mode Surface Waveguide as a Function of Ice Thickness

SECTION 6

PASSIVE COUNTERMEASURES AND IMPACT ON COMPOSITE BLADES

It is shown in this section that the vulnerability of Army helicopters due to possible enemy detection of microwave deicer leakage radiation is negligible. The vulnerability due to detection by radar, infrared and acoustic radiation is very high. The helicopter is a radar, infrared and acoustic target 100% of the time, in all kinds of weather and climate. Such equipment, presently in the enemy inventory in large numbers, will not require special development, has a high utilization factor against all kinds of airborne weapons not just helicopters, has a long range detection capability, is highly sophisticated, yields a high probability of detection and kill.

By comparison, specialized reconnaissance equipment developed to detect microwave deicer leakage radiation, not now in existence, would be utilized only a small fraction of the time during weather conditions conducive to ice formation and then only against helicopters. Even if this equipment were developed and deployed by the enemy, calculations (see below) show that it would have a range of no more than about 7 miles when liquid water content of the cloud was 1 gm/m^3 but drops to less than about 3 miles when the liquid water content of the icing cloud is 2 gm/m^3. The enemy would then have to procure this equipment in sufficient quantity to deploy at least one unit to every 5 square miles of battle area and be prepared to maintain it over long periods of non-use, summer, and winter when there is no possibility of ice formation.

Additionally as shown below, the use of microwave deicer on helicopters will permit the reduction in vulnerability to enemy radar by reduction in rotor blade radar cross-section. This reduction in radar vulnerability far outweighs the negligible increase in vulnerability due to leakage radiation.

At ranges of about 5 miles probability of detection by the unaided ear, radar, infrared and visual sighting is far greater than the probability of detection of deicer leakage radiation. The low countermeasure pay-off of equipment designed specifically to detect microwave deicer leakage radiation when compared to the high pay-off of radar, infrared and acoustics makes it extremely unlikely that such countermeasure equipment will appear in the enemy inventory.

RADAR REFLECTIVITY

The use of composite rotor blades offers reduced radar reflectivity because they are constructed without any (or a minimum of) metallic components. This advantage is lost, however, if conventional rotor blade deicers are required that incorporate metallic wires or mesh just below the surface of the leading edge. The microwave deicer offers the possibility of constructing rotor blade deicers completely out of nonmetallic materials that will not deteriorate the radar reflectivity of composite blades.

Techniques for accomplishing this were briefly discussed in the feasibility analysis, Reference 1. The experimental emphasis in the present program was placed primarily on demonstrating the microwave ice protection concept and experimental devices utilized metallic ground planes representing the metallic rotor blade. However, the ground plane is not basic to the propagation of surface waves: these waves can propagate in dielectric slabs, and the microwave ice protection concept, verified in this program, can be readily extended to dielectric-slab waveguides. The general theory of surface waveguides (including dielectric slabs) was presented in Reference 1.

Figure 28 shows how the power density varies in the dielectric slabs and the surface waveguide used in our experiments. The significant thing is that the dielectric slabs, Figure 28b, require twice the thickness of dielectric as required by the surface waveguide,

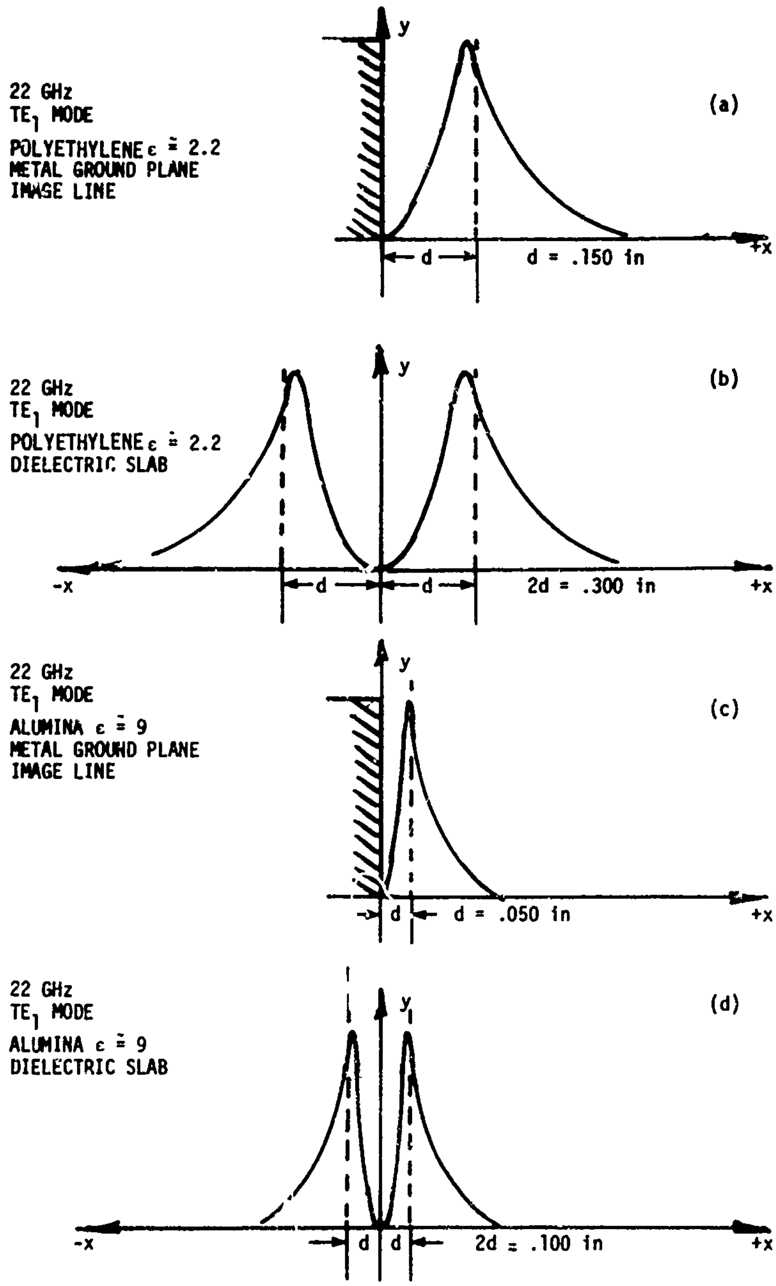

Figure 28. Power Density at 22 GHz for the TE_1 Mode for Dielectric Slabs and Image Lines (ordinate in watts/inch^2 abscissa in inches)

Figure 28a. For TE_1 modes, this can be reduced to one-third by the use of higher dielectric constant materials, such as alumina, $\varepsilon \approx 9$, Figure 28c and d. More significant perhaps is that, if the dielectric thickness becomes the limiting consideration, the TM_0 mode may be resorted to which offer thinner dielectrics at perhaps some penalty in shedding performance. Here also, as illustrated in Figure 29, the use of higher dielectric constant materials will also reduce the slab thickness significantly.

DETECTABILITY

Specific Attenuation Effects of Atmospheric Constituants

The principal attenuating medium in the atmosphere for the microwave region is:

1) Gaseous media (oxygen and water vapor)

2) Rainfall

3) Water cloud

4) Frozen phases of water

The effects of the gaseous media (oxygen and water vapor) were discussed in the feasibility analysis, Reference 1. Attenuation peaks around the 22-GHz absorption line of water molecules. Water vapor absorption exceeds molecular oxygen absorption. A graph of attenuation due to oxygen and water vapor was presented in the feasibility analysis, Figure 71, Reference 1.

Additional protection is provided by attenuation due to the liquid water content of the icing cloud. Clouds containing high liquid water content, supercooled water or rain (not discussed in Reference 1) produces the highest level of microwave attenuation. Clouds containing high levels of supercooled liquid water content are the primary cause of rotor blade icing and therefore it is expected that any leakage radiation of the microwave deicer will be heavily attenuated. Values

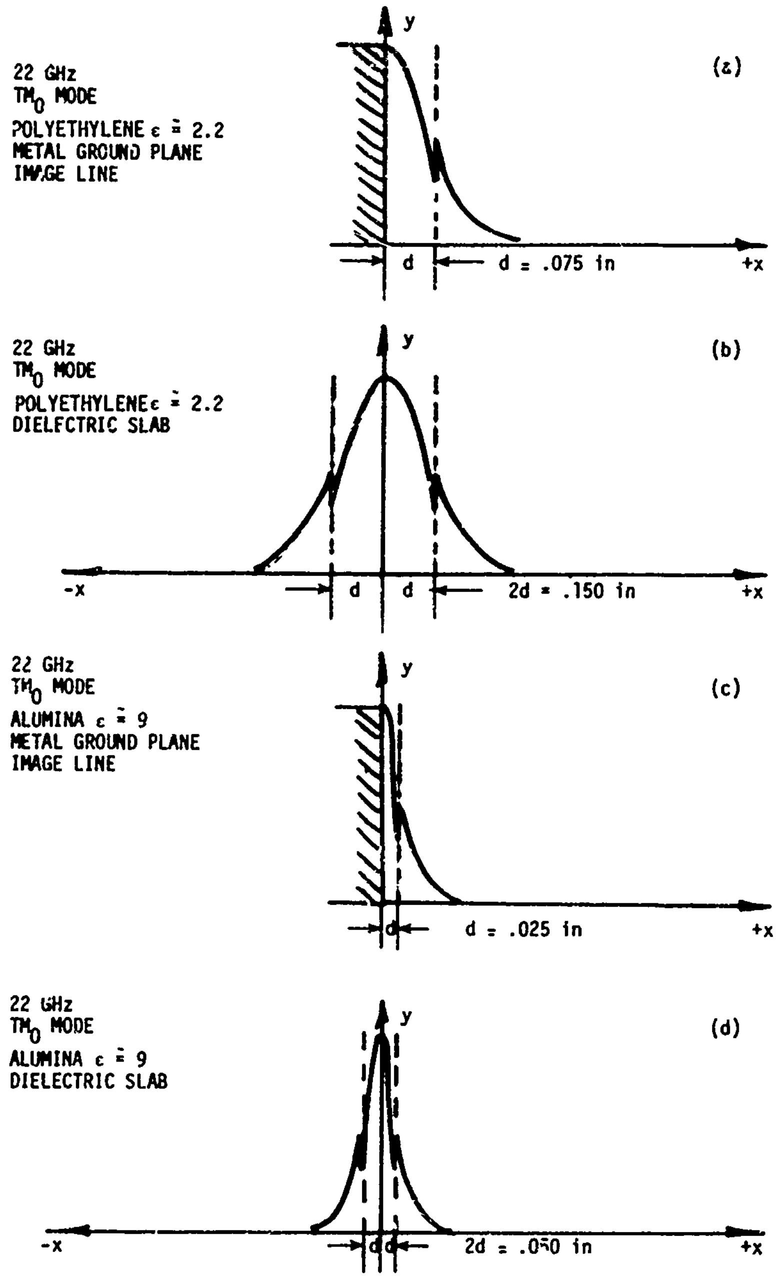

Figure 29. Power Density at 22 GHz for the TM_0 Modes for Dielectric Slabs and Image Lines (ordinate in watts/inch^2 abscissa in inches)

of attenuation constant due to liquid water content may be established from the following measurements at 18°C made by Gunn and East, Reference 14 and Medhurst, Reference 15 for rainfall.

Frequency (GHz)	Attenuation Constant α_r (db/km)
9.35	$0.0074\ R^{1.31}$
16.7	$0.045\ R^{1.14}$
24.2	$0.12\ R^{1.05}$
33.3	$0.22\ R^{1.0}$

The attenuation constant is represented in general form by:

$$\alpha_r = aR^b \qquad (12)$$

where a and b are constants which can be obtained from the above table and R is the rain rate in mm/hr. The liquid water content (LWC) is related to the rain rate R by the following equation:

$$LWC = AR^B \qquad (13)$$

which is commonly used in radar meteorology. Marshall and Palmer (Reference 16) as reported by Werner (Reference 17) give A = .09 and B = .84 for freezing rain and drizzle. Using these values the total

---

14 Gunn, L.L.S., and T.W.R. East: The Microwave Properties of Precipitation Particles, Quart, J. Roy, Meteorol. Soc., Vol. 80, pp. 522-545, October-December 1954.

15 Medhurst, R.G., "Rainfall Attenuation of Centimeter Waves: Comparison of Theory and Measurement". IEEE Transactions on Antennas and Propagation - March 1965.

16 Marshall, J. S. and Palmer, W., THE DISTRIBUTION OF RAINDROPS WITH SIZE, J. Meteor., 1948, pp. 165 - 166.

17 Werner, J.B., The Development of an Advanced Anti-Icing/Deicing Capability for U.S. Army Helicopters, Volume I - Design Criteria and Technology Considerations, Lockheed-California Company, USAAMRDL-TR-75-34A, Eustis Directorate, U.S. Army Air Mobility Research and Development Laboratory, Fort Eustis, Virginia, November 1975, AD A019044

attenuation at 2.5 mi, 5 mi and 10 mi due to liquid water have been computed as a function of liquid water content and rain rate.

LWC	R	α_r	TOTAL ATTENUATION AT 2.5 mi	5 mi	10 mi
gms/m^3	mm/h	db/km	db	db	db
.132		.098	0.35	0.7	1.5
.915	1	1.167	4.50	9	18.7
1.970	25	3.129	12.50	25	50.3
3.537	50	6.59	26.50	53	106
6.332	100	13.906	56.00	112	223
8.900	150	21.51	86.50	173	346

These values of attenuation will be that realized over and above that caused by gaseous water vaper discussed in Reference 1 and above.

Detectable Range

The maximum range at which the microwave deicer leakage radiation can be detected by an enemy reconnaissance receiver is established by calculating the range at which the received signal to noise ratio approaches 0 db. (This assumes that a scan search and target aquisition has been successfully accomplished and the target is within the beam of the reconnaissance receiver) This calculation requires the assumption of performance parameters of a reconnaissance receiver that the enemy can reasonably be expected to deploy in a battlefield environment. This receiver must be truck transportable, reasonably light weight and moderate in size, antenna diameter no greater than about 3 feet, noise temperature approximately 2500°K at 22 GHz, band width no greater than about 200 MHz.

If the microwave deicer leakage radiation is assumed to be no more than 100 watts (coupling efficiency greater than 90%) the signal to noise ratio as a function of range between the reconnaissance receiver and helicopter can be computed by the following equation:

$$\frac{S}{N} = C_t + G_t - L + G_r - k - T - B - L_s \tag{14}$$

where

C_t	= leakage radiation	= 20 dbw
G_t	= transmitter gain, isotropic	= 0 db
G_r	= reconnaissance receiver gain	= 35 db
k	= boltzman constant	= 228.6 db
T	= receiver noise temperature = $2500^\circ K$	= 34 db
B	= receiver band width 200 MHz	= 83 db
L	= path loss = $L_f + L_w + L_v$	
L_f	= free space loss	
L_w	= loss due to liquid water	
L_v	= loss due to water vapor	
L_s	= loss in power due to sweeping deicer generator ± 500 MHz	= 7 db

The signal to noise ratio as a function of range computed with the above equation is given in the following table where the maximum range (if acquired) is between 3 to 7 mi depending on the LWC.

Range	L_f	L_v	L_w Lwc = 1 gm/m^3	L_w Lwc = 2 gm/m^3	$\frac{S}{N}$ Lwc = 1 gm/m^3	$\frac{S}{N}$ LWC = 2 gm/m^3
mi	db	db	db	db	db	db
2.5	131.8	1	4.5	12.5	21.2	13.2
5.0	137.4	2	9	25	10.2	-5.8
10.0	143.4	4	18.7	50.3	-7.5	-39.1
20.0	149.4	8	18.7	50.3	-17.5	-49.1
40.0	155.4	16	18.7	50.3	-31.5	-63.1

The beam width of a 3-foot-diameter antenna at 22 GHz is on the order of 1° making it very difficult for the enemy of scan search, acquire, lock-on, launch and guide a missile at the intermittant leakage radiation of the microwave deicer that must fall within the 3 to 7 mile range. By comparison, as mentioned above, as a radar target the helicopter is on 100% of the time providing a high probability o. aquisition, lock-on, launch and guidance of the missile to the target at ranges up to 80 miles.

SECTION 7
RELIABILITY AND MAINTAINABILITY STUDIES

In Reference 8 samples of ultrahigh molecular weight polyethylene (UHMWPE), polyurethane and a section of the OH-6A helicopter hard-anodized rotor blade were subjected to the same sand and rain erosion tests, and the relative resistance to erosion of each material was experimentally established. With the known mean time between unscheduled maintainance (MTBUM) for the OH-6A aluminum blade, based upon field measurements, the MTBUMs of blades using UHMWPE and polyurethane were established.

Equations for the MTBUM, developed in Reference 8, are as follows:

$$MTBUM = \frac{LUV}{XY}\left[\frac{P(Y-X) + X}{P(V-U) + U}\right] \tag{13}$$

where:

- MTBUM = Mean time between unscheduled maintenance
- L = MTBUM of the OH-6A blade based on field data
- X = OH-6A blade test time before failure in <u>SAND</u> environment
- Y = OH-6A blade test time before failure in <u>RAIN</u> environment
- U = Elastomeric material test time before failure in <u>SAND</u> environment
- V = Elastomeric material test time before failure in <u>RAIN</u> environment
- P* = Percentage of time in sand environment
- p=(1-P)*= Percentage of time in rain environment

---

* It is assumed that the rotor flies in clear air most of the time, with no erosion taking place, and the remainder is spent in either a sand or a rain environment. P is the fractional portion of the remainder spent in a sand environment, whereas 1-P=p is the percentage spent in a rain environment.

It is clear that the erosion experienced is a function of the speed of the rotor and the angle of impingment of the sand or rain particles. The leading edge at the tip of a blade is subject to the most severe erosion due to its speed whereas areas of the rotor near the root are in a much less severe erosion environment.

As Reference 8 points out, while "an all-metal blade, such as that of the OH-6A, would be scrapped at the end of its MTBUM erosion period, the use of elastomeric erosion strips would allow the basic blade to be used indefinitely by stripping off the worn-out material and replacing it with new". It might further be added that, since the tip is the area that erodes most rapidly, the best erosion strips could be applied in areas near the tip while poorer (but good enough) erosion strips might be used on areas nearer the root providing the MTBUM of all the erosion material is not reduced.

With this concept it becomes possible to think of rotor blades incorporating two materials for the erosion strip: highly erosion-resistant material, such as polyurethane, for areas near the tip and a slightly poorer erosion-resistent material, such as UHMWPE, for all other areas. The MTBUM of such a compound erosion strip is established with Equation 13, by adding a term describing the effects of speed or rotor radius. In accordance with Reference 8, the MTBUM varies inversely with the square of the blade speed (i.e., erosion increases as the square of the speed) so that Equation 13 will appear as follows:

$$MTBUM = \frac{LUV}{XY}\left[\frac{P(Y-X)+X}{P(V-U)+U}\right]\left[\frac{S(r_t)}{S(r)}\right]^2 \qquad (14)$$

$$= \frac{LUV}{XY}\left[\frac{P(Y-X)+X}{P(V-U)+U}\right]\left[\frac{r_t}{r}\right]^2 \qquad (15)$$

where: $S(r)$ = Speed of erosion strip which is a function of r

$S(r_t)$ = Speed of erosion strip at tip r_t = tip radius

r = Radius of blade at segment of erosion strip

The MTBUMs of the tip and at 0.75 span for UHMWPE and polyurethane have been plotted in Figure 30 (corresponding to Figure 40 in Reference 8 for the tip only). The significant thing is that at approximately 0.75 span the MTBUM of UHMWPE is the same as the MTBUM of polyurethane used at the tip, so the use of UHMPE out to about 0.7 span and polyurethane from 0.7 to the tip will not deteriorate the MTBUM of the blade.

One of the possible failure modes of the microwave deicer is erosion of the surface waveguide by sand and rain. This analysis shows that compound surface waveguides composed of UHMWPE out to about 70. span fortified by a layer of polyurethane near the tip will go a long way in reducing this mode of failure and essentially increase the life of the microwave deicer.

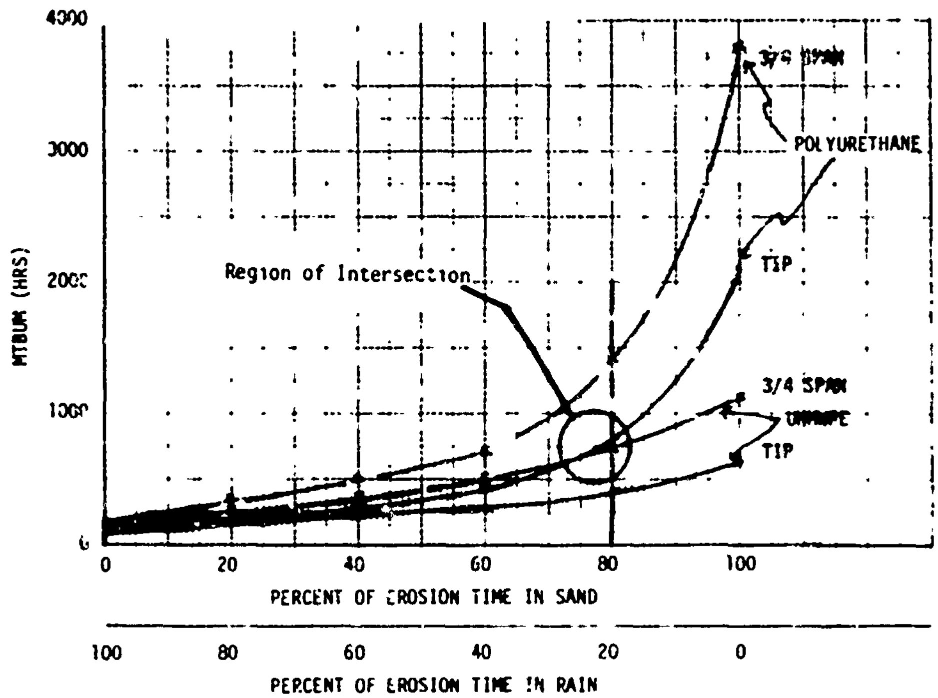

Figure 30. Mean Time Between Unscheduled Maintenance (MTBUM) Versus Percent Exposure to Sand and Rain Erosion

SECTION 8
POWER, WEIGHT, COST

SYSTEM POWER

The power drain and shed times for each helicopter studied is presented in Table 3 for ambient temperatures of -15°C and -20°C. The model used, described in Reference 1, is conservative yielding calculated shed times greater than actual shed times (surface wave power versus shed time was established from Table 4a and b). It should be recognized that power tube efficiency will improve with time (as discussed below) so the power drain for efficiencies of 30, 45, and 60% have been included in Table 3. Current, mature 2.45-GHz tubes have efficiencies in excess of 60% while current 22-GHz tubes offer only a maximum of 30%. Tubes being developed in the laboratory now have achieved 10 Kw 43% efficiency at 35 GHz, with theoretical predictions as high as 70% (see Appendix E).

Tube Technology - 22 GHz

As of 1977, the extended interaction oscillator (EIO) offers 1.2-Kw continuous wave (cw) power at 22 GHz with efficiencies between 20 and 30%. Higher efficiency is reasonable to expect in the future.

On the horizon, to be available in 2 to 3 years, is the Gyrotron, a new type of tube capable of extremely high continuous wave power and high efficiency. This tube stems from a mature technology developed in the Soviet Union within the last decade, where tubes like this are available today. The Energy Research and Development Administration (ERDA) has an outstanding contract to develop a 200-Kw continuous wave Gyrotron at 28 GHz with a maximum efficiency of 44%. The projected efficiency of this type of tube is as high as 70%. The internal structure of the Gyrotron is simpler than the EIO, which leads the developers to believe that the tube will eventually be less expensive than the EIO and provide the modest 1.2 Kw at the high efficiency required. (See Appendix E).

TABLE 3. HELICOPTER POWER DRAIN 400 WATTS PER BLADE
(CONSERVATIVE ESTIMATE)

HELICOPTER TYPE	TOTAL POWER REQUIRED PER HELICOPTER	POWER REQUIRED/TUBE AT DISTRIBUTION EFFICIENCY OF 80%	NO OF 1 Kw TUBES PER HELICOPTER	POWER DRAIN PER HELICOPTER			TIME TO SHED 0.250 in ICE (MEASURED AT MIDSPAN STAGNATION POINT)	
				TUBE EFFICIENCY			AMBIENT TEMPERATURE	
				30%	45%	60%	-20°C	-15°C
	Kw	Kw		Kw	Kw	Kw	sec	sec
UH-1							59.6	29.1
AH-1	0.8	1.0	1	3.3	2.2	1.6	69.1	33.75
OH-58							27	13.20
UTTAS							90.5	44.2
AAH	1.6	2.0	2	6.6	4.4	3.3	87.6	42.8
ASH							63.1	30.9
CH-47	2.4	3.0	3	10	6.6	5.0	69.1	33.75

TABLE 4. Time to Shed Ice Layer (Measured at Midspan Stagnation Point) Teflon Model, Ice Density = 0.9, Computed From eq B - 14 and 17 Reference 1 (lower ice density will result in shorter shed time)

PEAK POWER AVAILABLE $T_\infty = -15°C$

HELICOPTER	100 watts	200 watts	400 watts	800 watts	1600 watts
	sec	sec	sec	sec	sec
UH-1	116.42	58.21	29.1	14.5	7.27
AH-1	135.0	67.5	33.75	16.87	8.43
CH-47	136.0	67.5	33.75	16.87	8.43
OH-58	52.86	26.4	13.2	6.6	3.30
UTTAS	176.9	88.45	44.2	22.1	11.0
AAH	171.13	85.6	42.8	21.4	10.7
ASH	123.40	61.7	30.9	15.4	7.7

Note: Entries are time to shed (sec)

PEAK POWER AVAILABLE $T_\infty = -20°C$

HELICOPTER	100 watts	200 watts	400 watts	800 watts	1600 watts
	sec	sec	sec	sec	sec
UH-1	238.3	119.1	59.6	29.8	14.9
AH-1	276.4	138.2	69.1	34.5	17.3
CH-47	276.4	138.2	69.1	34.5	17.3
OH-58	108.2	54.1	27.0	13.5	6.8
UTTAS	362.2	181.1	90.5	45.3	22.6
AAH	350.3	175.1	87.6	43.8	21.9
ASH	252.6	126.3	63.1	31.6	15.8

Note: Entries are time to shed (sec)

Technology for 2.45- and 5.85-GHz Tubes

The technology for 2.45- and 5.85-GHz tubes, studied in Reference 1, is very mature, stemming primarily from World War II. Power out of 2.5 kw cw tubes is common with efficiencies up to 70%.

SYSTEM WEIGHT

The estimated system weight for each helicopter studied is presented in Table 5. The significant weight is the "incremental weight" which is the weight added to the helicopter by the inclusion of the microwave deicer.

Many of the devices making up the microwave deicer are constructed from materials and shapes similar to those used in the helicopter structure itself and can, by careful design, be integrated into the structure with only minimal increase in weight or loss of mechanica integrity of the original structure. Take for example, the rotor shaft and the feeder waveguide. The feeder waveguide is a hollow circularmetallic cylinder concentric with the rotor shaft. By careful design, it might be possible to construct combination shaft/feeders with no or only a minimal increase in weight. Similarly and more important, the deicer boot, constructed from dielectric materials, polyurethane, and polyethelene, may provide a net decrease in weight of new blades by eliminating the metallic erosion shield required for electro-thermal deicers and maintaining an all composite blade.

WEIGHT OF TUBE AND POWER SUPPLY

The major contributors to the system's weight are the power tube and its power supply. For the most part, these devices cannot be readily integrated into the helicopter structure. However, it should be recognized that tube efficiencies will improve with time, and tube and power supply weights will reduce accordingly. The power tube and the power supply weights used in Table 5 represent absolute weights of these devices (not incremental) assuming 30% efficiency of

TABLE 5. SYSTEM INCREMENTAL WEIGHT AND COST

			UH-1 AH-1 OH-58			UTTAS AAH ASH			CH-47		
			NO. REQ'D	COST $	INCRE-MENTAL WEIGHT lbs	NO. REQ'D	COST $	INCRE-MENTAL WEIGHT lbs	NO. REQ'D	COST $	INCRE-MENTAL WEIGHT lbs
MAIN ROTOR	BOOT		2	400	0	4	800	0	6	1200	0
	LAUNCHER		2	200	2	4	400	4	6	600	6
	POWER DIVIDER & DISTRIBUTOR		1	3000	4	1	3000	4	2	6000	8
	FEEDER		1	600	3	1	600	3	2	1200	6
	ROTARY JOINT		1	650	2	1	600	2	2	1300	4
TAIL ROTOR	BOOT		2	100	0	4	400	0	0	0	0
	LAUNCHER		2	200	2	4	400	4	0	0	0
	ROTARY JOINT		1	650	2	1	650	2	0	0	0
	FEEDER		1	600	2	1	600	2	0	0	0
COMMON EQUIPMENT	SWITCH		1	100	1	1	100	1	0	0	0
	CONTROL PANEL		1	400	4	1	400	4	1	400	4
	TUBE POWER SUPPLY		1	900	17	1	1350	34	1	1800	51
	POWER TUBE	2.45 GHz	1	1500	4.5	2	3000	9	3	4500	13.5
		5.85 GHz		1500	18		3000	36		4500	54
		22 GHz		4500	18		9000	36		13500	54
TOTALS		2.45 GHz		$9.3K	43.5		$12.3K	69		$17K	93
		5.85 GHz		$9.3K	57		$12.3K	96		$17K	133
		22 GHz		$12.3K	57		$18.35K	96		$17K	133

the tube. A rise in efficiency to 45% or 60% will produce a 25 to 50% drop in tube and power supply weight.

SYSTEM COST

System cost estimates for each helicopter type at 2.45, 5.85 and 22 GHz are presented in Table 5. The most significant cost differentials are between 22-GHz tubes and 5.85- and 2.45-GHz tubes. Cost estimates for the tube and power supply made in Reference 1 are used here.

SECTION 9

CONCLUSIONS

- Surface waveguide deicers can be used to shed ice when operating at 2.45 GHz.
- Shed performance is improved by operating deicers at 22 GHz.
- Analytical techniques for predicting surface waveguide performance have been verified experimentally.
- Maximum launch efficiency of 68% was obtained experimentally.
- Launch efficiencies in excess of 90% appear reasonable in optimized launchers.
- Dielectric loss properties of simulated rotor ice were measured.
- Cost, weight and power estimates of various helicopter types are presented.
- A compound surface waveguide composed of ultra high molecular weight polyethylene out to about 75% span fortified with a layer of polyurethane at the tip will increase the life of the microwave deicer.
- The vulnerability of Army helicopters due to possible detection of microwave deicer leakage radiation is negligible.
- Microwave deicers permit construction of rotor blades completely out of nonmetallic materials thereby reducing its radar cross-section.
- At an operating frequency of 22 GHz leakage radiation is attenuated significantly by the liquid water content of the icing cloud and water vapor absorption.
- Monitoring the power reflected from the microwave deicer boot provides an inherent means of detecting ice formation.
- Techniques for measuring ice thickness and ice accretion rate using resonant surface waveguides have been experimentally demonstrated. These devices are nonmechanical, have no moving parts, are essentially instantaneous and conform to the contour of the surface being monitored.

SECTION 10

RECOMMENDATIONS

- A comprehensive ongoing program should be initiated to develop microwave ice protection technology.
- Equip a UH-1 tail rotor with a microwave deicer. Install it on a whirlstand and test its performance in an icing tunnel. (See Appendix C).
- Develop a prototype system for the UH-1 helicopter and extend to other helicopters later.
- Research high-power, high-efficiency, low-weight microwave tubes specifically designed for microwave deicer service.
- Research dielectric materials further to find low-loss, high-dielectric constant materials with high resistances to sand and rain erosion for deicer service.
- Optimize rotor blade wave launchers that can be used at the tip of the blade or any intermediate point.
- Optimize radar cross-section reduction techniques for microwave deicers.
- Optimize wave launcher efficiency.
- Develop microwave ice detection technology (See Appendix D).

LIST OF SYMBOLS

Symbol		Definition	UNITS
c	=	Specific heat	cal/gm - °C
d_1	=	Thickness of surface waveguide	cm
d_2	=	Thickness of ice layer	cm
f_c	=	Cut off frequency	Hz
k_ε	=	Energy	watt-sec
k_s	=	Energy required to shed the ice sample	watt-sec
k_x	=	Internal eigenvalue	rad/cm
K_X	=	External eigenvalue	rad/cm
L	=	MTBUM of the OH-6A blade based on field data	Hrs
MTBUM	=	Mean time between unscheduled maintenance	Hrs
m	=	Mass of ice sample	gms
P	=	Percentage of time in sand environment	
$p=(1-P)$	=	Percentage of time in rain environment	
P_d	=	Power dissipated in the ice sample	watts
P_s	=	Power in surface wave	watts
r	=	Voltage standing wave ratio	numeric
r_i	=	Radius of blade at segment of erosion strip	cm
R_L	=	Return loss	db
$S(r)$	=	Speed of erosion strip which is a function of r	cm/sec
t_s =	=	Shed time	sec
U	=	Elastomeric material test time before failure in <u>SAND</u> environment	Hrs
V	=	Elastomeric material test time before failure in <u>RAIN</u> environment	Hrs
Y	=	OH-6A blade test time before fialure in <u>RAIN</u> environment	Hrs
β	=	Propogation constant	rad/cm
ϕ	=	Water flow rate	cc/sec
ε_i	=	Relative dielectric constant of material i	numeric
Γ	=	Reflection coefficient	numeric
j	=	$\sqrt{-1}$	

LIST OF SYMBOLS

LIST OF SYMBOLS		UNITS
η	= Launch efficiency	numeric
ρ	= Power density	watts/cm^2
ΔT	= Temperature rise	^oC
λ_g	= Guide wavelength	cm

REFERENCES

1. Magenheim, Bertram and Hains, Frank, Feasibility Analysis for a Microwave Deicer for Helicopter Rotor Blades, Mechanics Research Inc., USAAMRDL-TR-76-18, Eustis Directorate, U.S. Army Air Mobility Research and Development Laboratory, Fort Eustis, Virginia, May 1977.

2. M. Cohn, "Propagation in Dielectric-Loaded Parallel Plane Waveguide, "IRE Transactions on Microwave Theory and Techniques, pp. 202-208, April 1959.

3. M. Cohn, "TE Modes of Dielectric Loaded Trough Line," IRE Transactions on Microwave Theory and Techniques, pp. 449-454, July 1960.

4. D.D. King and S.P. Schlesinger, "Losses in Dielectric Image Lines, "IRE Transactions on Microwave Theory and Techniques, January 1967.

5. S.P. Schlesinger and D.D. King, "Dielectric Image Lines, "IRE Transactions on Microwave Theory and Techniques, July 1968.

6. R. Collin, Field Theory of Guided Waves, New York: McGraw-Hill, 1960.

7. Ramo, Whinnery and Van Duzer, Fields and Waves in Communications Electronics, New York: John Wiley & Sons, 1965.

8. Head, Robert E., Erosion Protection for the AH-1G Low Radar Cross-Section Main Rotor Blade, Volume I - Sand Rain Erosion Evaluation. Hughes Helicopters, USAAMRDL-TR-76-40A, Eustis Directorate, U.S. Army Air Mobility Research and Development Laboratory, Fort Eustis, Virginia, January 1977, AD A035961.

9. Cohn, Cassedy and Kott, "TE Mode Excitation on Dielectric Loaded Parallel Plane and Trough Waveguides, "IRE Transactions and Microwave Theory and Techniques, pp. 545-552, September 1960.

10. DuHamel, R.H. and Duncan, J.W., "Launching Efficiency of Wires and Slots for a Dielectric Rod Waveguide, "IRE Transactions of Microwave Theory and Techniques, July 1958.

11. Frost, A.D. McGeoch, C.R., and Mingins, C.R., "The Excitation of Surface Waveguides and Radiating Slogs by Strip-Circuit Transmission Lines, "IRE Transactions on Microwave Theory and Techniques, October 1956.

REFERENCES

12. Lofgren, Gary and Weeks, W.F., "Effect of Growth Parameters on Sub-Structure Spacing in NaCl Ice Crystals", Journal of Glaciology, Vol. 8, No. 52, 1969.

13. Rueggebert, Werner, 'Determination of Complex Permittivity of Arbitrarily Dimensioned Dielectric Modules at Microwave Frequencies, "IEEE Transactions on Microwave Theory & Techniques, Vol. MTT-19, No. 6, pp. 517-521, June 1971.

14. Gunn, L.L.S., and T.W.R., East: The Microwave Properties of Percipitation Particles, Quart, J. Roy, Meteorol. Soc., Vol. , , pp. 522-545, October-December 1954.

15. Medhurst, R.G., "Rainfall Attenuation of Centimeter Waves Comparison of Theory and Measurement". IEEE Transactions on Antennas and Propagation - March 1965.

16. Marshall, J.S., and Palmer, W., THE DISTRIBUTION OF RAINDROPS WITH SIZE, J. Meteor., 1948, pp. 165-166.

17. THE DEVELOPMENT OF AN ADVANCED ANTI-ICING DE-ICING CAPABILITY FOR U.S. ARMY HELICOPTERS, Volume 1 - Design Criteria and Technology Considerations, J.B. Werner - November 1975. USAAMRDL-TR-75-34A

18. Kisel, D.V., Korablev, G.S., Navel'yev, V.G., Petelin, M.I., and Tsimring, Sh. Ye., 'An Experimental Study of a Gyrotron, Operating at the Second Harmonic of the Cyclotron Frequency, with Optimized Distribution of the High-Frequency Field, Radio Engineering and Electronic Physics, Vol. 19 pp. 95-99, April 1974.

APPENDIX A

Static Ice Shed Test Data

The following is a summary of test data accumulated during the static ice shed tests described in Section 1. The first 12 tests are considered unreliable because sufficient time was not allowed between tests to assure temperature restabilization of the surface waveguide to ambient.

In a few tests, as indicated, an ice water spray was used in an attempt to better simulate natural icing due to supercooled clouds.

In a few tests, as indicated, an air gun was utilized in an attempt to blow away stagnent water produced by melting some of the ice thereby simulating to some extent the moving air stream around the rotor blade.

In a few tests, as indicated, the surface waveguide was tilted to permit drainage of stagnent water produced by melting some of the ice.

		TEST CONDITIONS - 2450 MHz														TEST RESULTS	
		ICE SAMPLE															
TEST NO.	TEST DATE	ICE COMPOSITION	ICE THICKNESS	ICE LENGTH x WIDTH	ICE DENSITY	TEMPERATURE SURFACE GUIDE	TRANSMITTER POWER	COUPLED POWER	REFLECTED POWER	POWER ON TIME	TERMINATION L = LOAD R = REFLECTOR	ICEWATER SPRAY	AIR GUN	LINE TILTED	SIMULATED CENTRIFUGAL LOAD	SHED TIME	REMARKS
			in	in	gm/cc	°C	WATTS	WATTS	WATTS	SEC	L R	ON or —	ON or —	YES or —	LB	SEC	
1	12-23-76	SALT 0.6%	3/16	3x1.6	0.9	-10*	400	220			L				8.4	7	CLEAN SHED
2	12-23-76	SALT 0.6%	3/16	3x1.6	0.9	-10*	400	220			L				8.4	7	CLEAN SHED
3	12-23-76	SALT 0.6%	3/16	3x1.6	0.9	-10*	400	220			L				8.4	—	SELF SHED
4	12-23-76	SALT 0.6%	3/16	3x1.6	0.9	-20*	400	220			L				8.4	9	CLEAN SHED
5	12-23-76	SALT 0.6%	3/16	3x1.6	0.9	-20*	400	220			L				8.4	15	CLEAN SHED
6	12-23-76	SALT 0.6%	3/16	3x1.6	0.9	-20*	400	220			L				8.4	12	CLEAN SHED
7	12-23-76	SALT 0.6%	3/16	3x1.6	0.9	-20*	1200	660			L				8.4	4	CLEAN SHED
		—	—	—	—	—	--										

*Temperature Measurements Uncertain in Tests 1 to 12 Model #2-TE_1 Mode 2 Layer Mode

		TEST CONDITIONS - 2450 MHz														TEST RESULTS	
		ICE SAMPLE															
TEST NO.	TEST DATE	ICE COMPOSITION	ICE THICKNESS	ICE LENGTH x WIDTH	ICE DENSITY	TEMPERATURE SURFACE GUIDE	TRANSMITTER POWER	COUPLED POWER	REFLECTED POWER	POWER ON TIME	TERMINATION L = LOAD R = REFLECTOR	ICEWATER SPRAY	AIR GUN	LINE TILTED	SIMULATED CENTRIFUGAL LOAD	SHED TIME	REMARKS
			in	in	gm/cc	°C	WATTS	WATTS	WATTS	SEC	L R	ON or —	ON or —	YES or —	LB	SEC	
8	12-28-76	SALT 0.6%	3/16	3x1.6	0.9	-20*	400	220	70		ECCO L				8.4	23	SOME MELTING
9	12-28-76	SALT 0.6%	3/16	3x1.6	0.9	-20*	400	220	70		L				8.4	5	CLEAN SHED
10	12-28-76	SALT 0.6%	3/16	3x1.6	0.9	-20*	400	220	70		L				8.4	15	CLEAN SHED
11	12-28-76	SALT 0.6%	3/16	3x1.6	0.9	-20*	400	220	70		L				8.4	17	CLEAN SHED
12	12-28-76	SALT 0.6%	3/16	3x1.6	0.9	-20*	1200	660	170		L				8.4	5	CLEAN SHED
13	12-29-76	SALT 0.6%	3/16	3x1.6	0.9	-20	1200	660	170		L				8.4	8	SOME MELTING
14	12-29-76	SALT 0.6%	3/16	3x1.6	0.9	-20	1200	660	170		L				8.4	11	SOME MELTING

*Eccosorb Model #2-TE_1 Mode 2 Layer Model

		TEST CONDITIONS - 2450 MHz														TEST RESULTS	
		ICE SAMPLE															
TEST NO.	TEST DATE	ICE COMPOSITION	ICE THICKNESS	ICE LENGTH x WIDTH	ICE DENSITY	TEMPERATURE SURFACE GUIDE	TRANSMITTER POWER	COUPLED POWER	REFLECTED POWER	POWER ON TIME	TERMINATION L = LOAD R = REFLECTOR	ICEWATER SPRAY	AIR GUN	LINE TILTED	SIMULATED CENTRIFUGAL LOAD	SHED TIME	REMARKS
			in	in	gm/cc	°C	WATTS	WATTS	WATTS	SEC	L R	ON or —	ON or —	YES or —	LB	SEC	
15	12-29-76	SALT 0.6%	3/16	3x1.6	0.9	-20	1200	660	170		*ECCO L				8.4	6	CLEAN SHED
16	12-29-76	SALT 0.6%	3/16	3x1.6	0.9	-20	1200	660	170		L				8.4	5	SOME MELTING
17	12-29-76	SALT 0.6%	3/16	3x1.6	0.9	-20	1200	660	150		L				8.4	6	SOME MELTING
18	12-29-76	SALT 0.6%	3/16	3x1.6	0.9	-20	1200	660	150		L				8.4	4	SOME MELTING
19	12-29-76	SALT 0.6%	3/16	3x1.6	0.9	-20	1200	660	200		L				8.4	15	SOME MELTING
20	12-30-76	SALT 0.6%	3/16	3x1.6	0.9	-20	1200	660	200		L				8.4	5	CLEAN SHED
21	12-30-76	SALT 0.6%	3/16	3x1.6	0.9	-20	800	440	–		L				8.4	13	SOME MELTING
22	12-30-76	SALT 0.6%	3/16	3x1.6	0.9	-20	800	440	100		L				8.4	9	CLEAN SHED

*Eccosorb Model #2-TE_1 Mode 2 Layer Model

TEST NO.	TEST DATE	TEST CONDITIONS - 2450 MHz														TEST RESULTS	
		ICE SAMPLE															
		ICE COMPOSITION	ICE THICKNESS	ICE LENGTH x WIDTH	ICE DENSITY	TEMPERATURE SURFACE GUIDE	TRANSMITTER POWER	COUPLED POWER	REFLECTED POWER	POWER ON TIME	TERMINATION L = LOAD R = REFLECTOR	ICEWATER SPRAY	AIR GUN	LINE TILTED	SIMULATED CENTRIFUGAL LOAD	SHED TIME	REMARKS
			in	in	gm/cc	°C	WATTS	WATTS	WATTS	SEC	L R	ON or —	ON or —	YES or —	LB	SEC	
22	12-30-76	SALT 0.6%	3/16	3x1.6	0.9	-20	800	440	100	—	L				8.4	18	CLEAN SHED
24	12-30-76	SALT 0.6%	3/16	3x1.6	0.9	-20	800	440	100	—	L				8.4	13	CLEAN SHED
25	1-3-77	SALT 0.6%	3/16	3x1.6	0.9	-20	400	220	—	—	L				8.4	31	SOME MELTING
26	1-3-77	SALT 0.6%	3/16	3x1.6	0.9	-20	400	220	—	—	L				8.4	31	SOME MELTING
27	1-3-77	SALT 0.6%	3/16	3x1.6	0.9	-20	2400	660	—	10	L				8.4	—	NO SHEDDING
28	1-3-77	SALT 0.6%	3/16	3x1.6	0.9	-20	2400	660	-	—	L				8.4	8	SOME MELTING
29	1-4-77	SALT 0.6%	3/16	3x1.6	0.9	-20	1800	990	—	—	L				8.4	8	SOME MELTING
30	1-4-77	SALT 0.6%	3/16	3x1.6	0.9	-20	1800	990	—	—	L				8.4	8	SOME MELTING

Remarks: Model #2 TE_1 Mode 2 Layer Model

		TEST CONDITIONS - 2450 MHz														TEST RESULTS	
		ICE SAMPLE															
TEST NO.	TEST DATE	ICE COMPOSITION	ICE THICKNESS	ICE LENGTH x WIDTH	ICE DENSITY	TEMPERATURE SURFACE GUIDE	TRANSMITTER POWER	COUPLED POWER	REFLECTED POWER	POWER ON TIME	TERMINATION L = LOAD R = REFLECTOR	ICEWATER SPRAY	AIR GUN	LINE TILTED	SIMULATED CENTRIFUGAL LOAD	SHED TIME	REMARKS
			in	in	gm/cc	°C	WATTS	WATTS	WATTS	SEC	L R	ON or —	ON or —	YES or —	LB	SEC	
31	1-11-77	SALT 0.3%	3/16	3x1.6	0.9	-20	800	440			L				8.4	10	CLEAN SHED
32	1-11-77	SALT 0.3%	3/16	3x1.6	0.9	-20	800	440			L				8.4	25	SOME MELTING
33	1-11-77	SALT 0.3%	3/16	3x1.6	0.9	-20	800	440			L				8.4	14	CLEAN SHED
34	1-11-77	SALT 0.3%	3/16	3x1.6	0.9	-20	800	440			L				8.4	20	CLEAN SHED
35	1-11-77	SALT 0.3%	3/16	3x1.6	0.9	-20	800	440			L				8.4	30	MELTING
36	1-12-77	SALT 0.3%	3/16	3x1.6	0.9	-20	800	440			L				8.4	4	MELTING
37	1-12-77	SALT 0.15%	3/16	3x1.6	0.9	-20	800	440		70	L				8.4	—	NO SHEDDING IN 70 SEC SOME MELTING
38	1-12-77	SALT 0.15%	3/16	3x1.6	0.9	-20	800	440		70	L				8.4	—	NO SHEDDING IN 70 SEC - MELTING

Remarks: Model #2 TE_1 Mode 2 Layer Model

TEST NO.	TEST DATE	TEST CONDITIONS - 2450 MHz: ICE SAMPLE: ICE COMPOSITION	ICE THICKNESS	ICE LENGTH x WIDTH	ICE DENSITY	TEMPERATURE SURFACE GUIDE	TRANSMITTER POWER	COUPLED POWER	REFLECTED POWER	POWER ON TIME	TERMINATION L = LOAD R = REFLECTOR	ICEWATER SPRAY	AIR GUN	LINE TILTED	SIMULATED CENTRIFUGAL LOAD	TEST RESULTS: SHED TIME	REMARKS
			in	in	gm/cc	°C	WATTS	WATTS	WATTS	SEC	L R	ON or —	ON or —	YES or —	LB	SEC	
39	1-13-77	SALT 0.15%	.25	15x1.9	0.9	-20	800	440	—	120	R	OFF		YES		—	MOST ICE MELTED AFTER 1 MIN -ALL ICE MELTED IN 2 MIN
40	1-13-77	TAP WATER	.25	15x1.9	0.9	-20	800	440		240	R	TURNED ON AFTER 60 SEC		YES			1 MIN-NO MELTING 2 MIN-DRAIN CHANNELS FORMED IN ICE 3 MIN-1/2 ICE MELTED 4 MIN-ALL ICE MELTED
41	1-13-77	TAP WATER	.25	15x1.9	0.9	-20	2400	1320			R	OFF		YES			1 MIN-2/3 ICE MELTED 2 MIN-ALL ICE MELTED
42	1-13-77	DIST	.25	15x1.9	0.9	-20	2400	1320			R	OFF		YES			1 MIN-2/3 ICE MELTED 2 MIN-ALL ICE MELTED

Remarks: Model #2 TE_1 Mode 2 Layer Model

TEST NO.	TEST DATE	TEST CONDITIONS - 2450 MHz: ICE SAMPLE: ICE COMPOSITION	ICE THICKNESS	ICE LENGTH x WIDTH	ICE DENSITY	TEMPERATURE SURFACE GUIDE	TRANSMITTER POWER	COUPLED POWER	REFLECTED POWER	POWER ON TIME	TERMINATION L = LOAD R = REFLECTOR	ICEWATER SPRAY	AIR GUN	LINE TILTED	SIMULATED CENTRIFUGAL LOAD	TEST RESULTS: SHED TIME	REMARKS
			in	in	gm/cc	°C	WATTS	WATTS	WATTS	SEC	L R	ON or —	ON or —	YES or —	LB	SEC	
43	1-17-77	DIST	3/16	3x1.6	0.9	-20	800	440	—	60	L	OFF			8.4	—	NO SHEDDING IN LESS THAN 60 SEC
44	1-18-77	DIST	3/16	3x1.6	0.9	-20	800	440	100	60		ON			8.4		1/3 ICE MELTED IN LESS THAN 60 SEC
45	1-18-77	DIST	3/16	3x1.6	0.9	-18	2400	1320	—	30	R	ON			8.4	30	ALL ICE MELTED IN LESS THAN 30 SEC.
46	1-18-77	DIST	3/16	3x1.6	0.75	-13	2400	1320	—	12	R	ON			8.4	12	ALMOST ALL ICE MELTED IN LESS THAN 12 SEC
47	1-18-77	DIST	3/16	3x1.6	0.9	-15	2400	1320	—	240	R	OFF			8.4	240	ALL ICE MELTED AFTER 240 SEC
48	1-19-77	DIST	3/16	3x1.6	0.90	-20	2400	1320	—	190	R	OFF			8.4		STARTED TO MELT AFTER 190 SEC
49	1-19-77	DIST	3/16	3x1.6	0.75	-20	2400	1320	—	20	L	ON			8.4		1/2 ICE MELTED AFTER 20 SEC

Remarks: Model #2 TE_1 Mode 2 Layer Model

TEST NO.	TEST DATE	TEST CONDITIONS - 2450 MHz: ICE SAMPLE: ICE COMPOSITION	ICE THICKNESS	ICE LENGTH x WIDTH	ICE DENSITY	TEMPERATURE SURFACE GUIDE	TRANSMITTER POWER	COUPLED POWER	REFLECTED POWER	POWER ON TIME	TERMINATION L = LOAD R = REFLECTOR	ICEWATER SPRAY	AIR GUN	LINE TILTED	SIMULATED CENTRIFUGAL LOAD	TEST RESULTS: SHED TIME	REMARKS
			in	in	gm/cc	°C	WATTS	WATTS	WATTS	SEC	L R	ON or —	ON or —	YES or —	LB	SEC	
50	1-20-77	DIST	3/16	3x1.6	0.9	-20	1600	880		20	R					20	3rd LAYER=0.6% SALT 1/2 ICE MELTED
51	1-20-77	DIST	3/16	3x1.6	0.9	-13	2400	1320		15	R					15	3rd LAYER=DIST WATER 1/2 ICE MELTED
52	1-20-77	DIST	3/16	3x1.6	0.9	-13	2400	1320		40	R					40	3rd LAYER=DIST WATER 1/2 ICE MELTED
53	1-20-77	DIST	3/16	3x1.6	0.9	-13	2400	1320		40	R					40	3rd LAYER=10 MIL CELULOSE ACETATE TAPE-ACRYLATE ADHESIVE
54	1-21-77	DIST	3/16	3x1.6	0.9	-13.7	2400	1320		50	R					50	3rd LAYER= 8 MIL FILAMENT TAPE
55	1-21-77	DIST	3/16	3x1.6	0.9	-15.1	2400	1320		75	R					75	3rd LAYER=8 MIL FILAMENT TAPE ALL ICE MELTED
56	1-21-77	DIST	3/16	3x1.6	0.9	-17	2400	1320		80	R					80	3rd LAYER=8 MIL FILAMENT TAPE-ALL ICE MELTED

Remarks: Model #2 TE_1 Mode Various Types of 3rd Layer

TEST NO.	TEST DATE	TEST CONDITIONS - 2450 MHz														TEST RESULTS	
		ICE SAMPLE															
		ICE COMPOSITION	ICE THICKNESS	ICE LENGTH x WIDTH	ICE DENSITY	TEMPERATURE SURFACE GUIDE	TRANSMITTER POWER	COUPLED POWER	REFLECTED POWER	POWER ON TIME	TERMINATION L = LOAD R = REFLECTOR	ICEWATER SPRAY	AIR GUN	LINE TILTED	SIMULATED CENTRIFUGAL LOAD	SHED TIME	REMARKS
			in	in	gm/cc	°C	WATTS	WATTS	WATTS	SEC	L R	ON or —	ON or —	YES or —	LB	SEC	
57	1-21-77	DIST	3/16	3x1.6	0.9	-12	2400	1320		25	R				8.4	25	POWDERED HIGH LOSS LENNITE BETWEEN TWO 8 MIL LAYERS OF TAPE - MINOR MELTING
58	1-21-77	DIST	3/16	3x1.6	0.9	-13.7	2400	1320		50	R				8.4	50	SAME 3rd LAYER 1/3 MELTED
59	1-21-77	DIST	3/16	3x1.6	0.9	-20	2400	1320		170	R				8.4	170	SAME 3rd LAYER - ALL ICE MELTED

Remarks: Model #2 TE_1 Mode 3rd Layer Model

TEST NO.	TEST DATE	TEST CONDITIONS - 2450 MHz														TEST RESULTS	
		ICE SAMPLE															
		ICE COMPOSITION	ICE THICKNESS	ICE LENGTH x WIDTH	ICE DENSITY	TEMPERATURE SURFACE GUIDE	TRANSMITTER POWER	COUPLED POWER	REFLECTED POWER	POWER ON TIME	TERMINATION L = LOAD R = REFLECTOR	ICEWATER SPRAY	AIR GUN	LINE TILTED	SIMULATED CENTRIFUGAL LOAD	SHED TIME	REMARKS
			in	in	gm/cc	°C	WATTS	WATTS	WATTS	SEC	L R	ON or —	ON or —	YES or —	LB	SEC	
60	1-25-77	CRREL SNOW #6	APPROX 1/4	—	0.3	-18	2400	1320		120	R					55	CRRELSAMPLES WERE TOO SOFT TO LOAD WITH THE LOADING MECHANISM SAMPLES WERE PLACED ON LINE AND TIME TO START MELTING HAS RECORDED
61	1-25-77	CRREL SNOW #6	.35	15x1.63	0.3	-20	2400	1320		120	R					70	
62	1-25-77	CRREL SNOW #6	.35	15x1.63	0.3	-15	2400	1320		120	R		ON			55	

Remarks: Model #2 TE_1 Mode Shed Tests Using CRREL Snow Samples

TEST NO.	TEST DATE	TEST CONDITIONS - 2450 MHz: ICE SAMPLE: ICE COMPOSITION	ICE THICKNESS	ICE LENGTH x WIDTH	ICE DENSITY	TEMPERATURE SURFACE GUIDE	TRANSMITTER POWER	COUPLED POWER	REFLECTED POWER	POWER ON TIME	TERMINATION L = LOAD R = REFLECTOR	ICEWATER SPRAY	AIR GUN	LINE TILTED	SIMULATED CENTRIFUGAL LOAD	TEST RESULTS: SHED TIME	REMARKS
			in	in	gm/cc	C	WATTS	WATTS	WATTS	SEC	L R	ON or —	ON or —	YES or —	LB	SEC	
63	2-11-77	TAP	.189	3x1.75	.9	-20	2000	860			WATER L		OFF		8.4	90	MOST OF ICE MELTED MELTING BEGAN IN 70 SEC
64	2-11-77	TAP	.189	3x1.75	.9	-14.1	2000	860			WATER L		ON		8.4	85	MOST OF ICE MELTED REFLECTED POWER DIPPED
65	2-11-77	TAP	189	3x1 75	.9	-17.4	2000	860	STABLE		WATER L		ON		8.4	100	NO WATER ON LINE REFLECTED POWER REMAINED STABLE-1/2 ICE MELTED-HOT SPOTS
66	2 11-77	TAP	189	3x1.75	.9	-16.4	2000	860	STABLE		WATER L		ON		8.4	80	EVIDENCE OF HOT SPOTS
67	2-14-77	TAP	.095	3x1.75	.9	-20.[illegible]	2000	860			WATER L		OFF		8.4	75	MOST OF ICE MELTED BEFORE SHEDDING
68	2-15-77	TAP	.095	3x1.75	.9	-19.1	2000	860	STABLE		WATER L		ON		8.4	120	ONLY A SMALL PORTION OF ICE SHED
69	2-15-77	TAP	.189	3x1.75	.9	-17.3	1000	430			WATER L		OFF		8.4	240	CLEAN SHEDDING HALF ICE MELTED

Remarks: Model #3 TE_1 Mode

TEST NO.	TEST DATE	TEST CONDITIONS - 2450 MHz: ICE SAMPLE: ICE COMPOSITION	ICE THICKNESS	ICE LENGTH x WIDTH	ICE DENSITY	TEMPERATURE SURFACE GUIDE	TRANSMITTER POWER	COUPLED POWER	REFLECTED POWER	POWER ON TIME	TERMINATION L = LOAD R = REFLECTOR	ICEWATER SPRAY	AIR GUN	LINE TILTED	SIMULATED CEN TRIFUGAL LOAD	TEST RESULTS: SHED TIME	REMARKS
			in	in	gm/cc	°C	WATTS	WATTS	WATTS	SEC	L R	ON or —	ON or —	YES or —	LB	SEC	
70	2-15-77	TAP	.189	3x1.75	.9	-14.4	1000	430			WATER LOAD L		ON		8.4	155	HALF ICE SHED
71	2-16-77	TAP	.189	3x1.75	.9	-17.4	800	344			WATER LOAD L		OFF		8.4	—	NO SHEDDING SAMPLE MELT-ED AWAY
* 72	2-16-77	TAP	.189	.98x 1.75	.9	-12.7	2000	860			WATER LOAD L		OFF		3	50	MELTED (SMALLER ICE SAMPLE)
73	2-16-77	TAP	.189	.98 x 1.75	.9	-18.4	1000	430			WATER LOAD L		OFF		3	160	MELTED
74	2-16-77	TAP	.189	.98 x 1.75	[illegible]	-11.3	1000	430			WATER LOAD L		OFF			55	MELTED
75	2-17-77	TAP	.189	1.5x 1.75	.9	-15	1000	430			WATER LOAD L		ON			NONE	NO SHEDDING OR MELTING DURING 1st 5 MIN
76	2-17-77	TAP	.189	.98x 1.75	.9	-19	1000	430			WATER LOAD L		OFF			360	ALL ICE MELTED
77	2-17-77	TAP	.189	.98x 1.75	.9	-13	1000	430			WATER LOAD L		OFF			360	ALL ICE MELTED

Remarks: Model #3 TE_1 Mode Tests 72 to 77 Use A 1" Ice Sample

TEST NO.	TEST DATE	TEST CONDITIONS - 2450 MHz														TEST RESULTS	
		ICE SAMPLE															
		ICE COMPOSITION	ICE THICKNESS	ICE LENGTH x WIDTH	ICE DENSITY	TEMPERATURE SURFACE GUIDE	TRANSMITTER POWER	COUPLED POWER	REFLECTED POWER	POWER ON TIME	TERMINATION L = LOAD R = REFLECTOR	ICEWATER SPRAY	AIR GUN	LINE TILTED	SIMULATED CENTRIFUGAL LOAD	SHED TIME	REMARKS
			in	in	gm/cc	°C	WATTS	WATTS	WATTS	SEC	L R	ON or —	ON or —	YES or —	LB	SEC	
78	2-17-77	TAP	.189	1x1.75	.9	-11.8	1000	430			WATER LOAD L		ON		.75	30	CLEAN SHED
79	2-17-77	TAP	.189	1x1.75	.9	-11.8	1000	430			WATER LOAD L		OFF		.5	30	CLEAN SHED
80	2-18-77	TAP	.189	1x1.75	.9	-13.6	1000	430			WATER LOAD L		OFF		.5	80	CLEAN SHED
81	2-18-77	TAP	.189	1x1.75	.9	-17	1000	430			WATER LOAD L		OFF		.5	80	MELTED DISREGARD TEST
82	2-18-77	TAP	.189	1x1.75	.9	-19.1	1000	430			WATER LOAD L		ON		.5	70	CLEAN SHED
83	2-18-77	TAP	.189	1x1.75	.9	-17.7	2000	860			WATER LOAD L		ON		.5	20	CLEAN SHED
84	2-18-77	TAP	.189	1x1.75	.9	-18.4	2000	860			WATER LOAD L		ON		.5	40	CLEAN SHED

Remarks: Model #3 TE_1 Mode Tests 78 to 112 Utilize a 0.025 Cellulose Acetate Tape with Acrylate Adhesive

TEST NO.	TEST DATE	ICE SAMPLE: ICE COMPOSITION	ICE SAMPLE: ICE THICKNESS	ICE SAMPLE: ICE LENGTH x WIDTH	ICE SAMPLE: ICE DENSITY	TEMPERATURE SURFACE GUIDE	TRANSMITTER POWER	COUPLED POWER	REFLECTED POWER	POWER ON TIME	TERMINATION L = LOAD R = REFLECTOR	ICEWATER SPRAY	AIR GUN	LINE TILTED	SIMULATED CENTRIFUGAL LOAD	SHED TIME	REMARKS
TEST CONDITIONS - 2450 MHz																TEST RESULTS	
			in	in	gm/cc	°C	WATTS	WATTS	WATTS	SEC	L R	ON or —	ON or —	YES or —	LB	SEC	
85	2-21-77	TAP	.189	1x1.75	.9	-18	2000	860		—	WATER LOAD L		ON		0.5	40	
86	2-21-77	TAP	.189	1x1.75	.9	-19	2000	860		—	WATER LOAD L		ON		0.5	50	
87	2-21-77	TAP	.189	1x1.75	.9	-17.7	500	215		5 MIN	WATER LOAD L		ON		0.5	NO SHED	NO SHEDDING
88	2-21-77	TAP	.189	1x1.75	.9	-17.0	500	215		6 MIN	WATER LOAD L		ON		0.5	NO SHED	NO SHEDDING
89	2-23-77	TAP	.189	1x1.75	.9	-10	1000	430		—	WATER LOAD L		OFF		0.5	30	CLEAN SHED
90	2-23-77	TAP	.189	1x1.75	.9	-10.1	1000	430		—	WATER LOAD L		OFF		0.5	25	CLEAN SHED
91	2-23-77	TAP	.189	1x1.75	.9	-11.4	1000	430		—	WATER LOAD L		OFF		0.5	35	CLEAN SHED
92	2-23-77	TAP	.189	1x1.75	.9	-10.4	2000	860		—	WATER LOAD L		OFF		0.5	7	CLEAN SHED

Remarks: Model #3 TE_1 Mode 3 Layer Model Cellulose Acetate Tape Acrylate Adhesive 0.025"

TEST NO.	TEST DATE	TEST CONDITIONS - 2450 MHz														TEST RESULTS	
		ICE SAMPLE															
		ICE COMPOSITION	ICE THICKNESS	ICE LENGTH x WIDTH	ICE DENSITY	TEMPERATURE SURFACE GUIDE	TRANSMITTER POWER	COUPLED POWER	REFLECTED POWER	POWER ON TIME	TERMINATION L = LOAD R = REFLECTOR	ICEWATER SPRAY	AIR GUN	LINE TILTED	SIMULATED CENTRIFUGAL LOAD	SHED TIME	REMARKS
			in	in	gm/cc	°C	WATTS	WATTS	WATTS	SEC	L R	ON or —	ON or —	YES or —	LB	SEC	
93	2-24-77	TAP	.189	.98x 1.75	.9	-10	2000	860			WATER LOAD L		OFF		0.5	10	.025" 3rd LAYER CLEAN SHED
94	2-24-77	TAP	.189	.98x 1.75	.9	-20	2000	860			WATER LOAD L		OFF		0.5	20	.025" 3rd LAYER CLEAN SHED
95	2-25-77	TAP	.189	.98x 1.75	.9	-12.2	2000	860			WATER LOAD L		OFF		0.5	10	.025" 3rd LAYER CLEAN SHED
96	2-25-77	TAP	.189	.98x 1.75	.9	-10.3	2000	860			WATER LOAD L		OFF		0.5	20	.025" 3rd LAYER CLEAN SHED
97	2-25-77	TAP	.189	.98x 1.75	.9	-12.1	500	215			WATER LOAD L		OFF		0.5	80	.025" 3rd LAYER CLEAN SHED
98	2-25-77	TAP	.189	.98x 1.75	.9	-9.5	500	215			WATER LOAD L		OFF		0.5	60	.025" 3rd LAYER CLEAN SHED
99	2-25-77	TAP	.189	.98x 1.75	.9	-10.8	500	215			WATER LOAD L		OFF		0.5	30	.025" 3rd LAYER CLEAN SHED
100	2-28-77	TAP	.189	.98x 1.75	.9	-12	500	215			WATER LOAD L		OFF		0.5	100	.025" 3rd LAYER CLEAN SHED

Remarks: Model #3 TE_1 Mode 3 Layer Model .025 MIL Cellulose Acetate Tape Acrylate Adhesive

TEST NO.	TEST DATE	TEST CONDITIONS - 2450 MHz: ICE SAMPLE: ICE COMPOSITION	ICE THICKNESS	ICE LENGTH x WIDTH	ICE DENSITY	TEMPERATURE SURFACE GUIDE	TRANSMITTER POWER	COUPLED POWER	REFLECTED POWER	POWER ON TIME	TERMINATION L = LOAD R = REFLECTOR	ICEWATER SPRAY	AIR GUN	LINE TILTED	SIMULATED CENTRIFUGAL LOAD	TEST RESULTS: SHED TIME	REMARKS
			in	in	gm/cc	°C	WATTS	WATTS	WATTS	SEC	L R	ON or —	ON or —	YES or —	LB	SEC	
101	2-28-77	TAP	.189	.98x 1.75	.9	-13.8	2000	860			WATER LOAD L				0.5	10	VERY CLEAN SHED
102	2-28-77	TAP	.189	.98x 1.75	.9	-14	2000	860			WATER LOAD L				0.5	35	SOME MELTING
103	3-1-77	TAP	.189	.98x 1.75	.9	-15.9	2000	860			WATER LOAD L				0.5	35	SOME MELTING
104	3-1-77	TAP	.189	.98x 1.75	.9	-14.6	2000	860			WATER LOAD L				0.5	40	SOME MELTING
105	3-2-77	TAP	.189	.98x 1.75	.9	-15	1000	430			WATER LOAD L				0.5	65	SOME MELTING
106	3-2-77	TAP	.189	.98x 1.75	.9	-14	1000	430			WATER LOAD L				0.5	60	SOME MELTING
107	3-2-77	TAP	.189	.98x 1.75	.9	-14	1000	430			WATER LOAD L				0.5	40	CLEAN SHED
108	3-2-77	TAP	.189	.98x 1.75	.9	-14.5	1000	430			WATER LOAD L				0.5	50	CLEAN SHED

Remarks: Model #3 TE_1 Mode 3 Layer Model .025 Cellulose Acetate Tape Acrylate Adhesive

TEST NO.	TEST DATE	TEST CONDITIONS - 2450 MHz														TEST RESULTS	
		ICE SAMPLE															
		ICE COMPOSITION	ICE THICKNESS	ICE LENGTH x WIDTH	ICE DENSITY	TEMPERATURE SURFACE GUIDE	TRANSMITTER POWER	COUPLED POWER	REFLECTED POWER	POWER ON TIME	TERMINATION L = LOAD R = REFLECTOR	ICEWATER SPRAY	AIR GUN	LINE TILTED	SIMULATED CENTRIFUGAL LOAD	SHED TIME	REMARKS
			in	in	gm/cc	°C	WATTS	WATTS	WATTS	SEC	L R	ON or —	ON or —	YES or —	LB	SEC	
109	3-2-77	TAP	.189	.98x 1.75	.9	-14	500	215			WATER LOAD L				0.5	85	SOME MELTING
110	3-3-77	TAP	.189	.98x 1.75	.9	-15	500	215			WATER LOAD L				0.5	150	SOME MELTING
111	3-3-77	TAP	.189	.98x 1.75	.9	-14.7	500	215			WATER LOAD L				0.5	80	CLEAN SHED
112	3-3-77	TAP	.189	.98x 1.75	.9		500	215			WATER LOAD L				0.5	110	SOME MELTING

Remarks: Model #3 TE_1 Model 3 Layer Model .025 Cellulose Acetate Tape Acrylate Adhesive

TEST NO.	TEST DATE	TEST CONDITIONS - 2450 MHz														TEST RESULTS	
		ICE SAMPLE															
		ICE COMPOSITION	ICE THICKNESS	ICE LENGTH x WIDTH	ICE DENSITY	TEMPERATURE SURFACE GUIDE	TRANSMITTER POWER	COUPLED POWER	REFLECTED POWER	POWER ON TIME	TERMINATION L = LOAD R = REFLECTOR	ICEWATER SPRAY	AIR GUN	LINE TILTED	SIMULATED CENTRIFUGAL	SHED TIME	REMARKS
			in	in	gm/cc	°C	WATTS	WATTS	WATTS	SEC	L R	ON or —	ON or —	YES or —	LB	SEC	
113	3-4-77	SALT 0.6%	3/32	3x1.6	0.9	-18.6	1200	648			WATER LOAD L				4	30	CLEAN SHED
114	3-4-77	SALT 0.6%	3/32	3x1.6	0.9	-18.7	1200	648			WATER LOAD L				4	50	CLEAN SHED
115	3-4-77	SALT 0.6%	3/32	3x1.6	0.9	-18.0	1200	648			WATER LOAD L				4	20	CLEAN SHED
116	3-4-77	SALT 0.6%	3/32	3x1.6	0.9	-17.0	1200	648			WATER LOAD L				4	25	CLEAN SHED
117	3-7-77	SALT 0.6%	3/32	3x1.6	0.9	-18.0	1800	972			WATER LOAD L				4	20	CLEAN SHED
118	3-7-77	SALT 0.6%	3/32	3x1.6	0.9	-18.6	1800	972			WATER LOAD L				4	18	CLEAN SHED
119	3-7-77	SALT 0.6%	3/32	3x1.6	0.9	-19.0	600	324			WATER LOAD L				4	40	CLEAN SHED
120	3-7-77	SALT 0.6%	3/32	3x1.6	0.9	-18.4	600	324			WATER LOAD L				4	55	CLEAN SHED

Remarks: Model #2 TM_0 Mode 2 Layer Model

TEST NO.	TEST DATE	TEST CONDITIONS - 2450 MHz														TEST RESULTS	
		ICE SAMPLE															
		ICE COMPOSITION	ICE THICKNESS	ICE LENGTH x WIDTH	ICE DENSITY	TEMPERATURE SURFACE GUIDE	TRANSMITTER POWER	COUPLED POWER	REFLECTED POWER	POWER ON TIME	TERMINATION L = LOAD R = REFLECTOR	ICEWATER SPRAY	AIR GUN	LINE TILTED	SIMULATED CENTRIFUGAL LOAD	SHED TIME	REMARKS
			in	in	gm/cc	°C	WATTS	WATTS	WATTS	SEC	L R	ON or —	ON or —	YES or —	LB	SEC	
121	3-7-77	SALT 0.6T	3/32	3x1.6	0.9	-17.0	600	324			WATER LOAD L				4	70	CLEAN SHED
122	3-8-77	SALT 0.6%	3/16	3x1.6	0.9	-19.2	1200	648			WATER LOAD L				4	40	SOME MELTING
123	3-8-77	SALT 0.6%	3/16	3x1.6	0.9	-17.4	1200	648			WATER LOAD L				4	45	SOME MELTING
124	3-8-77	TAP	3/32	3x1.6	0.9	-18.0	1200	648		420	WATER LOAD L				4	—	NO SHEDDING
125	3-8-77	TAP	3/32	3x1.6	0.9	-13.0	2400	1296			WATER LOAD L				4	—	NO SHEDDING
126	3-8-77	TAP	3/32	3x1.6	0.9	-10.0	2400	1296			WATER LOAD L				4	160	MELTED

Remarks: Model #2 TM_0 Mode 2 Layer Model

		TEST CONDITIONS - 2450 MHz														TEST RESULTS	
		ICE SAMPLE															
TEST NO.	TEST DATE	ICE COMPOSITION	ICE THICKNESS	ICE LENGTH x WIDTH	ICE DENSITY	TEMPERATURE SURFACE GUIDE	TRANSMITTER POWER	COUPLED POWER	REFLECTED POWER	POWER ON TIME	TERMINATION L = LOAD R = REFLECTOR	ICEWATER SPRAY	AIR GUN	LINE TILTED	SIMULATED CENTRIFUGAL LOAD	SHED TIME	REMARKS
			in	in	gm/cc	°C	WATTS	WATTS	WATTS	SEC	L R	ON or —	ON or —	YES or —	LB	SEC	
127	3-10-77	DIST	3/32	3x1.6	0.9	-18.6	800	440			WATER LOAD L				3	5	CLEAN SHED
128	3-10-77	DIST	3/32	3x1.6	0.9	-18.0	800	440			WATER LOAD L				3	15	CLEAN SHED
129	3-11-77	DIST	3/32	3x1.6	0.9	-19.0	2400	1320			WATER LOAD L				3	3	CLEAN SHED
130	3-11-77	DIST	3/32	7 1/2 x1.6	0.9	-18.4	2400	1320			WATER LOAD L				3	11	CLEAN SHED
131	3-14-77	DIST	3/32	3x1.6	0.9	-18.0	1200	660			WATER LOAD L				3	11	CLEAN SHED
132	3-14-77	DIST	3/32	3x1.6	0.9	-19.0	1200	660			WATER LOAD L				3	19	CLEAN SHED
133	3-14-77	DIST	3/32	3x1.6	0.9	-18.3	1200	660			WATER LOAD L				3	19	CLEAN SHED
134	3-14-77	DIST	3/32	3x1.6	0.9	-17.6	800	440			WATER LOAD L				3	20	CLEAN SHED

Remarks: Model #1 TE_1 Mode Lossy Layer Consisted of Resistive Material α=0.08 dB/in

		TEST CONDITIONS - 2450 MHz														TEST RESULTS	
		ICE SAMPLE															
TEST NO.	TEST DATE	ICE COMPOSITION	ICE THICKNESS	ICE LENGTH x WIDTH	ICE DENSITY	TEMPERATURE SURFACE GUIDE	TRANSMITTER POWER	COUPLED POWER	REFLECTED POWER	POWER ON TIME	TERMINATION L = LOAD R = REFLECTOR	ICEWATER SPRAY	AIR GUN	LINE TILTED	SIMULATED CENTRIFUGAL LOAD	SHED TIME	REMARKS
			in	in	gm/cc	°C	WATTS	WATTS	WATTS	SEC	L R	ON or —	ON or —	YES or —	LB	SEC	
135	3-14-77	DIST	3/32	3x1.6	0.9	-17.6	800	440			WATER LOAD L				3	20	CLEAN SHED
136	3-15-77	DIST	3/32	3x1.6	0.9	-18.9	400	220			WATER LOAD L				3	52	CLEAN SHED
137	3-15-77	DIST	3/32	3x1.6	0.9	-18.0	400	220			WATER LOAD L				3	58	CLEAN SHED
138	3-15-77	DIST	3/32	3x1.6	0.9	-18.4	1200	560			WATER LOAD L				3	5	CLEAN SHED
139	3-15-77	DIST	3/32	3x1.6	0.9	-18.3	800	440			WATER LOAD L				3	30	CLEAN SHED

Remarks: Model #1 TE_1 Mode 3 Layer Model Lossy Layer Consisted of Resistive Material α=0.08 dB/in

		TEST CONDITIONS - 2450 MHz														TEST RESULTS	
		ICE SAMPLE															
TEST NO.	TEST DATE	ICE COMPOSITION	ICE THICKNESS	ICE LENGTH x WIDTH	ICE DENSITY	TEMPERATURE SURFACE GUIDE	TRANSMITTER POWER	COUPLED POWER	REFLECTED POWER	POWER ON TIME	TERMINATION L = LOAD R = REFLECTOR	ICEWATER SPRAY	AIR GUN	LINE TILTED	SIMULATED CENTRIFUGAL LOAD	SHED TIME	REMARKS
			in	in	gm/cc	°C	WATTS	WATTS	WATTS	SEC	L R	ON or —	ON or —	YES or —	LB	SEC	
140	3-22-77	DIST	3/32	3x1.6	0.9	-18.6	1200	660			WATER LOAD L				3	45	2 LAYERS CLEAN SHED
141	3-22-77	DIST	3/32	3x1.6	0.9	-18.9	1200	660			WATER LOAD L				3	40	2 LAYERS CLEAN SHED
142	3-22-77	DIST	3/32	3x1.6	0.9	-18.6	1200	660			WATER LOAD L				3	60	2 LAYERS POLYURETHANE MELTED IN SPOTS
143	3-22-77	DIST	3/32	3x1.6	0.9	-19.3	1200	660		120	WATER LOAD L				3		1 LAYER SPOT MELTING IN POLYURETHANE

Remarks: Model #1 TE_1 Mode 3 Layer Model 1 or 2 Layers of Polyurethane Each 0.024 in. thick

TEST NO.	TEST DATE	TEST CONDITIONS - 2450 MHz														TEST RESULTS	
		ICE SAMPLE															
		ICE COMPOSITION	ICE THICKNESS	ICE LENGTH x WIDTH	ICE DENSITY	TEMPERATURE SURFACE GUIDE	TRANSMITTER POWER	COUPLED POWER	REFLECTED POWER	POWER ON TIME	TERMINATION L = LOAD R = REFLECTOR	ICEWATER SPRAY	AIR GUN	LINE TILTED	SIMULATED CENTRIFUGAL LOAD	SHED TIME	REMARKS
			in	in	gm/cc	°C	WATTS	WATTS	WATTS	SEC	L R	ON or —	ON or —	YES or —	LB	SEC	
144	3-24-77	DIST	3/32	3x1.6	0.9	-18.6	1600	880			WATER LOAD L				3	45	MINOR MELTING
145	3-24-77	DIST	3/32	3x1.6	0.9	-17.9	1600	880			WATER LOAD L				3	60	MINOR MELTING
146	3-24-77	DIST	3/32	3x1.6	0.9	-17.9	800	440			WATER LOAD L				3	100	MINOR MELTING
147	3-24-77	DIST	3/32	3x1.6	0.9	-18.5	800	440			WATER LOAD L				3	130	MINOR MELTING
148	3-24-77	DIST	3/32	3x1.6	0.9	-18.0	2400	1320			WATER LOAD L				3	20	CLEAN SHED
149	3-24-77	DIST	3/32	3x1.6	0.9	-18.5	2400	1320			WATER LOAD L				3	28	CLEAN SHED

Remarks: Model #1 TE_1 Mode Model 1 Layer Polyurethane 0.025" Thick Adhesive Removed

APPENDIX B

DERIVATIONS OF LOSS TANGENT EQUATIONS

The attenuation constant of a surface waveguide is defined by

$$\alpha_t = \frac{W_D}{2W_T} \qquad \text{(B-1)}$$

where:

α_t = Attenuation constant

W_D = The power dissipated

W_T = Total power transferred

The power dissipated per unit length is due to dielectric heating of the surface waveguide and any ice layer. The total attenuation constant is thus:

$$\alpha_t = \frac{\frac{\omega\varepsilon_1 \ell \tan\delta_1}{2}\int_0^{d_1} |E_y|^2 dx + \frac{\omega\varepsilon_1 \ell \tan\delta_i}{2}\int_{d_1}^{d_2} |E_y|^2 dx}{2W_T} \qquad \text{(B-2)}$$

ω = Radian frequency

ε_1 = Dielectric constant (dielectric and ice)

ℓ = Width of surface guide

$\tan \delta_i$ = Loss tangent of ice

$\tan \delta_1$ = Loss tangent of dielectric

E_y = Transverse electric field intensity

d_1 = Thickness of dielectric

d_2 = Thickness of dielectric plus ice layer

x = Coordinate axis normal to surface

$$E_y = \frac{j\omega\varepsilon E}{k_x} \sin k_x X \qquad \text{(B-3)}$$

In B-2, the simplifying assumption is made that the real part of the dielectric constant of ice, ε_2, is approximately the same as the dielectric layer.

The total power transfer, W_T, is:

$$W_T = \frac{\beta\omega\varepsilon E^2 \ell}{2}\left[\frac{1}{k_x^2} \quad S(d_2) + \frac{\cos^2 k_x d_1}{2K_x^3}\right] \tag{B-4}$$

where:

$$S(d) = \frac{d}{2} - \left[\frac{\sin 2k_x d}{4k_x}\right] \tag{B-5}$$

Substituting Equations B-3 and B-4 into Equation B-2 gives:

$$\alpha_t = A[\tan \delta_1 \; S(d_1) + \tan \delta_i \; (S(d_2) - S(d_1))] \tag{B-6}$$

where:

$$A = \frac{k_1^2}{2k_x^2 \beta\left(\frac{1}{k_x^2} S(d_2) + \frac{\cos^2 k_x d_2}{2K_x^3}\right)} \tag{B-7}$$

Equation B-6 may now be solved to yield tne desired tan δ_i:

$$\tan \delta_i = \frac{\frac{\alpha_t}{A} - \tan \delta_1 \; S(d_1)}{S(d_2) - S(d_1)} \tag{B-8}$$

To use B-8, the attenuation of the ice loaded line, α_t, must be determined all the other terms are known.

Theoretically, α_t could be measured by classical attenuation techniques but it is so small for short line lengths that this method is impractical.

It is instead determined by measuring the power dissipated in the ice sample, W_i and calculating the power dissipated in the line, W_l under the ice sample as follows.

The attenuation constant of the ice loads line is:

$$\alpha_t = \frac{-10 \log\left[\dfrac{W_T - W_l - W_L}{W_T}\right]}{L} \text{db/unit length} \qquad \text{(B-9)}$$

where: W_T = Power incident on the iced section
W_l = Power dissipated in the line
W_i = Power dissipated in the ice
L = Length of iced section

The power lost in the base dielectric W_l is calculated from Equation B-9 by first assuming the loss in the ice is zero or $W_i = 0$ (real part of the dielectric constant of ice is the same as the dielectric) or

$$\alpha_l = \alpha_t \approx \frac{-10 \log\left[1 - \dfrac{W_l}{W_T}\right]}{L} \qquad \text{(B-10)}$$

where: α_l = Attenuation constant due to losses in the dielectric assuming no losses in the ice.

Equation B-10 is solved for the argument of the log function to give:

$$1 - \frac{W_l}{W_T} = 10^{-\alpha_l L/10} \qquad \text{(B-11)}$$

and α_l is obtained from Equation B-6 by assuming $\tan \delta_i = 0$.

The power lost in the ice is determined by measuring the time required to heat the ice sample from ambient temperature to 0°C or until the ice just begins to melt. Then:

$$W_i = \frac{mc(0 - T_\infty)}{t_1} \quad (4.186) \text{ watts} \tag{B-12}$$

where: m = Mass of the ice

c = Specific heat of ice

t_1 = Time required to raise the ice from 0°C to T_∞

T_∞ = Ambient temperature

Substituting Equation B-11 into Equation B-9 yields α_t

$$\alpha_t = \frac{-10 \log \left[10^{-\alpha_1 L/10} - \frac{W_i}{W_T} \right]}{L} \tag{B-13}$$

α_1 is obtained from Equation B-6 assuming $\tan \delta_i - 0$

W_i is obtained from Equation B-12

α_t is then substituted into Equation 8 to obtain $\tan \delta_i$, the loss tangent of the ice.

APPENDIX C

WHIRLING ARM METHOD OF TESTING MICROWAVE ICE PROTECTION CONCEPT

SIMULATED ICING ENVIRONMENT

These tests will demonstrate the performance of a microwave deicer, mounted on the tail rotor of a UH-1 helicopter, in a simulated rotor blade icing environment. An artists conception of the recommended whirling-arm apparatus is illustrated in Figure C-1 and a schematic diagram in Figure C-2. A perspective view of the tail rotor deicer boot and wave launcher are illustrated in Figures C-2 and C-4, respectively.

The recommended tests will consist of three major tasks:

1) Design, fabricate and test the microwave deicer for the UH-1 Tail Rotor in accordance with concepts demonstrated experimentally in this program.
2) Design, fabricate and test the whirling-arm apparatus.
3) Perform deicing and anti-icing tests in a simulated icing environment such as the NASA Lewis Icing Research Tunnel.

Deicing Performance T[illegible]

In this test, droplet impact ice simulating light, moderate and heavy icing will be permitted to accrete on the deicer boot as the tail rotor is rotated at various angular velocities. The microwave energy required to shed the ice is then measured as a function of the parameters listed below:

1. Degree of Icing (Liquid Water Content LWC)
   a. Light $0.12 < LWC < .5$ gm/m^3
   b. Moderate $0.5 < LWC < 1.0$ gm/m^3
   c. Heavy $1.0 < LWC$ gm/m^3
2. Ambient Temperature 0 to -20°C
3. Droplet Size
4. Blade Temperature
5. Air Speed

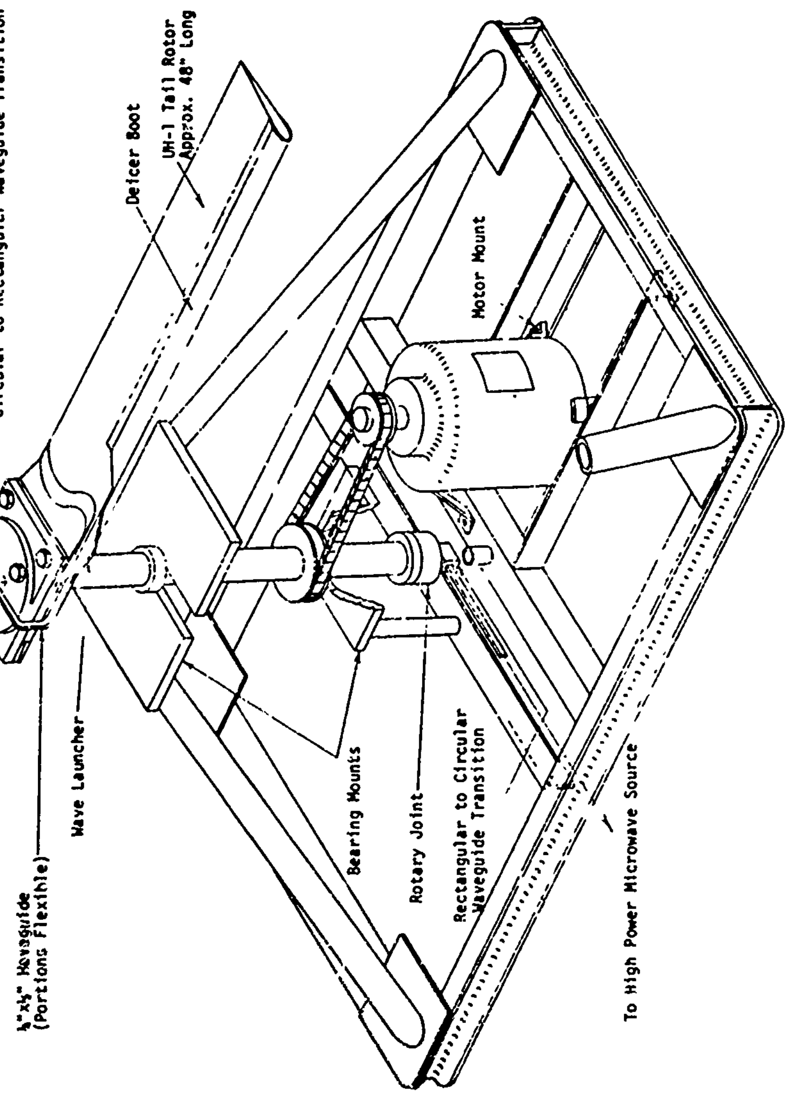

FIGURE C-1. ARTISTS CONCEPTION OF WHIRLING-ARM TEST STAND

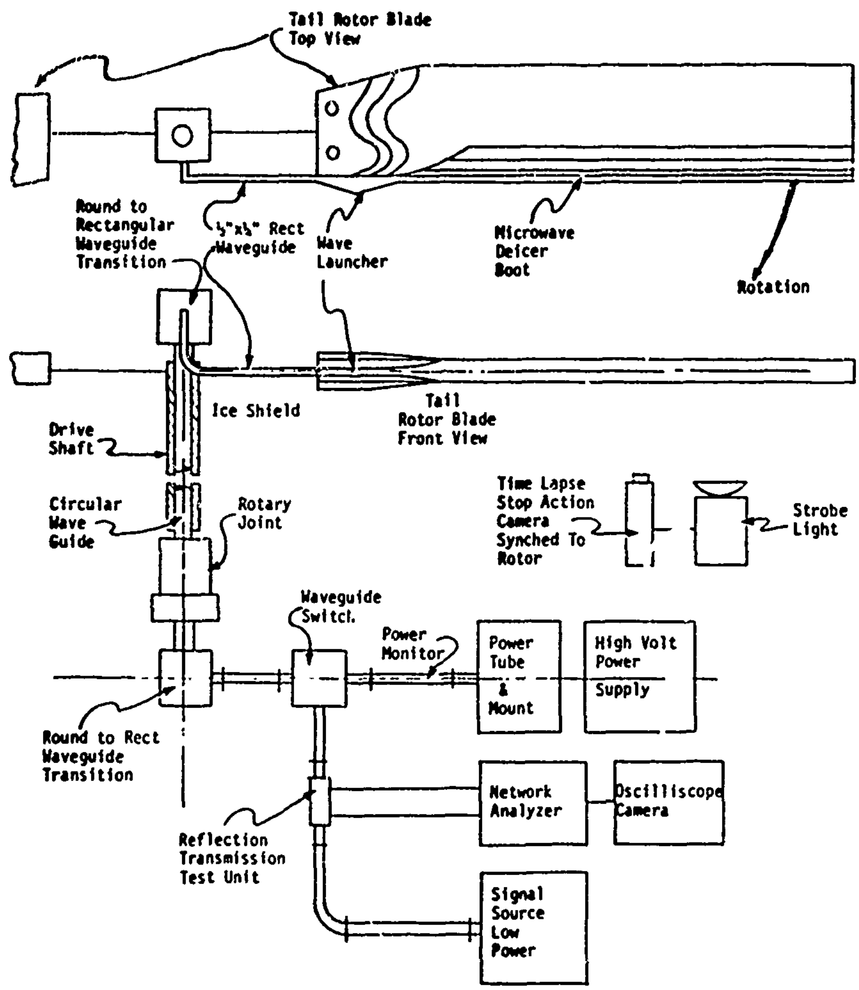

FIGURE C-2. SCHEMATIC DIAGRAM WHIRLING ARM TEST STAND

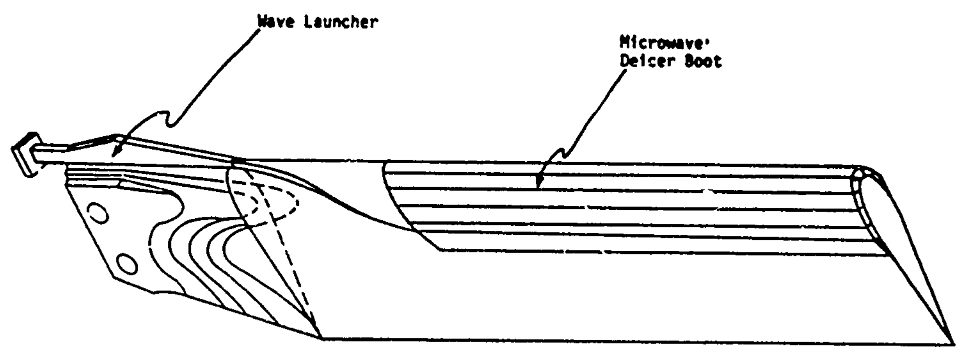

FIGURE C-3. PERSPECTIVE VIEW UH-1 TAIL ROTOR EQUIPPED WITH MICROWAVE DEICER BOOT AND WAVE LAUNCHER

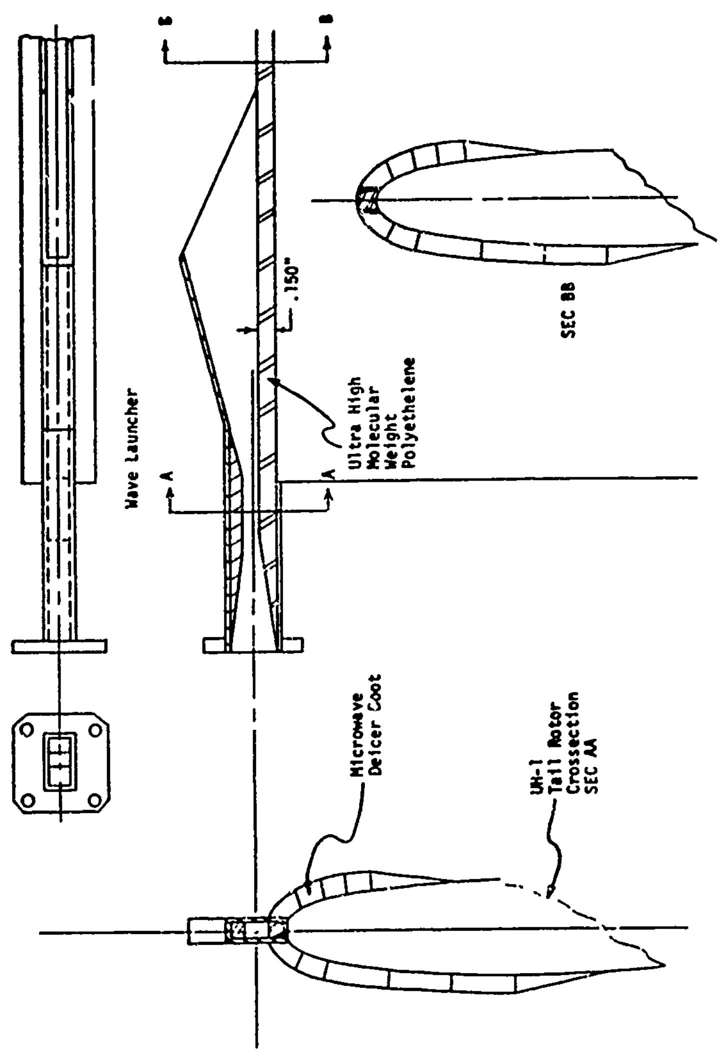

FIGURE C-4. CROSSECTION - DEICER BOOT AND WAVE LAUNCHER

6. Angular Velocity (Centrifugal Force)
7. Ice Thickness (Time in Icing)
8. Time to Shed

The shedding process will be recorded with the time lapse stop-action camera and stroboscope synchronized to the blade rotation. The camera record will establish the shed time, the degree of shedding and the size and the shape of the shed fragments.

Anti-Icing Performance Tests

In this test, the microwave energy, at various levels, is turned on prior to any ice accumulation on the blade and the power required to keep the rotor blade just ice free is measured as a function of the following parameters:

1. Degree of Icing
    a. Light $0.12 < LWC < 0.5\ gm/m^3$
    b. Moderate $0.5 < LWC < 1.0\ gm/m^3$
    c. Heavy $1.0 < LWC\ \ gm/m^3$
2. Ambient Temperature
3. Blade Temperature
4. Air Speed
5. Angular Velocity

The condition of the blade is recorded with time lapse, stop action stroboscopic photography.

APPENDIX D
MICROWAVE ICE DETECTORS

Breadboard microwave ice detectors, thickness gauges and accretion rate meters can be developed based upon the experimental findings made in Section 5.

These devices will be nonmechanical, have no moving parts, and conform to the contour of the surface being monitored. The readout will be essentially instantaneous, giving ice presence, ice thickness and ice accretion rate as functions of time. The devices will be small, lightweight and rugged so that they can be placed almost anywhere on the skin of the aircraft, including the rotor blade and engine inlet ducts.

Ice Detection Background

An ice detector is a necessary component of any icing protection system for a helicopter, but at present no completely satisfactory instrument for this application exists. Helicopter rotor blades are dangerously sensitive to small amounts of ice, and the pilot, at present, receives no direct evidence of its formation. Present day icing forecasts, based upon prior statistics, are frequently inaccurate and subjective and offer no sure way for the pilot to become aware of the presence of ice. The only absolutely certain way to become aware of a dangerous icing condition is to detect the ice and measure its severity with suitable, rapidly responding ice detectors. This must be done in sufficient time for the pilot to determine if the icing severity is within the capability of ice protection system or permit timely evasive manuevers.

BASIC CONCEPTS

The basic concept that would be used in an ice detector is that ice is a good dielectric and that its dimensions, e.g., thickness and accretion rate, will affect the performance of surface waveguides on which it is permitted to accumulate. Two physical phenomena demonstrated experimentally in this program are utilized. These are:

(a) Tuning or shifting of the resonant frequency of surface waveguides on which ice is allowed to accumulate (Figures 26 and 27).

(b) Decreasing of the cut-off frequency of surface waveguide on which ice is allowed to accumulate.

Several ice detectors are described which are based upon phenomena a and b; all will produce simplified signals for cockpit readout of ice presence, ice thickness and ice accretion rate. These are:

1) A resonant surface waveguide, phased locked-loop ice detector
2) A resonant surface waveguide, quadrature hybrid ice detector
3) A cut-off, go no-go Ice Presence Indicator
4) Cut-off Swept Frequency Ice Thickness and Accretion Rate Meter

Resonant Frequency Ice Detectors (Types 1 and 2)

These ice detectors make use of the shift in the resonant frequencies of surface waveguides on which ice is allowed to accumulate, as illustrated in Figures 26 and 27. The degree of shift of the resonance and its time rate of change are proportional to the ice thickness and accretion rate respectively. Both devices (1 and 2 above) convert the frequency shift to proportional dc voltages, which can be read on conveniently located cockpit readout meters and calibrated in ice thickness and ice accretion rate. The readouts are continuous and instantaneous, there being no moving parts or inertia to contend with.

Cut-Off Ice Detectors (Types 3 and 4)

These ice detectors make use of the decrease in the cut-off frequency of the TE_1 mode surface waveguide caused by the thickening of the waveguide by the accumulation of ice.

In the simple go/no-go ice presence indicator, the microwave oscillator is set just below cut-off of the surface waveguide so that no energy may propagate down the guide and be detected. As the ice accumulates, effectively thickening the surface waveguide, the cut-off frequency is lowered below the frequency of the oscillator; at which time, energy can propagate and be detected, indicating the presence of ice.

A more sophisticated device utilizing the cut-off principle is the swept-frequency device. This device will meter the ice thickness and accretion rate. In this device, the microwave oscillator repetitively sweeps from a frequency below cut-off to a frequency above cut-off, propagation through the guide occurring at the instant its cut-off frequency is reached. As ice accumulates on the surface guide, reducing its cut-off frequency, propagation occurs earlier and earlier during the sweep. The time this occurs is an indication of ice thickness. Instrumentation that measures this instant in the form of a voltage pulse or other means can be used to provide a convenient cockpit readout.

APPENDIX E

POWER DRAIN OF A MICROWAVE DEICER AT 33.7 GHz USING AN EXPERIMENTAL GYROTRON

In the gyrotron, constructed in the Soviet Union, Reference 18 an output power of 10 kw at an efficiency of 40% was obtained. An outline drawing of this tube is presented in Figure E-1. Power output, efficiency and power lost are plotted versus beam current in Figure E-2. The results of using this tube to design a microwave deicer, the power drain and the time to shed, assuming an ambient temperature of -20°C and 800 watts power per blade, for a microwave deicer using this tube, are presented in Table E-1. The higher frequency reduces the surface waveguide thickness to 0.1 inch.

[18] Kisel, D.V., Korablev, G.S., Navel'yev, V.G., Petelin, M.I., and Tsimring, Sh. Ye., "An Experimental Study of a Gyrotron, Operating at the Second Harmonic of the Cyclotron Frequency, With Optimized Distribution of the High-Frequency Field, "Radio Engineering and Electronic Physics, Vol. 19 pp. 95-99, April 1974.

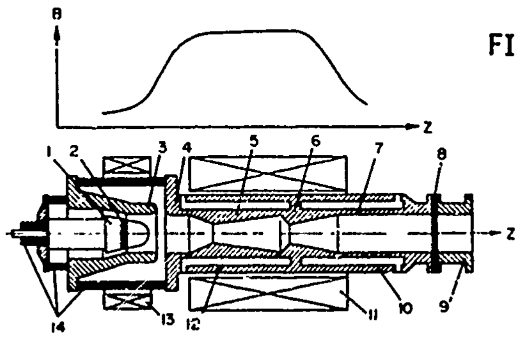

FIGURE E-1. OUTLINE DRAWING OF SOVIET GYROTRON PROTOTYPE. 1-CATHODE; 2-EMITTING STRIP; 3-FIRST ANODE; 4-SECOND ANODE; 5-CAVITY; 6-OUTPUT COUPLING APERTURE; 7-BEAM COLLECTOR; 8-OUTPUT WINDOW; 9-OUTPUT WAVEGUIDE; 10 and 12-WATER JACKETS; 11-MAIN SOLENOID; 13-ELECTRON GUN SOLENOID; 14-INSULATORS. OVERALL LENGTH OF THIS DEVICE IS IS APPROXIMATELY 20 cm.

Excerpted from Reference 18

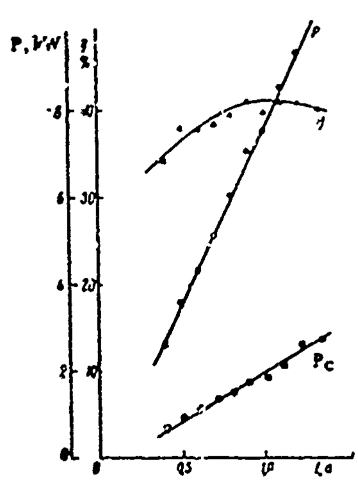

FIGURE E-2. THE DEPENDENCE OF THE EFFICIENCY (η), CAVITY LOSSES (P_c) AND GYROTRON OUTPUT POWER P ON THE BEAM CURRENT I IN THE CONTINUOUS MODE OF OPERATION:

$U_c = 19$ kV.

Excerpted from Reference 18

TABLE E-1. HELICOPTER POWER DRAIN, USING GYROTRON AT 35 GHz T_∞ = -20°C, 800 WATTS PER BLADE

HELICOPTER TYPE	TOTAL POWER REQUIRED	POWER REQ'D/TUBE @ DISTRIBUTION EFFICIENCY OF 80%	NO. OF TUBES PER HELICOPTER	POWER DRAIN PER HELICOPTER	TUBE EFFICIENCY	SHED TIME
	kw	kw		kw	η	sec
UH-1 AH-1 OH-58	1.6	2.0	1	5.7	35%	29.8 34.55 13.5
UTTAS AAH ASH	3.2	4.0	1	10.4	38%	45.25 43.80 31.55
CH-47	4.8	6.0	1	15.2	39%	34.55